Identification of Umbrella Constraints in Power Generation Scheduling Problems

Ali Jahanbani Ardakani

Department of Electrical & Computer Engineering
McGill University
Montréal, Canada

August 2014

A thesis submitted to McGill University in partial fulfillment of the requirements for the degree of Doctor of Philosophy.

Abstract

In this dissertation we propose a methodology to reduce the size of optimization problems used for market clearing and planning studies purposes in power systems. Solving these optimization problems is essential for daily operation of power systems and to ensure their security and dependability. However, the biggest challenge in solving these problems are their large sizes. Nonetheless, the empirical evidence and previous research suggest that these problems contain many redundant constraints. We propose a methodology, called umbrella constraint discovery (UCD), which identifies the constraints of these problems that contribute in forming the feasible set of solutions (umbrella constraints) and removes the ones that do not contribute. These redundant constraints do not have any effect on the solution of the problem, yet, they occupy memory and require CPU time. UCD is an optimization-based approach which identifies the umbrella constraints through the enforcement of a consistency logic on the set of constraints. In this dissertation, we apply UCD on security-constrained optimal power flow and unit commitment problems for different standard test systems. One of the advantages of UCD is that it lends itself well to decomposition. We propose decomposition techniques to further expedite the solution of UCD problems. Different decomposition approaches which exploit the structure of the parent problem are tested and the most efficient ones are identified.

We also perform a sensitivity analysis on umbrella sets by varying the system load. The results show that the umbrella sets are relatively insensitive to the changes of system loads. This means that the system operators should not need to run UCD for each change of load in the system, but rather they can use the results of UCD for the similar conditions of their system. Additionally, the system operators can solve UCD problem for the entire system load profile over the span of a year and use the union of all umbrella sets corresponding

to each hour. We show that the size of this set is still very small in comparison with the original constraint set.

Then, we introduce a new formulation that benefits from less computational complexity than UCD, called partial UCD. This new method exploits the experience of running UCD on the network at hand and by making some reasonable assumptions, it reduces the computational burden for identifying non-umbrella constraints. This formulation is indeed an approximation of UCD and can quickly identify non-umbrella constraints. Therefore, it can be used as a pre-processing step to UCD solution.

To further investigate the efficacy of the proposed methodology, we apply UCD and partial UCD on mixed-integer linear problems. We elaborate how the benefits of application of the proposed methodology can be further exploited the proposed methodology can improve the solution time of mixed-integer linear problems.

Finally, we explore the possibility of predicting heuristically the umbrella set of a network if enough historical information of UCD results are available. We used neural networks to demonstrate that this task is possible and the results are encouraging.

Résumé

Dans cette thése, nous proposons une méthodologie qui permet la réduction de la taille des problèmes d'optimisation utilisés dans les études d'équilibre du marché et de planification des réseaux électriques. La résolution de ces problèmes d'optimisation est essentielle au fonctionnement quotidien des réseaux élelectriques et à assurer leur sécurité et leur fiabilité.

Cependant, le plus grand défi dans la résolution de ces problèmes consiste en la taille de ceux-ci. Néanmoins, les données empiriques, ainsi que les recherches antérieures, suggèrent que ces problèmes contiennent de nombreuses contraintes redondantes. Nous proposons une méthodologie, nommée la Découverte des Contraintes Parapluie (DCP), qui identifie les contraintes de ces problèmes qui contribuent à former l'ensemble des solutions réalisables (les contraintes parapluie) et supprime les contraintes qui n'y contribuent pas. Ces contraintes redondantes n'ont aucun effet sur la solution des problèmes et pourtant elles occupent de la mémoire et consomment du temps machine (CPU). DCP est une approche fondée sur l'optimisation qui identifie les contraintes parapluie par l'application d'une logique de cohérence sur l'ensemble des contraintes. Dans cette thèse, nous appliquons la DCP dans l'analyse de répartition de puissance optimale sous contraintes de sécurité et dans la gestion de la production électrique sur des réseaux standards d'éssai différents. Un des avantages de la DCP est qu'elle se prête bien à la décomposition. Nous proposons des techniques de décomposition afin d'accélérer la génération des solutions des problèmes DCP. Différentes approches de décomposition qui exploitent la structure du problème majeur sont testées et les plus efficaces sont identifiées.

Nous effectuons également une analyse de sensibilité sur les ensembles parapluie en variant la charge du réseau. Les résultats démontrent que les ensembles parapluie sont relativement insensibles aux changements des charges du réseau. Cela signifie que les ges-

tionnaires du réseau de transport n'auront pas la nécéssité d'exécuter la DCP pour chaque variation de la charge du réseau ; mais plutôt, ils peuvent utiliser les résultats de la DCP obtenus dans des conditions similaires à leur réseau de transport.

En outre, les gestionnaires du réseau de transport peuvent résoudre le problème de la DCP pour l'ensemble du profil de charge du réseau sur la durée d'une année et utiliser l'assemblage de tous les ensembles parapluie correspondant à chaque heure. Nous montrons que la taille de cet ensemble est largement inférieure à celle de l'ensemble des contraintes d'origine.

Ensuite, nous introduisons une nouvelle formulation qui bénéficie d'une complexité de calcul moindre à celle de la DCP, nommée DCP partielle. Cette nouvelle méthode exploite l'expérience de l'exploitation de la DCP sur le réseau connu et en faisant certaines hypothèses raisonables. Ceci réduit la charge de calcul de l'ordinateur pour identifier les contraintes non-parapluie. Cette formulation est en effet un rapprochement de la DCP et peut identifier rapidement les contraintes non-parapluie. Par conséquent, elle peut être utilisée comme une étape de pré-traitement à la solution de la DCP.

Afin d'approfondir l'efficacité de la méthode proposée, nous appliquons la DCP et la DCP partielle sur des problèmes linéaires avec nombres entiers. Nous élaborons sur la façon dont les bénifices de l'application de la méthodologie proposée peuvent être exploitées davantage afin d'améliorer le temps de solution des problèmes linéaires avec nombres entiers.

Enfin, nous explorons la possibilité de prédire de manière heuristique l'ensemble parapluie d'un réseau si suffisamment d'information historique des résultats de DCP sont disponibles. Nous avons utilisé des réseaux neuronaux afin de démontrer que cette tâche est possible et que les résultats sont encourageants.

Dedication

To Rana

Acknowledgments

My deepest recognition goes to my supervisor, Professor François Bouffard for his unconditional help, excellent knowledge of the field and his great supervision during my study. He had always been an academic and emotional support for me during very rough years of my Ph.D. He is the most knowledgeable supervisor and the wisest and caring friend that I have ever come across. There are no words to express my gratitude for all of the help and support he offered to me during my studies at McGill University. One simply could not wish for a more supportive and friendlier supervisor. I take my hat off to you.

I wish to thank my Ph.D. committee members, Professor Francisco D. Galiana, Professor Benoit Boulet and Professor Dennis Dionysios Giannacopoulos for their guidance and support. I would like to also thank my examiners, Prof. Ross Baldick from the University of Texas at Austin, and Prof. Michael Kokkolaras from McGill University for their very constructive comments and insights.

This work would have not been completed without financial support from the FRQ-NT and McGill Engineering Doctoral Award. Also, the author acknowledges the support from the IBM Academic Initiative for the access to a royalty-free CPLEX license.

I would like to also thank my good friend Seyed Ehsan Safavieh from Albert-Ludwigs-Universität Freiburg, Germany. A special thank goes to Mohammad El Chehaly for his help. I praise the enormous amount of help from my friends in Power System Laboratory at McGill University. Thank you my friends: Dr. Ali Shojaei, Dr. Amir Kalantari, Dr. Hamed Golestani Far, Prof. Houshang Karimi, Omar Saadeh, Mostafa Momen, Dr. Sameh El Khatib, Amir Abiri-Jahromi, Aboutaleb Haddadi, Dr. Mojtaba Vaezi, Dr. Hamid Mahboubi, Harmeet Cheema, Dmitri Rimorov, Seyed Ali Gorji Zadeh, Seyed Nasrollah Tabatabaei, Hussam Nosair, Salman Md. Nazir, Navdeep Dhaliwal, Carlos Martinez, Jonathan Robinson, Christopher Tegho and Sajad Darabi.

Contents

1 Introduction **1**

1.1 Fundamentals of Modern Power System Security Enforcement 2

1.2 Operational Cost Optimization in Power Systems 6

1.2.1 Economic Dispatch 6

1.2.2 Unit Commitment 8

1.3 Optimal Power Flow 9

1.4 Problem Identification 14

1.5 Dissertation Outline 21

1.6 Claim of Originality 23

2 Umbrella Constraint Discovery **26**

2.1 Introduction 27

2.2 Preventive SCOPF 29

2.2.1 SCOPF Problem Formulation 30

2.2.2 Compact Formulation 31

2.3 Umbrella Constraints and Umbrella Sets 33

2.4 Identifying Umbrella Constraints 36

2.4.1 Preliminaries 37

2.4.2 Efficient Umbrella Constraint Discovery 39

2.4.3 Some Remarks 41

Computational Complexity of UCD-II 41
UCD-II Infeasibility and Solution Uniqueness 41
Generality of UCD-II 42
2.5 Decomposition 43
2.5.1 Separation 43
2.5.2 Divide-and-Conquer 44
2.5.3 Partitioning 46
Contingency-Based Partitioning 46
Line-Based Partitioning 47
2.6 Three-Bus Example 48
2.6.1 Lagrange Multipliers of UCD-II Constraints 51
2.7 Test Results 53
2.7.1 IEEE RTS 53
2.7.2 Contingency-Based Partitioning 56
Line-Based Partitioning 56
2.7.3 118 Bus System 58
Line-Based Partitioning of UCD-II 59
Contingency-Based Partitioning of UCD-II 61
2.8 Sensitivity Analysis 62
2.8.1 Three-Bus System 63
Load Change at Bus 3 63
Load Change at Bus 2 70
2.8.2 IEEE RTS 72
Change of Load at Bus 7 73
Change of Load at Bus 8 75
Discussion 76
2.9 Discussion 84

2.10 Summary and Conclusion 85

3 Partial Umbrella Constraint Discovery 87

3.1 Introduction 87

3.2 Computational Inefficiencies in UCD 88

3.3 Partial UCD 89

3.3.1 Formulation of Partial UCD 90

3.3.2 Size of P-UCD 93

3.4 Partial UCD Test Results 95

3.4.1 Application on IEEE RTS 95

3.4.2 Application on IEEE 118 Bus System 97

3.5 Summary and Conclusion 103

4 Application to Unit Commitment Problems 105

4.1 Introduction 105

4.2 UCD and Mixed-Integer Problems 106

4.3 Formulation of the Unit Commitment Problem 109

4.4 Application of UCD to SCUC 113

4.4.1 Application of UCD on Static Unit Commitment 114

4.4.2 Application of UCD on Dynamic Unit Commitment 118

4.4.3 Discussion 120

4.5 Summary and Conclusion 121

5 Prediction of Umbrella Sets 122

5.1 Introduction 122

5.2 Neural Networks 123

5.3 Test System 124

5.4 Implementation 125

5.5 Error Types 127

5.6 Modified Training Algorithm 129
5.7 Conclusion 131

6 Conclusion **133**
6.1 Dissertation Overview 133
6.2 Recommendations for Future Work 137

A IEEE Reliability Test System Data **139**

B IEEE 118 Bus System Data **143**

References **153**

List of Figures

1.1 Basic structure of a power system 3
1.2 SCOPF solution through iterative economic dispatch/SFT 15

2.1 Demonstration of umbrella and non-umbrella constraints 36
2.2 Necessary steps for applying UCD on SCOPF problems 48
2.3 Three-bus system. 49
2.4 Feasibility set of solutions for three-bus system 50
2.5 Demonstration of redundant, weakly redundant and umbrella constraints . 53
2.6 IEEE Reliability Test System 1996 55
2.7 Feasible set of the three-bus system with 10 MW load at bus 3 65
2.8 Feasible set of the three-bus system with 30 MW load at bus 3 66
2.9 Feasible set of the three-bus system with 50 MW load at bus 3 67
2.10 Feasible set of the three-bus system with 70 MW load at bus 3 68
2.11 Feasible set of the three-bus system with 90 MW load at bus 3 69
2.12 Corrolation between system load changes and umbrella sets 79
2.13 Contribution of each line in the yearly umbrella set of IEEE RTS 80
2.14 Contribution of each contingency in the yearly umbrella set of IEEE RTS . 81
2.15 Share of each constraint in the yearly umbrella set of IEEE RTS 83

3.1 Illustration of partial UCD 92
3.2 The lines contributing to the umbrella set of 118 bus system. 101

3.3 The contingencies contributing to the umbrella set of 118-bus system. . . . 102

4.1 Feasible set of region of a given example with continuous variables 108
4.2 Feasible set of an example with binary variables 109
4.3 Steps for running UCD on MIPs 114
4.4 The feasible set of an MIP 116
4.5 The feasible set of the above problem with the new constraint 117

5.1 A general neural network with one hidden layer. 124

List of Tables

1.1 ISOs different daily markets 9

2.1 Generation Parameters 48
2.2 Umbrella set for different loadings in bus 3 of the three-bus system 64
2.3 Umbrella set for different loadings in bus 2 of the three-bus system 71

3.1 Summary of UCD Solution Times 103

4.1 Application of UCD on UC and SCUC 120

5.1 Comparison of ANNs trained with BP 127
5.2 Comparison of average performance of ANNs trained with BP 127
5.3 False negative and false positive errors in the networks trained with BP . . 128
5.4 Comparison of ANNs trained by PSO 130
5.5 Comparisons of neural networks 131

A.1 IEEE RTS bus data. 140
A.2 IEEE RTS generator data. 141
A.3 IEEE RTS branch data. 142

B.1 IEEE 118 bus system data. 144
B.2 IEEE 118 bus system generation data 146

List of Acronyms

SCOPF	Security-constrained optimal power flow
SCUC	Security-constrained unit commitment
UCD	Umbrella constraint discovery
P-UCD	Partial umbrella constraint discovery
ANN	Artificial neural networks

Nomenclature

The list of main symbols used in this dissertation is defined below. Other symbols might be used in the dissertation and will be defined as needed throughout the text.

Indices

i	Index of buses running from 1 to I.
k	Index of contingencies running from 0 to K.
ℓ	Index of transmission lines running from 1 to L.
j and j'	Index of constraints running from 1 to J.

Sets

$\mathcal{J}$	Set of constraints.
$\tilde{\mathcal{J}}$	Subset of $\mathcal{J}$.
$\mathcal{U}$	Set of umbrella constraints.
$\overline{\mathcal{U}}$	Set of non-umbrella constraints.
$\mathcal{J}_\lambda^\ell$	Subset of $\mathcal{J}$ in line-based decomposition.
$\mathcal{J}_\lambda^k$	Subset of $\mathcal{J}$ in contingency-based decomposition.
$\mathcal{J}_\pi$	Subset of $\mathcal{J}$ containing generation-based or potential umbrella constraints.

Variables

p_i	Power generated at bus i.
s_i	Slack variable in UCD-II formulation.
$u_{i,t}$	Binary variable indicating status of generator i at time t.
$r_{i,t}$	Spinning reserve contribution from generator i at time t.

Functions

$f(\cdot)$	Some arbitrary objective function.
$C(\cdot)$	Energy production cost function for generators.
$S(\cdot)$	Start-up and shut down cost function for generators.

Parameters

I	Number of buses in the system.
L	Number of lines in the system.
$\overline{f}_\ell$	Capacity of transmission line ℓ.
T	Time horizon.
UT_i	Minimum up time for generator i.
DT_i	Minimum down time for generator i.
d_i	Load at bus i.
H	Generation shift factor matrix.
$h_{\ell,i}(k)$	Coefficients of generation shift factor matrix representing change of power transfer in line ℓ during contingency k for changes in power produced in bus i.
SR_t	Total spinning reserve requirement for the system at time t.
Δ_i	Ramp up/down limit of generating unit i.

Chapter 1

Introduction

The electricity industry has changed very positively the living standards of most human beings since its dawn in the late 19^{th} century. Electricity has been generated in centralized power plants and transferred to load centers, be it cities or industrial sites, using transmission lines. A general sketch of a typical electricity system is shown in Fig. 1.1. Traditionally, the operation of the electric systems was following a centralized "command-and-control" paradigm. In this paradigm, most of the electric systems' infrastructure were owned by governments and electric networks in all (voltage) levels were run by the government-supervised entities.

During 1970s and 1980s, some countries started restructuring industries which were historically owned by governments by introduction of market and competition. Restructuring brought in many advantages for these industries, including lower costs and rates of products. The restructuring of electricity industry started in 1980s by countries such as Chile (1982), England and Wales (1990) and Norway (1990) [1]. In the United States of America, the Energy Policy Act marked the start of restructuring of the electricity industry by mandating open access to the tranmission systems in 1992. In April 1996, the Federal En-

ergy Regulatory Commission (FERC) issued Orders 888 and 889 which mandated further access to the transmission systems by the creation of independent system operators (ISO). In Order 888, FERC delineates 11 characteristics of ISOs. Consequent to the formation of ISOs, in December 1999, FERC issued Order 2000 in which the voluntary formation of Regional Transmission Operators (RTOs) is encouraged and 12 characteristics and functions of this type of entity are enumerated. RTOs along with ISOs ensure a non-discriminatory access to transmission networks. There are currently nine ISOs and RTOs functioning in the United States of America and Canada. The regions which do not have an RTO or ISO should conform to FERC's open access mandate [2].

Since the appearance of ISOs/RTOS, utilities have merged and created large entities. For example, an RTO in United States of America called PJM, serves more than 61 million people in 13 states and the District of Columbia. Interconnecting power systems increases the reliability of the whole system, but at the same time, introduces challenges and uncertainties for the operation and planning of the power system.

1.1 Fundamentals of Modern Power System Security Enforcement

ISOs/RTOs ensure the reliable operation of power systems while running a competitive electricity market. In a restructured power system, most of the traditional tasks of utilities are moved to ISOs. Some of the ISOs' responsibilities are the following:

— Long-term regional planning,

— Managing the wholesale electricity market,

— Operation of the electric power systems.

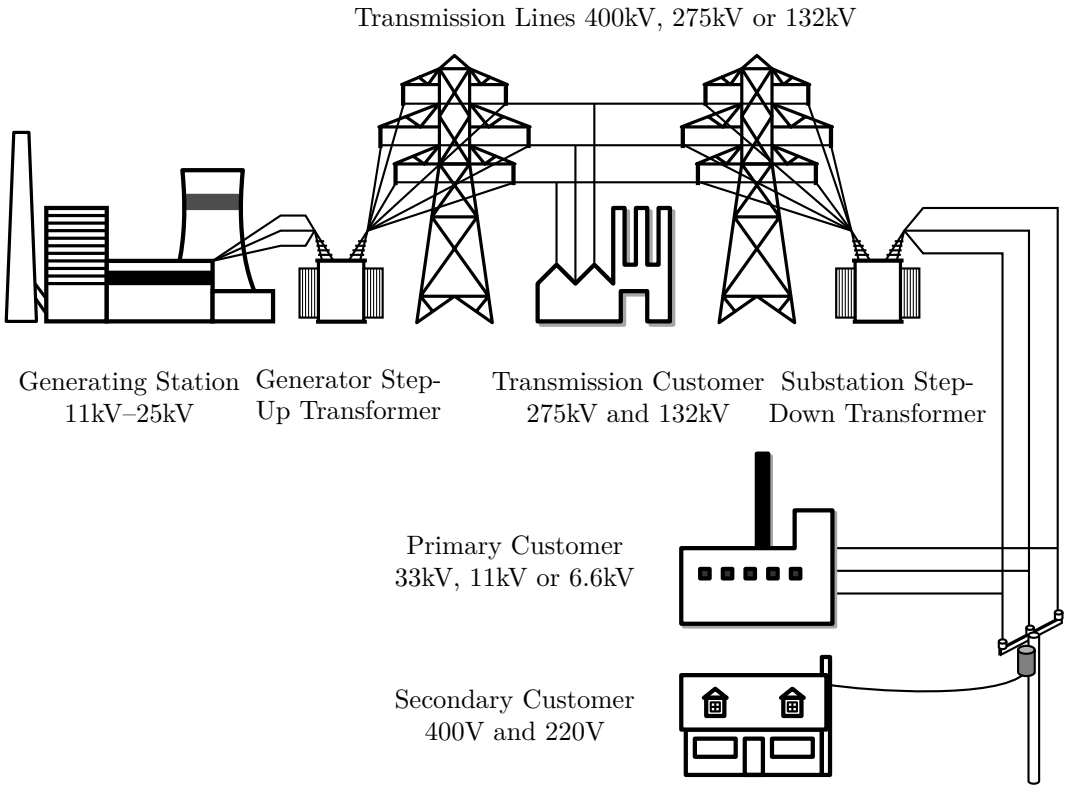

Figure 1.1 Basic structure of a power system [3], [4]

ISOs make long-term regional planning decisions while trying to address the needs of all utilities and consumers within their region for the reliability and economic benefits. They run different wholesale power markets: day-ahead market, hour-ahead market and real-time market, while ensuring fair and non-discriminatory access to transmission networks by all market participants. In the aspect of their operation responsibility, ISOs seek to minimize the cost of electricity production while maintaining the system's reliability. By minimization of the general cost of system operation, ISOs should eventually contribute to reducing the cost of electricity for consumers.

In the context of power systems, reliability consists of *security* and *adequacy*. In this dissertation, we mostly deal with security rather than adequacy. Security of a power system is its resilience against possible disturbances; this is in contrast to adequacy which is concerned with having appropriate generation and transmission infrastructure to serve the forecasted load [5].

There are five operating states in which a power system can be [6, 7]:

— In the *normal state*, the system load is satisfied and all of the system constraints are respected. All equipment are functioning within their limits and the available reserve in the system is enough to provide the level of security, should the system be subjected to stresses.

— If all system constraints are satisfied, but the occurrence of some disturbances could make some equipment to become overloaded, the system is in the *alert state*. By taking preventive actions, the system operator can restore the system to the normal state.

— If a disturbance occurs before taking preventive actions when the system is in the alert state, the system enters the *emergency state*. In this state, some of the system

inequality constraints such as equipment capacities are violated. However, the system is still intact and corrective control actions are required to take the system back to at least the alert state.

— If the system is in the emergency state and no corrective action is taken, the system will disintegrate and enter the *in extremis state*. In this state equality and inequality constraints are violated and system loads are lost. The system operator should take emergency control actions to stop a total system collapse.

— By taking emergency actions the system collapse can be stopped and the system will enter *restorative state*. By taking control actions the system can enter alert or normal state of operation.

In order to secure the operation of power systems, system operators mainly follow two control paradigms to ensure the system security: preventive and corrective security control. In preventive security control, the system operators set the system control variables in such a way that, without taking any action, system constraints are not violated if one of the postulated contingencies occur in the system. On the other hand, in corrective security control, if a contingency occurs, some of the system constraints are violated, but, the system operators take predetermined actions in order to relieve those violations. Those actions are determined by solving OPF problems considering the possible contingencies in the system to avoid sliding the system into any insecure operating states. The accommodation of corrective actions in SCOPF models allows the system operators to run the network at a lower cost compared to a pure preventive control model. At the same time, the cost of system operation using either corrective or preventive control is higher than the cost of operation obtained by an economic dispatch problem since they include more constraints [8].

Additionally, the level and diversity of uncertainties present in large-scale interconnected electricity transmission and distribution networks are rising steadily. These increases will speed up over the coming years with the massive integration of renewable generation, the electrification of road transport and the continuous ageing of legacy network infrastructures. To better manage these uncertainties and to better exploit the potential of the carbon-free electricity from renewable resources, planning and operation tools available for assisting system operators will have to model more explicitly the potential impacts of this wider spectrum of uncertainties in order to keep the power system in its secure operation state.

1.2 Operational Cost Optimization in Power Systems

To minimize the cost of system operation, ISOs use different tools to model the power system and to identify the combination of generators that could yield the most economic state of the system while satisfying the forecasted load in the operation day. Indubitably, the most economic state of the system must satisfy all of the technical constraints of the network. We specifically talk about three optimization tools: economic dispatch, optimal power flow (OPF) and security-constrained optimal power flow (SCOPF). New York ISO estimated that the use of security-constrained economic dispatch can bring savings about 100 million dollars annually amounting to two billion dollars from 1977 to 1999 [9].

1.2.1 Economic Dispatch

One of the first attempts to optimize the power system was to minimize the cost of the power generation given the different cost curves of generators in early 1930s [10]. To do so, the system operators would form an optimization problem called “economic dispatch”. The goal of economic dispatch problem was to allocate the total demand to different generators

in such a fashion that the total demand is met and, at the same time, the total cost of power generation is minimized. Back in 1930s, economic dispatch problems were solved by experienced engineers using their judgment or by "specially-developed slide rules" [10]. In economic dispatch problems, the network is either not modeled at all or its constraints are simplified [11]. Since this method ignores many of the constraints which are governing operation of power systems, this method could yield a sub-optimal or infeasible solution. Many efforts have been made since late 1950s and early 1960s to solve optimal real power flow problems [12] with objective functions such as loss minimization using exact [13] or approximate models [14].

Moreover, the economic dispatch problem does not include the possible abnormalities (so-called contingencies) that may happen in real-time operation. Also, system voltages and angles are not modeled within the problem. Therefore, if a contingency happens in a system, it is possible that the system may slide into an insecure operation mode.

A general economic dispatch formulation can be represented as follows [15]

$$\min_{p} \sum_{i=1}^{I} C_i(p_i) \tag{1.1}$$

subject to

$$\sum_{i=1}^{I} p_i = \sum_{i=1}^{I} d_i \tag{1.2}$$

$$\underline{p}_i \leq p_i \leq \bar{p}_i; \qquad i = 1, \ldots, I \tag{1.3}$$

where $C_i(\cdot)$ is the cost of generation of one megawatt in generating unit i, I is the number of buses in the system including load and generating buses and d_i is the load at bus i. Finally, p_i is the generation level at bus i, and $\underline{p}_i$ and $\bar{p}_i$ are the minimum and maximum

generation levels at bus i.

1.2.2 Unit Commitment

To meet the forecast load, sufficient generation capacity needs to be brought online prior to dispatch. In an ISO setting, each generator who wishes to participate in the electricity market, submits a bid for generation to the ISO before the operation day. Using this information, the ISO clears the market while ensuring that the forecast load can be satisfied subject to generators' technical constraints. During the market clearing process, the ISO utilizes a mathematical model called a security-constrained unit commitment (SCUC) [16–22] to determine which generator should be turned on and what would be their level of output for each hour of the next day. The SCUC problem considers network constraints and possible contingencies in the system as well as the technical constraints of the units. By taking these constraints into account, operators ensure secure operation of the system in the event of occurrence of any postulated contingency. This constitutes a preventive security control action.

The objective function of unit commitment problems has traditionally been the minimization of the fuel cost of power production and start up and shut down costs. However, the models can be modified to accommodate maximization of social welfare as the objective function [23]. It can be shown that despite the dissimilarities between these two forms of unit commitment problem, they both are very similar in purpose [1]. Along with the commitment of units for supplying the load, there is always some capacity committed as reserve to buffer the errors in the load forecast. Again, it is the unit commitment that determines the generators which will provide the reserve for the operating day. The unit commitment problem formulation will be explained comprehensively in Chapter 4.

Table 1.1 ISOs different daily markets [24]

ISO Name	Day-Ahead	Hour-Ahead	Real-Time
CAISO	✓	✓	✓
MISO	✓	✗	✓
New England	✓	✗	✓
New York	✓	✗	✓
PJM	✓	✗	✓

1.3 Optimal Power Flow

When the unit commitment results are obtained, the owners of the committed units are notified about the status of their units for the operating day and the output of their units. On the day of operation, the load forecast for the hour of operation is modified based on the new information about the load. ISOs solve optimal power flow problems to fine tune the output of committed generators. Some ISOs run hour-ahead markets where participants submit their bids an hour ahead of the operation. When the operation hour arrives, ISOs clear a real-time market (five minutes ahead of operation) based on the results of the optimal power flow with the values of the actual load. Table 1.1 shows the list of some of the ISOs in the United States of America and the markets that they clear daily.

Optimal power flow problems have different variations and their applications go beyond market clearing. In fact, the optimal power flow is used very often in other contexts in ISOs. They run an OPF every day, every hour and every five minutes to find the optimal state of the network [10]. The OPF as a tool can help decision-makers in ISOs in different situations. The following is a list of examples of the use of SCOPF and its variations in some situations [25].

1. Not everything goes as planned in power systems all of the times. Different abnormal

situations may arise while operating a complex network with so many elements such as power systems. These abnormal situations (contingencies) could be in the form of transmission lines failures, generators outages, transformer failures, *etc.* In such situations, solving OPF problems can help ISOs to identify the minimum cost control actions necessary to bring back the network to the "normal" state.

2. If the load of the system changes in such manner that makes some of the transmission lines overloaded, the system operator should take actions to correct the power transmission of those overloaded lines. Solving an OPF problem subjected to line constraints can give the operators the most economic combination of generators that satisfies the system demand and at the same time relieves the congested lines. This function of OPF in a deregulated environment can be referred to as "congestion management".
3. If voltages of a power system violate their allowed ranges, the operator takes corrective actions to bring the voltages to their limits. The solution of OPF can identify the control actions that will bring the voltages back into their normal limits.
4. In both the preventive or corrective security control paradigms, the OPF is in the heart of decision making for the system operators.
5. When a power system is in the secure state, system operators solve OPF to further minimize the cost of system operation.
6. In a deregulated environment, the OPF, and its extension SCOPF, can be used to calculate locational marginal electricity prices. This is a common practice in several ISOs such as California ISO (CAISO), ISO New England and PJM [26].

The OPF problem was formulated for the first time in 1962 by Carpentier [27]. The objective of an OPF problem could be to minimize the cost of power production while

satisfying a number of network constraints. These constraints include voltage limits, line flow limits, transformer flow limits, tap changer limits, *etc.* With recent developments in mixed integer programming solution methods in the past 20 years, integer decision variables have also been integrated into OPF problems. A simple form of an OPF problem can look like the following [25]

$$\min_{p,\delta} \quad \sum_{i=1}^{I} C_i(p_i) \tag{1.4}$$

subject to

$$\underline{p}_i \leq p_i \leq \bar{p}_i \qquad i = 1, \ldots, I \tag{1.5}$$

$$p_i - d_i = P_i(\delta) \qquad i = 1, \ldots, I \tag{1.6}$$

$$-\bar{f}_\ell \leq f_\ell(\delta) \leq \bar{f}_\ell \qquad \ell = 1, \ldots, L \tag{1.7}$$

where $P_i(\delta)$ is the power flow in lines connecting to bus i, $f_\ell(\delta)$ is the power flow in line ℓ and δ is the vector of bus voltage angles. Equation (1.4) is the objective function of the OPF problem. Constraint (1.5) bounds the power generation in each unit within its limits. Equation (1.6) is the load balance constraints which ensures the balance of load and generation in the system. Constraint (1.7) enforces the transmission line flow limits.

The resilience of a power system against credible contingencies is one of the most important aspects of all power systems. If a contingency happens in real-time operation, the system variables must stay within their allowed limits either without intervention of the system operator (preventive control) or with the intervention of some pre-defined corrective actions (corrective control). To ensure the security of power systems, some constraints are

included in the OPF problems to model the uncertainties arising from the system operation under contingencies. This extension of OPF problem is called security-constrained OPF (SCOPF) and was, for the first time, proposed in 1974 [28]. To implement an SCOPF, "security constraints" should be added to the OPF problem. These constraints enforce some more limits on lines and other system variables by taking into account the post-contingency description of the power system.

The SCOPF has been used for planing studies such as: (i) shunt var planning; (ii) transfer capability studies; (iii) reactive interchange studies; (iv) loss optimization studies. SCOPF calculations can be used to determine sizing and location of new capacitors in the system in order to maintain normal operation of the system in the non-contingent case. In this case, the objective function would be the capital cost of capacitors to be minimized satisfying both pre- and post-contingency limits of the system. The SCOPF problem solution can also determine the optimal settings of control variables for flexible ac transmission system (FACTS) devices with the goal to improve the market-clearing [29]. Moreover, SCOPF calculations can be used as a pricing tool for electricity since the marginal prices are provided by the solution of the problem. These prices can be calculated for binding power system constraints, power production capacities, equipment regulation limits, area interchanges and transactions, losses and bus powers [30].

The conventional SCOPF formulation considering corrective actions is as follows [8, 26, 31]:

$$\min_{\mathbf{x}_0,\ldots,\mathbf{x}_K,\mathbf{u}_0,\ldots,\mathbf{u}_K} f_0(\mathbf{x}_0,\mathbf{u}_0) \tag{1.8}$$

$$\text{subject to} \quad \mathbf{g}_0(\mathbf{x}_0,\mathbf{u}_0) = \mathbf{0} \tag{1.9}$$

$$\mathbf{h}_0(\mathbf{x}_0,\mathbf{u}_0) \leq \mathbf{L}_l \tag{1.10}$$

$$\mathbf{g}_k^s(\mathbf{x}_k^s,\mathbf{u}_0) = \mathbf{0} \tag{1.11}$$

$$\mathbf{h}_k^s(\mathbf{x}_k^s,\mathbf{u}_0) \leq \mathbf{L}_s \tag{1.12}$$

$$\mathbf{g}_k(\mathbf{x}_k,\mathbf{u}_k) = \mathbf{0} \tag{1.13}$$

$$\mathbf{h}_k(\mathbf{x}_k,\mathbf{u}_k) \leq \mathbf{L}_m \tag{1.14}$$

$$|\mathbf{u}_k - \mathbf{u}_0| \leq \overline{\Delta \mathbf{u}}_k \tag{1.15}$$

where $k = 0,\ldots,K$ where K is the number of contemplated contingencies in the system and we define that $k = 0$ corresponds to the non-contingent state of the system. f_0 is the objective function of the problem. $\mathbf{x}_k$ are the state variables of the system such as voltage magnitudes and angles while $\mathbf{x}_k^s$ represents the system state variables right after occurrence of a contingency and before the system operator's intervention. $\mathbf{u}_k$ are the control variables of the system such as active power output of generators or tap changer values of transformers. $\mathbf{L}_l$ represents the normal transmission line limits, $\mathbf{L}_m$ represents the medium-term transmission line limits and $\mathbf{L}_s$ represents the emergency line flow limits of the system. $\overline{\Delta \mathbf{u}}_k$ denotes the maximum change that is allowed between k^{th} contingency and the non-contingent state for control variable $\mathbf{u}_k$, which acts as binding constraint between no-contingency and k^{th} contingency state [26]. If $\overline{\Delta \mathbf{u}}_k = 0$, no corrective action will be allowed and the problem will become the same as a preventive SCOPF. If $\overline{\Delta \mathbf{u}}_k \to \infty$, all corrective actions can be implemented without any limits, which turns the above problem

to an OPF without considering any contingency. We note that the desired corrective actions should not violate generation and line limit constraints. The equality constraints (1.9), (1.11) and (1.13) in the above model represent the ac/dc load flow equations while inequality constraints (1.10), (1.12) and (1.14) impose the transmission line flow limits in the system, control variables limits and state variable limits, if any.

The mainstream approach in industry to solving such SCOPF is to use a generation dispatch module and the simultaneous feasibility test (SFT) [32]. The generation dispatch produces generating unit set points which are validated by the SFT for line flow violations in both pre- and post-contingency states. Violations that are identified are used to generate new linear constraints for the generation dispatch. These new constraints are based on shift factors, which can also account for the nonlinearity of the power flow, and they are then added to the the generation dispatch to eliminate those previously-identified violations. This dispatch-SFT iterative process runs until no more violations are found. This is typical of security-constrained day-ahead market clearing algorithms and locational marginal pricing calculations used in large ISOs and RTOs in the United States (see, for example, [33]). Fig. 1.2 shows the steps taken in the successive economic dispatch/simultaneous feasibility test algorithm to solve the SCOPF.

1.4 Problem Identification

The reliability of power systems has always been a very important aspect of the planning and operation of electricity networks. The reliability and security aspects of power systems are usually highlighted after the occurrence of a major blackout such as the blackout of August 14, 2003. On that day, around 4:10 PM EDT, a major black out occurred in the Northeast of the U.S. (including states such as New York, Ohio and New Jersey)

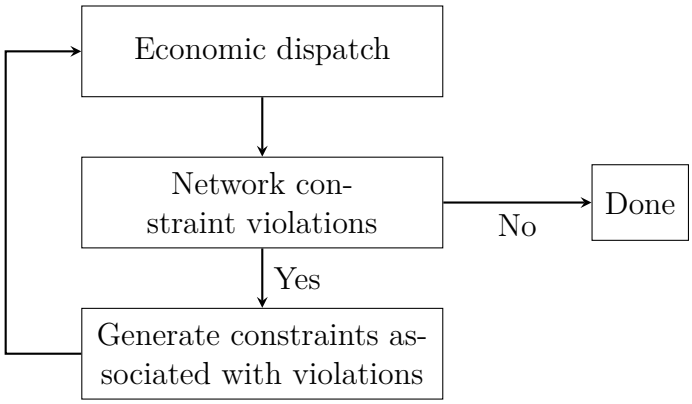

Figure 1.2 Flowchart showing the successive economic dispatch/simultaneous feasibility test algorithm to solve the SCOPF.

and Ontario, Canada (cities such as Toronto and Ottawa). It was estimated that the blackout affected 55 million people and caused several fatalities. In the aftermath of this blackout, U.S.-Canada Power System Outage Task Force final report, published in April 2004 [3], delineated several causes contributing to the blackout. The report highlights the reliability issues arising from insecure operation of the heavily loaded and densely woven interconnected North American power grid. Therefore, operation of power systems under stress limits the manoeuvre options of the operators and will give less time to the operators to decide on corrective actions, if a contingency occurs in the system. Consequently, there is a constant need for developing new tools and at the same time making the algorithms faster in order to help the system operators make crucial decisions during system contingency and increase their knowledge and awareness about the state of the system.

The classic way to address the modeling issues is to formulate the planning problems of the network operators as security-constrained optimal power flow (SCOPF) problems, especially to deal with unplanned generation and transmission equipment outages (*a.k.a.* contingencies) [26].

However, this modeling approach is undermined by the dimensions of the resulting

SCOPF optimization problem formulations stemming from the large-scale nature of power systems, the wide spectrum of potential uncertain events and their associated consequences.

The operators rely on these optimization problems, most significantly, OPF, SCOPF and SCUC to ensure the reliable and secure operation of the systems before and after occurrence of a contingency [31]. Given the small time window that operators have to solve SCOPF/OPF problems to secure the system operation, it is vital to be able to solve SCOPF/OPF problems very fast and robustly.

On the other hand, SCOPF/OPF problems have proven to be very difficult to solve. The size of these problems is colossal and the complexity and non-convexity of their constraints and the presence of many integer variables make them prone to difficult convergence [11,28]. For example, for IEEE 118 bus system, the corresponding SCOPF problem contains 65 730 constraints. For the real-life networks, the number of constraints could be in order of millions. However, previous work [34, 35] and operator experience showed that only a few of the constraints associated with the different contingencies have the potential to be of importance in their final solution. In other words, most of the SCOPF constraints are redundant. Those redundant constraints do not have the potential to contribute to the feasible set of solutions; however, they use resources in the process of solving those problems. Different simplification approaches have been implemented on SCOPF/OPF problems to make them tractable since their first appearance.

In the field of operations research, there has been many studies trying to identify the redundant constraints in linear problems [36–43]. Most notably, [44] presents a comparative study of some approaches for identification of redundant constraints. The proposed methods do not guarantee identification of *all* redundant constraints and, therefore, each will leave out some redundant constraints. More exact methods need more computations and solution time to identify more redundant constraints.

In [45], its authors propose a modification to the method proposed in [46] to reduce the computational effort and solution time of the problem.

In addition, Benders Decomposition [47] is one of the first approaches to be used to simplify OPF problems and it continues to be one of the tools that is used nowadays. In Benders decomposition, the problem is divided into a *master* problem and some *sub-problems*. In the first step, the master problem is solved and using its results, the sub-problems are solved. If any of the problem constraints are violated, a new constraint (cut) is added to the master problem. By iterating this approach, the optimal solution is found while satisfying all constraints. Reference [48] proposes a decomposition of SCOPF problems based on Benders decomposition to overcome the size issue of SCOPF problems due to incorporation of constraints arising from contingencies. Reference [49] explains solving a security-constrained unit commitment problem using Benders decomposition in details. In [8], Benders decomposition is utilized to solve the economic dispatch problem including the security constraints with corrective control after occurrence of a contingency.

Running a full ACOPF problem with improved models for system constraints would result in more precise power dispatches and improved market signals [9]. However, the solution time for these models will increase to impractical levels very easily. Linearized (dc) OPF, on the other hand, linearizes ac OPF problems based on several assumptions. In dc OPF, we assume that all voltages in the system have magnitude of 1 per unit and at the same time ignores the shunt capacitance and resistance of transmission lines. It also assumes that the voltage angles remains close to zero. Based on these assumptions, a linear dc formulation of the network is derived [15]. The dc OPF is used to calculate locational marginal electricity prices [50]. DC approximation can be combined with ac OPF to speed up the solution process and improve the efficiency of solution of ac OPF problems [51]. DC models are also used in many security-constrained unit commitment [52, 53]. [54]

discusses the computational challenges introduced to OPF in the new deregulated market environment. The article uses three different algorithms for solving OPF problems. The paper addresses the problem of abrupt price changes around break points in the price/power curve by presenting alternative algorithms and formulations.

The number of constraints of SCOPF problems are significantly larger than the OPF problems. These constraints arise from the operation of the system under postulated contingency. The number of constraints in SCOPF and OPF problems are the major drawback for solving these problems. One of the areas of the research on OPF and SCOPF has long been to identify the "unnecessary" or "redundant" constraints, especially, in SCOPF problems.

One method for reduction of the number of constraints is to identify the contingencies that push the system out of its secure region and include only the constraints arising from those contingencies. This method is called contingency filtering or contingency selection and consists of two classes, namely, contingency ranking and contingency screening. The contingency filtering has been a hot topic for research for many decades [55–74].

Most of contingency filtering approaches rely on a severity index which indicates how severe a contingency would affect the system. The severity is measured based on line thermal limits and voltage limit violations. If the severity index is above a certain threshold for a contingency, that contingency is selected to be included in the SCOPF calculations. The severity index calculations depend upon results collected from post-contingency load flow calculations or Lagrange multipliers as in [35,75]. Other contingency filtering methods include neural networks [73], fuzzy sets [72], calculation of eigenvalues [69], fast Fourier transform [64], *etc.* Other legacy methods for contingency selection are based on overload performance indices [15], concentric relaxation [15,76] and bounding [15,77] are not entirely driven towards SCOPF calculations. They are more concerned with establishing bounds

on system variables to preserve the security of the system and with determining the "radii of impact" of contingencies in network space.

Research looking into the characterization of feasible operating regions of electricity networks has been ongoing for over 30 years, with great emphasis on voltage and dynamic stability; see key references [26,75,78–87]. Yet, the formalization of the concept of umbrella contingency was first introduced in [35]. So far, very little specific research has looked into the potential for identifying systematically umbrella contingencies and constraints and their computational saving potential. Most notably, in [75], authors propose a contingency filtering technique by introducing *dominated* and *non-dominated* contingencies. The conjecture is that the larger the violation of a constraint, the more non-dominated that constraint. Reference [87] uses the technique proposed in [75] to reduce the size of SCOPF problems and solve them iteratively. Its authors aim to identify a subset of postulated contingencies which encloses all binding contingencies in order to reduce the size of the corresponding SCOPF and reduce the solution time. Further work in [51] proposes an iterative use of a dc SCOPF approximation of the full ac SCOPF problem in order to reduce the solution time of ac SCOPF problems. Additionally, [52] implements an iterative ac SCOPF solution approach on large-scale systems.

Zhai *et al.* [53] approach the problem of inactive constraint elimination based on a relaxation technique for network-constrained unit commitment, yet without considering contingencies. The work of [88] uses robust optimization as a mean to address the large number of constraints involved when dealing with $n - K$ generation failures on a single-node power system model. Nevertheless, the approach does not consider the outage of network lines and incorporation of such constraints will render the problem intractable. A key feature of all these proposals is that if one changes the SCOPF objective function, the sets of "dominant and dominated" contingencies/binding constraints can change as a

result.

For further reading on the subject, the reader can refer to these review papers [11, 26, 89, 90]. Papers [30, 31, 91] present a review on the challenges of SCOPF problems.

One of the main contributions in this field is [35]. In this work, authors strive to find the contingencies that enclose the feasibility region of the problem. Unlike the methods that were presented before, the results of this work, is independent of the objective function of the SCOPF problem. The work in this dissertation is motivated by findings of [35]. The only drawback the method proposed in [35] was that it failed to find *all* umbrella constraints and those identified required the solution of the full SCOPF problem.

Here we distinguish between the two concepts of *binding* or *active* constraints and that of *potentially binding* or *umbrella* constraints. Binding constraints are those which the optimal solution is located on them. In other words, on the optimum solution, the equality of binding constraints is satisfied [92]. On the other hand, umbrella constraints are those constraints that construct the feasibility region of an optimization problem. These constraints might not be binding for a specific solution which is obtained to minimize or maximize a specific objective function, but they have the "potential" to become binding for a different objective function. Most of the research in power systems is focused on identifying binding constraints in SCOPF and SCUC problems. This approach might be acceptable for a vertically integrated power system, but surely it is not suitable for a deregulated market with high penetrations of renewable energies and stochastic analysis. In such a volatile environment, the objective function of generation scheduling problem may change repeatedly. Therefore, it is needed to run the process of finding the binding constraints of the problem each time the objective function changes. On the other hand, if the potential binding constraints are known, the generation scheduling problem could be run only objected to those constraints and there is no need to re-identify those constraints

every time that the objective function changes. This means significant time savings for system operators which could be used towards making better decisions and give them more time to implement more elaborate control actions. Any improvement in the solution of OPF problems can bring significant savings from the power production costs. If only the solution of OPF problems could be improved by 5%, there will be around 19 billion dollars annual savings, based on 2009 power production statistics in the United States of America [10].

In this research, we propose an optimization-based formulation to identify the umbrella constraints of linearized SCOPF problems. By the same token, we demonstrate that this approach can be used on any convex optimization problem.

1.5 Dissertation Outline

Chapter 2: Umbrella Constraint Discovery

A formulation for the proposed approach for identifying "umbrella constraints" is presented, elaborated and tested in this chapter. In so doing, we introduce the problem for formulation for Umbrella Constraint Discovery (UCD). First, a na ive version of UCD (UCD-I) is presented in details and its difficulties and issues are discussed. Later, a much more efficient formulation to identify umbrella constraints, which we call Umbrella Constraint Discovery II (UCD-II) is presented. This method is applied on several test systems and its efficiency is shown. A decomposition method is introduced to reduce the computational burden of UCD-II. A sensitivity analysis is performed to show the insensitivity of membership of constraints in the umbrella set for wide ranges of load on two sample networks. We conclude this chapter with challenges of the proposed methods.

Chapter 3: Partial Umbrella Constraint Discovery

In this chapter, an approximation of the umbrella constraint discovery problem is intro-

duced to overcome the shortcomings of the original umbrella constraint discovery problems. The new formulation, called *partial* UCD, benefits from a new approach which needs fewer cross-constraint comparisons to identify non-umbrella constraints. Partial UCD is tested on different test systems and its solution time is significantly shorter than UCD-II. Partial UCD can also be used as a complementary tools to many algorithms that try to iteratively identify binding constraints as it can significantly reduce the size of the problems with very little computational effort.

Chapter 4: Application on SCUC

Application of UCD and partial UCD is extended to power generation planning problems with binary variables, namely, security constrained unit commitment (SCUC) problems. It is shown that UCD can significantly reduce the size of SCUC problems as well. We show in this chapter that the structure of SCUC problems is such that they do not contain proportionally as many non-umbrella constraints as SCOPFs. Especially, the generation-based set of constraints of these problems have very few non-umbrella constraints. Other benefits of applying UCD on SCUC problems is investigated in this chapter.

Chapter 5: Prediction of Umbrella Constraints

Given the non-trivial computational requirements of UCD problem solution, in this chapter we explore the possibility of predicting the umbrella set of a given network. We apply a heuristic method based on artificial neural networks to achieve this goal. This is done through a learning process whereby it is used to train the ANN to identify umbrella constraints based on nodal load distribution. The importance of types of prediction errors in neural networks are highlighted and a modified training algorithm for neural networks are introduced. We show that it is indeed possible to exploit the cyclic nature of electric load and consequently umbrella sets for the purpose of predicting umbrella sets.

Chapter 6: Conclusion

This chapter summarizes the main contributions and achievements of this research. Furthermore, future research directions are outlined.

Appendices

In the appendices, the data used for test networks are presented. Also, some of these information are uploaded to a website to be easily accessible for interested researchers.

1.6 Claim of Originality

The following results of this research are the main contributions of the author to the advancement of knowledge:

1. The most significant contribution of this dissertation is the proposal of an optimization-based formulation, called Umbrella Constraint Discovery (UCD). The dissertation provides a clear definition of umbrella and non-umbrella constraints in optimization problems and introduces a formulation for systematic identification of *all* umbrella constraints in any convex optimization problem. Some of the unique aspects of this formulation are the followings:
   (a) This formalization is a linear programming problem and can be easily solved using off-the-shelf linear solvers.
   (b) The Lagrange multipliers of the constraints of this formulation can be used to flag weakly redundant constraints.
   (c) In the process of identifying umbrella constraints, the algorithm provides the geometric "distance" between a non-umbrella constraint and the feasible set of solutions. This distance could be used by operators to know how far a line is from potentially being congested.

(d) Using the proposed formulation, system operators can build an umbrella set of contingencies which contains all possible contingencies that may contribute the umbrella set of constraints. These contingencies are the critical contingencies that the operator should be prepared if any of them were to happen.

(e) If an optimization problem is infeasible, the corresponding UCD problem will also be infeasible. The converse of this statement holds as well.

(f) If the original optimization problem is an MIP, the corresponding UCD problem will convert the original constraints to linear constraints before analyzing them. This feature helps to keep the UCD problem an LP and tractable and at the same time, find the most compact formulation of the original MIP.

(g) This formalization can be used as a benchmark for any other approach which attempts to identify umbrella/binding constraints, since it has been mathematically proven that UCD can identify all of the umbrella constraints in a given convex optimization problem.

(h) This formulation is not exclusive to linear problems. It can be applied to any convex problem.

2. The main feature of UCD is its decomposability. This feature comes very handy in identifying umbrella constraints for large systems where corresponding UCD problems are colossal. The UCD problem is split into sub-problems and the structure of UCD allows to solve the sub-problems independently. This feature favors the use of parallel computation to speed up the solution time of UCD problems. In this work, several decomposition approaches are proposed and the efficiency of these approaches are analyzed. Moreover, recommendations are made with respect to how decomposition should be set up in SCOPF problems. We exploit the problem structure in such a

way that faster umbrella constraint discovery is favoured.

3. An approximation of UCD, called *partial* UCD, is proposed to identify the umbrella constraints much faster. Partial UCD avoids some of the computational inefficiencies in UCD to identify non-umbrella constraints and to pre-screen the constraints before entering UCD. Partial UCD has been applied on different test systems to verify its capabilities.

4. The UCD is applied on problems with binary variables to explore the benefits that UCD can offer in solving Mixed Integer problems (MIPs). UCD can help in strong branching in MIPs. Also, the experience of applying UCD on SCUC shows that the structure of SCUC problems does not contain many non-umbrellas.

5. The dissertation proposes to use artificial neural networks to predict the membership of umbrella sets. The nature of umbrella set membership prediction requires avoiding false negative errors and therefore a custom training algorithm is developed to respond to this need.

Chapter 2

Umbrella Constraint Discovery

This chapter presents in complete details the concepts behind umbrella constraints and umbrella sets in security-constrained optimal power flow problems. We highlight the basic observations that differentiate umbrella and non-umbrella constraints. Subsequently, we present an initial optimization approach for the identification of umbrella and non-umbrella constraints. Later, we discuss the shortcomings and inefficiencies of this formulation. We move on to present a much more efficient formulation for the identification of umbrella constraints which overcomes the shortcomings of the original formulation. Moreover, we propose a decomposition method to expedite the process of identifying umbrella constraints. The proposed formulation is implemented on SCOPF problems associated to different standard test systems. The test results are carefully elaborated and interpreted. These tests provide key evidence of the power of our proposal to allow for much shorter solution times for problems subjected to their umbrella constraints only. Additionally, a sensitivity analysis is performed on two sample test systems to analyze the sensitivity of the umbrella set of an SCOPF problem to changes in system parameters, in this case loads at different network buses. The results of this work also confirms the general expectation that SCOPF

problems have large proportions of non-umbrella constraints.

2.1 Introduction

The level and diversity of uncertainties present in large-scale interconnected electricity transmission and distribution networks are rising steadily. These increases will speed up over the coming years with the massive integration of renewable generation, the electrification of road transport and the continuous ageing of legacy network infrastructures. To better manage these uncertainties while ensuring power system security and to better exploit the potential of the carbon-free electricity from renewable resources, planning and operation tools available for assisting system operators will have to model more explicitly the potential impacts of this wider spectrum of uncertainties. The classic way to address this modeling issue is to formulate the planning problems of the network operators as security-constrained optimal power flow (SCOPF) problems, especially to deal with unplanned generation and transmission equipment outages (*a.k.a.* contingencies) [26]. This modeling approach is undermined by the dimensions of the resulting SCOPF optimization problem formulations stemming from the large-scale nature of power systems, the wide spectrum of potential uncertain events and their associated consequences. Observations made in previous work [34, 35] and operator experience showed that only a few of the constraints associated with the different contingencies modeled within SCOPF problems have the potential to be of importance in their final solution. This led to the proposal for the definition of what we call an "umbrella contingency" [35]. Umbrella contingencies are those abnormal operating states which are together sufficient to provide security cover for all other abnormal states. The set of umbrella contingencies, and by extension the set of umbrella constraints, defines the minimum set of constraints describing the feasible set of

the problem over which it is sufficient to solve the SCOPF to achieve the same original secure full SCOPF solution. There is considerable potential for computational improvements in the solution of SCOPF problems if they are subjected to much reduced sets of constraints which only correspond to those of the umbrella constraints. The computational improvements should be in terms of core memory and in potential solution speed-ups.

This dissertation contributes to the field of SCOPF computation by introducing two formulations for the umbrella constraint discovery (UCD) problem, which finds the *complete set* of umbrella constraints as a *pre-processing step to the SCOPF solution*. One UCD formulation is based on mixed-integer linear optimization and the second, which is much more efficient, is a linear program. We introduce a convergent decomposition technique for solving the UCD problem. We validate the potential of UCD in streamlining SCOPF solution processes, where we show for the IEEE 118 bus test system [93] a potential SCOPF constraint count reduction of 99.31% leading to an SCOPF solution time representing 0.57% of the solution time with its original full set of constraints. Finally, we use the IEEE Reliability Test System—1996 (RTS) [94] to show that UCD outcomes are relatively insensitive to SCOPF parameter variations, with UCD results remaining valid over wide ranges of system load, and where umbrella set membership is correlated to system demand. We argue that the latter properties allow for umbrella sets to be pre-calculated offline and/or reused when systems are planned under sets of similar conditions.

In this formulation, we do not rely on any heuristic, as in some of the methods in the literature, to assess whether or not a network constraint has the potential to impact network operation. UCD can determine systematically all the constraints the network operator must consider. In fact, UCD could be used to validate the results of heuristic contingency screening methods, as it can determine if a flagged contingency truly does contribute constraints towards the umbrella set or not. On the other hand, contingency

screening methods could be used in conjunction with UCD to reduce its computational burden by potentially reducing the number of constraints UCD has to assess in the first place.

In the next section, we formulate the SCOPF problem that we will be using in this dissertation.

2.2 Preventive SCOPF

Preventive and corrective controls are two main operational paradigms to shield power systems against contingencies. In this dissertation, we will only consider outages of lines as postulated contingencies. Moreover, we use preventive control to model the system without loss of generality. As will be shown later in this chapter, the proposed method can be applied on any convex optimization problem.

The goal of the preventive SCOPF problem is to find the dispatch levels for each generating unit such that the operational cost of a network is minimized while all relevant technical constraints corresponding to pre- and post-contingency states are satisfied simultaneously. Here, only branch contingencies can be considered, as purely preventive control actions cannot properly deal with losses of generation or demand variations—corrective generation-based actions are always needed after such contingencies in order to rematch the system load. Therefore, the optimal values of the control variables, generation levels here, are to remain constant following the occurrence of any credible line or transformer contingency. In most instances of preventive SCOPF problems [1], the network technical constraints include: (i) the system power balance; (ii) generation upper and lower production limits; and, (iii) line flow limits enforced on the basis of the dc power flow both in pre-

1. In the remainder of this dissertation, the acronym SCOPF refers to the preventive SCOPF, unless otherwise stated.

and post-contingency states. Other control variables and constraints could be included, like phase shifter set points and unit commitment decisions as well as their corresponding constraints. Without loss of generality here and for the sake of brevity, we shall not include those in this work. The focus of this work is the simplification of the SCOPF formulation, which we hypothesize should have a positive impact on its solution process. Additionally, in Chapter 4, we apply UCD on unit commitment problems and we investigate the benefits of applying UCD on those problems.

2.2.1 SCOPF Problem Formulation

The SCOPF objective function shown in (2.1) generally minimizes the cost of operation

$$\min_{p} \sum_{i=1}^{I} C_i(p_i) \tag{2.1}$$

where $C_i(\cdot)$ is the generation cost function at bus i, p_i the generation level at bus i, and I is the number of network buses. The above objective function is subjected to the system-wide load balance, for which we ignore losses here,

$$\sum_{i=1}^{I} p_i = \sum_{i=1}^{I} d_i \tag{2.2}$$

and where d_i is the load at bus i. Generation levels have to be bounded at each node $i = 1, \ldots, I$ as well

$$\underline{p}_i \leq p_i \leq \bar{p}_i \tag{2.3}$$

Here $\underline{p}_i$ and $\bar{p}_i$ are respectively the lower and upper dispatch limits of generation at bus i.

In addition, there are two constraints associated with each transmission line: one associated with its upper limit and the other with its lower limit. Each line limit constraint pair

has to be included to bound the line usage in all pre- and post-contingency states. Hence, for all lines in the network, $\ell = 1, \ldots, L$, and for all line contingency states, $k = 0, \ldots, K$, the SCOPF solution has to satisfy

$$-\bar{f}_\ell(k) \leq \sum_{i=1}^{I} h_{\ell i}(k)(p_i - d_i) \leq \bar{f}_\ell(k) \tag{2.4}$$

where L is the number of lines of the network, $\bar{f}_\ell(k)$ is the upper limit of line ℓ in contingency state k, and $h_{\ell i}(k)$ is the linear generation shift factor (*a.k.a.* power transmission distribution factor (PTDF)) relating power injection at bus i to the flow in line ℓ while contingency state k is occurring [15,32]. We point out that contingency state $k = 0$ corresponds to the pre-contingency, *i.e.* normal operating condition. For ease of exposition here, we shall consider contingency states k where a single transmission component is down ($N-1$ security); however, this can be generalized to multiple component contingencies ($N-m$ security).

2.2.2 Compact Formulation

We can convert all of the constraints, (2.2)–(2.4), to "less than or equal" form. In order to convert the system-wide load balance, (2.2), which is an equality constraint, to the "less than or equal" form, we first convert the constraint to two inequalities, one in the form of "less than or equal", (2.5), and the other one in the form of "greater than or equal", (2.6).

$$\sum_{i=1}^{I} p_i \leq \sum_{i=1}^{I} d_i \tag{2.5}$$

$$-\sum_{i=1}^{I} p_i \geq \sum_{i=1}^{I} d_i \tag{2.6}$$

For notational conciseness, we shall consider the SCOPF formulation, (2.1)–(2.4), in

the following compact form

$$\min f(p) \tag{2.7}$$

subject to

$$Ap \leq b \tag{2.8}$$

where p is a vector of dimension $I \times 1$ lumping all of the network's bus-wise generation levels, $f(p)$ is some objective function, A is a constant matrix with dimensions $J \times I$, and b is a constant vector with dimensions $J \times 1$, where $J = 2 + 2I + 2(L + K(L-1))$. The horizontal dimension of A corresponds to the number of buses in the network, I, while its vertical dimension (as well as that of b), J, corresponds to (i) two rows standing in for the power balance (2.5) and (2.6); (ii) $2I$ rows for the upper and lower generation limits (2.3); and, (iii) $2(L+K(L-1))$ rows for all the line limits in both pre- and post-contingency states (2.4).The objective function, $f(p)$ is immaterial in the proposed formulation. Therefore, it could be an arbitrary function such as the system operation cost, maximum flow on a transmission line, network losses, *etc.*

The number of constraints for the corresponding SCOPF problem of the IEEE Reliability Test System—1996 (RTS) [94] accumulates to 2 864 constraints. The network has 24 buses and 38 lines. We consider the outages of each line as postulated contingency of the system, except for line 11 [2]. Each line contributes two constraints in both no-contingency state and each contingency state of the system. Obviously, the line that we are considering its outage will not contribute any constraint to the problem. The constraints arising from the operation of lines will total to 2 816 constraints. There will be 48 constraints to limit the lower and upper limits of power at each bus. Finally, there are two constraints to ensure the system-wide load balance, (2.5) and (2.6). We can see that most of the constraints are

2. The reason for this will be explained in details in Section 2.7.1

coming from line constraints and their operation in contingency states. Therefore, for a network with a large list of postulated contingencies and large number of lines, the size of SCOPF problems could easily make the problem intractable and significantly increase the solution time.

2.3 Umbrella Constraints and Umbrella Sets

The size of SCOPF problems is usually the biggest challenge in solving them in large practical networks (*i.e.* with large I and L). Imposing all pre- and post-contingency constraints at the same time can make the SCOPF calculations significantly arduous and may lead to memory shortage and CPU time overruns [26]. It is common knowledge that in SCOPF problems most of the constraints are not essential in constructing the problem's set of feasible solutions and, consequently, are irrelevant in finding the optimal solution [26,35]. These non-essential constraints always remain non-binding (inactive), but they do contribute to the use of memory and CPU time during the solution process. Hence, the hypothesis here is that by identifying and removing these unnecessary constraints before solving an SCOPF problem, one should be able to increase numerical stability of the solution process and find a solution using fewer computing resources.

This observation and hypothesis lead us, following the general idea of [35], to define the concepts of *umbrella constraint* and *umbrella set*:

Definition 1 (Umbrella constraint) *Let $\mathcal{J}$ be the set of indices corresponding to all the constraints (rows) of an optimization problem formulated as* (2.7) *and* (2.8)*, and let $j \in \mathcal{J}$. Constraint (row) j is an umbrella constraint of $\mathcal{J}$ if and only if removing it from $\mathcal{J}$ alters set of feasible solutions of the original optimization problem.*

Definition 2 (Umbrella set) *The umbrella set $\mathcal{U} \subseteq \mathcal{J}$ of an optimization problem is*

the set containing the minimum *number of constraints (rows) necessary to form its set of feasible solutions. Removing any member of the umbrella set* $\mathcal{U}$ *would alter the set of feasible solutions of the original optimization problem, while adding any of the constraints in the non-umbrella set,* $\overline{\mathcal{U}} \subseteq \mathcal{J}$*, for which* $\mathcal{U} \cap \overline{\mathcal{U}} = \emptyset$ *and* $\mathcal{U} \cup \overline{\mathcal{U}} = \mathcal{J}$*, would not change the set of feasible solutions.*

Here the term "umbrella" implies that some constraints provide "cover" for other less stringent constraints. Umbrella constraints are also sometimes called "necessary" constraints in the optimization literature [40]. Solving an optimization problem constrained by its umbrella set only would result in the same set of feasible solutions as the original problem and the same optimal solution (for the same objective function). In fact, the umbrella set of an optimization problem is independent from its objective function. This leads us to underline that, unlike in [35], umbrella constraints do not have to be binding (active) at the optimum of an optimization problem, while binding (active) constraints have to be in the umbrella set, by necessity. In fact, umbrella constraints are the only constraints that have the "potential" to be binding. Some of the umbrella constraints might not be binding for a specific objective function; however, if the objective function and consequently the optimal solution changes, these constraints might become binding. We recall that in [35] only binding constraints were deemed to form the set of umbrella constraints. The fact that constraints' Lagrange multipliers were nonzero at the optimal solution of an SCOPF problem was used as the litmus test for classifying constraints as umbrella. That approach was practically sound; however, it failed to identify *all* the members of the umbrella set, while it required that the full SCOPF problem be solved first to obtain its Lagrange multipliers. The fact that the umbrella set is independent of the objective function, makes this work more valuable for cases where the same set of constraints are used for different

objective functions, *e.g.* applications in big ISOs where markets are cleared repeatedly over the same network.

The umbrella constraint and set concepts are illustrated in Fig. 2.1, for an optimization problem in two variables with six linear constraints. It can be seen that this is a feasible problem and the feasible set of solutions is indicated by the coloured area. By inspection of Fig. 2.1, one can see that constraints 5 and 6 do not contribute in shaping the feasible region of the problem. Their presence or lack thereof would not make any difference, and they could simply be ignored. Constraints 1–4, on the other hand, are essential to describe the interior of the feasible region. Eliminating any of these constraints would change the problem's feasible set and could lead to a change of the optimal solution; therefore, they form the umbrella set for this problem. It is worth emphasizing that there is a difference between an umbrella constraint and a binding (active) constraint. Binding constraints are part of the umbrella set out of necessity. However, if a constraint is in the umbrella set, it does not need to be binding at the optimum. The binding character of a constraint is established by subjecting the umbrella set to the problem's objective function. For example, we can see from Fig. 2.1 that constraints 1–4 are umbrella, but only constraints 2 and 3 are binding, since the optimum solution, shown by the dot, is located at the intersection of these two constraints. All other constraints are non-binding (including 1 and 4, which are umbrella).

Because the number of constraints contained in umbrella sets for practical SCOPF problems is usually much smaller than that of their original counterparts, we expect that solving SCOPF problems subjected to their umbrella sets only could save on memory and CPU time. Now the question is: How can we find the umbrella set for any SCOPF problem formulated as in (2.7) and (2.8)? We provide an answer in the next section.

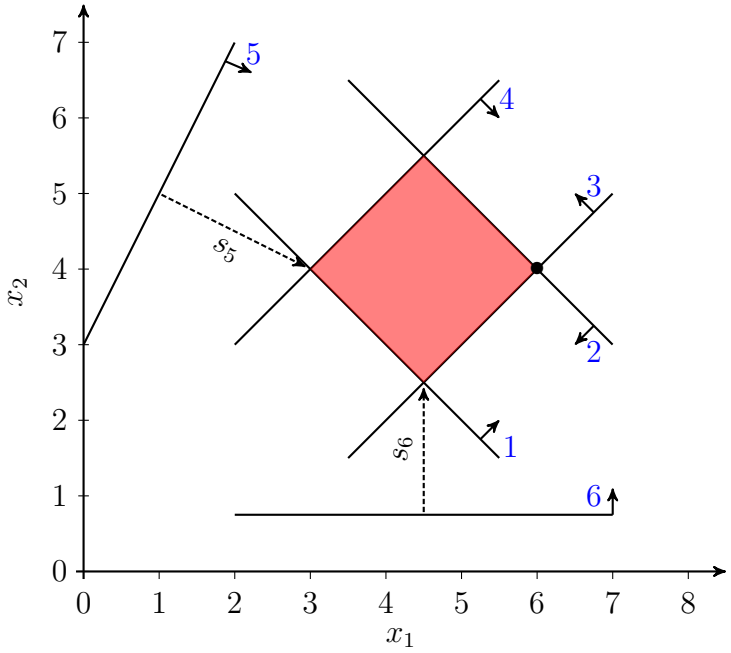

Figure 2.1 Umbrella and non-umbrella constraints; binding and non-binding constraints. Numbered arrows show the direction of the feasible half-planes induced by individual constraints.

2.4 Identifying Umbrella Constraints

For an optimization problem with J linear constraints, as formulated in (2.7) and (2.8), the brute force answer to the above question is to consider the $2^J - 1$ possible umbrella sets and proving that each of them is either umbrella or not. This approach is obviously counterproductive for practical SCOPF problems. In this dissertation, we propose and demonstrate the validity of a much more efficient optimization approach for identifying the members of the umbrella set of linearly-constrained SCOPF problems. However, the formulation is easily applicable to any convex optimization problem.

2.4.1 Preliminaries

In this section, we give the preliminary observations that led to the proposal of an effective formulation for identifying umbrella constraints. What sets apart umbrella and non-umbrella constraints come from the following two observations: we observe that *there is always at least* one point *lying on an umbrella constraint that is feasible with respect to all other constraints in a linear SCOPF problem.* In other words since the umbrella constraints are the most inner constraints, in a feasible optimization problem (*i.e.* non-empty feasible set of solutions), they will always satisfy all other constraints, including other umbrella constraints. When a point *lies on* on a constraint, it means that the inequality constraint is being satisfied with equality. Also, we observe, in the case of a non-umbrella constraint, that *there is* no single point *available on the constraint that can be feasible with respect to all other constraints of the problem.* We would like to point out that we might be able, under special circumstances, to find points on non-umbrella constraints that satisfy all other constraints *individually*; however, there is no point on non-umbrella constraints that can satisfy all other constraints, especially all umbrella constraints *simultaneously.*

In Fig. 2.1 for example, we can find at least one point on constraint 1 that satisfies all the other constraints, including all umbrellas *i.e.* constraints 2–4, and non-umbrellas, *i.e.* constraints 5 and 6. Otherwise, picking constraint 6, which is non-umbrella, we are not able to find any point on that constraint that is feasible with respect to all the other constraints simultaneously.

These two observations form the basis of the initial idea for the classification of umbrella/non-umbrella constraints implemented next.

Let a_j denote the vector corresponding to the j^{th} row of matrix A and b_j the j^{th} element of the b vector of the system of inequalities in (2.8). Let us also define an arbitrary vector

$\mathbf{w}_j \in \mathbb{R}^I$. We claim that constraint j is umbrella if and only if there exists a point $\mathbf{w}_j$ which lies on the hyperplane $\mathbf{a}_j^T\mathbf{w}_j = b_j$ and is consistent with respect to all constraints $j' = 1, \ldots, J$, *i.e.* $\mathbf{w}_j$ satisfies $\mathbf{a}_{j'}^T\mathbf{w}_j \leq b_{j'}$ for all j'.

Proposition 1 (Umbrella Constraint Discovery I (UCD-I)) *Let $u_j \in \{0, 1\}$, for all $j = 1, \ldots, J$, satisfy the assignment*

$$u_j = \begin{cases} 0, & \textit{if constraint } j \textit{ is umbrella} \\ 1, & \textit{otherwise.} \end{cases} \tag{2.9}$$

Solving the following mixed-integer mathematical program determines the set of umbrella constraints of problem (2.7), (2.8)

$$\min_{\mathbf{w}, u \in \{0,1\}^J} \sum_{j=1}^{J} u_j \tag{2.10}$$

subject to, for all $j = 1, \ldots, J$,

$$\mathbf{a}_{j'}^T\mathbf{w}_j \leq b_{j'} \qquad j' = 1, \ldots, J \tag{2.11}$$

$$(1 - u_j)\mathbf{a}_j^T\mathbf{w}_j \geq (1 - u_j)b_j \tag{2.12}$$

where $\mathbf{w} \in \mathbb{R}^{IJ}$ and $\mathbf{w}_j \in \mathbb{R}^I$. The interpretation of UCD-I above goes as follows: the lower bound on the objective function (2.10) is 0, which corresponds to the case where all constraints in (2.8) are umbrella. If constraint j is indeed umbrella ($u_j = 0$) then (2.11) and (2.12) can be satisfied simultaneously thus implementing the rule on the existence of a consistent $\mathbf{w}_j$ stated in opening of this section. In that case, $\mathbf{w}_j$ can lie on the hyperplane $\mathbf{a}_j^T\mathbf{w}_j = b_j$, as implemented by the combination of (2.11) for $j' = j$ and (2.12) for j. In

that case, the point $\mathbf{w}_j$ also happens to be feasible with respect to all the other constraints $j \neq j'$ of (2.11). Otherwise, if constraint j is not umbrella, the only way the above problem can remain feasible is if u_j is set to 1, effectively removing the j^{th} constraint from (2.12).

We note that UCD-I is a nonlinear mixed-integer problem due to the presence of the products $(1 - u_j)\mathbf{a}_j^T\mathbf{w}_j$. Nonetheless, it is well-known that such products of binary and continuous variables can be linearized at the expense of more constraints and auxiliary continuous variables [95]. Hence, UCD-I can be transformed into a mixed-integer linear program (MILP) for which good commercial solvers are available. It remains, however, that UCD-I itself is not a trivial problem, first because of its combinatorial nature—MILPs are NP-complete in theory [92]—and second because of its large size—it has $J(J + 1)$ constraints, IJ continuous and J binary variables. It is trivial to parallelize solution of UCD-I since the problem can be separated across $j \in J$.

2.4.2 Efficient Umbrella Constraint Discovery

Given the obvious drawbacks of UCD-I, we demonstrate next that the above problem formulation can be recast as a much more computationally-efficient linear program. For that purpose, we now define a new set of variables $s_j \in \mathbb{R}_+$ for $j = 1, \ldots, J$.

Proposition 2 (Umbrella Constraint Discovery II (UCD-II)) *Let $s_j \geq 0$, for all $j = 1, \ldots, J$, satisfy the assignment*

$$s_j = \begin{cases} 0, & \textit{if constraint } j \textit{ is umbrella} \\ > 0, & \textit{otherwise.} \end{cases} \tag{2.13}$$

Solving the following linear program (LP) determines the set of umbrella constraints of

(2.7), (2.8)

$$\min_{\mathbf{w}, s \geq 0} \sum_{j=1}^{J} s_j \tag{2.14}$$

subject to, for all $j = 1, \ldots, J$,

$$\mathbf{a}_{j'}^T \mathbf{w}_j \leq b_{j'} \qquad\qquad j' = 1, \ldots, J \tag{2.15}$$

$$\mathbf{a}_j^T \mathbf{w}_j + s_j \geq b_j \tag{2.16}$$

The interpretation of UCD-II is quite similar to that of UCD-I. If all constraints are umbrella, then $s_j = 0$ for all j, thus achieving the lower bound of the objective function. If a constraint j is truly umbrella ($s_j = 0$) then (2.15) and (2.16) can be satisfied together, meaning that there exists a $\mathbf{w}_j$ that can lie on the hyperplane $\mathbf{a}_j^T \mathbf{w}_j = b_j$ while still remaining feasible with respect to all the other constraints $j' \neq j$. In the opposite case, to maintain feasibility of the whole problem, we have to increase the value of s_j until we can find a value of $\mathbf{w}_j$ which can lie on the (geometrically-translated) hyperplane $\mathbf{a}_j^T \mathbf{w}_j = b_j - s_j$ while satisfying all other constraints in (2.15). In fact, the slack variables s_j serve to virtually bring all non-umbrella constraints into the umbrella set as a way to ensure the feasibility of UCD-II. This is unlike in UCD-I where the binary variable u_j effectively removed the requirement for $\mathbf{w}_j$ to lie on $\mathbf{a}_j^T \mathbf{w}_j = b_j$ as a mean to keep the problem feasibility. Lastly, the objective function (2.14) ensures that the least amount of constraint translation is performed to ensure global UCD-II problem feasibility and solution uniqueness.

It is interesting to attempt to interpret the meaning of the variables s_j in UCD-II. One can see s_j as the minimum distance to cover for constraint j to "enter" the umbrella set. For example, consider the arrows labeled s_5 and s_6 in Fig. 2.1. These arrows show the direction and the distance to cover when translating constraints 5 and 6 to have them join the

umbrella set already formed by constraints 1–4. The optimal values s_j^* and their sensitivities (*e.g.* $\partial s_j^*/\partial b$) could serve to predict under which conditions particular constraints become members of the umbrella set or end up leaving it.

2.4.3 Some Remarks

Computational Complexity of UCD-II

UCD-II is an LP, and, as LPs can be solved in polynomial time [92], this reformulation represents a major computational improvement over UCD-I. However, UCD-II is much larger than the original SCOPF problem in (2.7), (2.8) (which is also an LP). UCD-II has $J(I+1)$ variables and $J(J+2)$ constraints, as opposed to I variables and J constraints for the SCOPF. Therefore, even for small power systems, the dimensions of UCD-II become unmanageable. For example, UCD-II for the small-sized IEEE 118 bus standard test system [93]—with $I = 118$ and $J = 65\,730$ when implementing $N-1$ security—cannot be solved directly. We demonstrate how to overcome this difficulty in Section 2.5 through the introduction of a decomposition approach.

UCD-II Infeasibility and Solution Uniqueness

It is worth noting that if the original SCOPF is infeasible, so is UCD-II and vice-versa. This is because the constraints of the SCOPF, (2.8), are effectively contained in UCD-II (represented therein by (2.15)). Moreover, UCD-II solutions are always unique in spite of the fact that the original SCOPF may have duplicate constraints—for example, when the SCOPF contains line flow limits for identical parallel lines. Duplicate constraints should always be umbrella or non-umbrella together.

Generality of UCD-II

As a final remark, we underline the general applicability of UCD-II for identifying umbrella constraints in mathematical programs. First, UCD-II can be applied to linear optimization problems with discrete decision variables. This is because what really matters in terms of umbrella constraint set membership are the coefficients of the matrix A and the right-hand side vector b in (2.8). In fact, by solving UCD-II on the constraint set of a pure integer program (IP), one can obtain the feasible space closest to the IP's convex hull prior to the calculation of cutting planes. We will discuss the application of UCD-II on problems with integer variables in Chapter 4.

In addition, UCD-II can be formulated and solved if the set of constraints of the original optimization problem describes a convex set. In other words, solving

$$\min_{w,s\geq 0} \sum_{j=1}^{J} s_j \tag{2.17}$$

subject to, for all $j = 1, \ldots, J$,

$$g_{j'}(\mathbf{w}_j) \leq 0 \qquad\qquad j' = 1, \ldots, J \tag{2.18}$$

$$g_j(\mathbf{w}_j) + s_j \geq 0 \tag{2.19}$$

finds the set of umbrella constraints if subsets $\{x \in \mathbb{R}^N : g_j(x) \leq 0\}$ are convex for each $j = 1, \ldots, J$. This claim is true as both the constraint set and the objective of (2.17)–(2.19) are also convex.

2.5 Decomposition

It is clear from the above discussion that UCD-II, in spite of being formulated as an LP, is still intractable for practical SCOPF problems. We saw that the size of the UCD-II problem can grow intractably large. We noticed that the process of finding umbrella constraints can be broken down into smaller sub-problems. In fact, we demonstrate next that UCD-II lends itself well to decomposition, especially as applied to the SCOPF problem.

2.5.1 Separation

By inspection of (2.14)–(2.16), we find that UCD-II is separable because both s_j and $\mathbf{w}_j$ can be solved for independently of any other $s_{j'}$ and $w_{j'}$, $j \neq j'$. Hence, by solving the following problem independently for each $j = 1, \ldots, J$ we can uncover the set of umbrella constraints

Proposition 3 (Separated UCD-II (S-UCD-II))

$$\min_{\mathbf{w}_j, s_j \geq 0} s_j \tag{2.20}$$

subject to

$$\mathbf{a}_{j'}^T \mathbf{w}_j \leq b_{j'} \qquad j' = 1, \ldots, J \tag{2.21}$$

$$\mathbf{a}_j^T \mathbf{w}_j + s_j \geq b_j \tag{2.22}$$

where $\mathbf{w}_j \in \mathbb{R}^I$. The problem (2.20)–(2.22) has $I+1$ variables and $J+1$ constraints, which is essentially the same size as the original SCOPF, (2.7)–(2.8), and it can be solved for each instance $j = 1, \ldots, J$ by running J parallel linear optimizations. This natural decomposition for UCD-II is obviously welcome. However, the number of separated subproblems is

large for practical SCOPF problems, and the theoretical computational complexities associated with solving the SCOPF and the separated UCD-II are essentially the same. This lukewarm progress thus prompts a further consideration of the structure of the SCOPF and its impact on the solution of UCD-II.

2.5.2 Divide-and-Conquer

The bulk of the constraints contributing to increasing the size of the SCOPF and UCD-II problems come from the line flow constraints (2.4); there are $2(L+K(L-1))$ of them in the SCOPF and the S-UCD-II problems. The proposal here is to partition the set of line flow constraints present in UCD-II in a classic divide-and-conquer optimization approach [96]. The divide-and-conquer optimization approach we are proposing for UCD-II relies on the following principle:

Lemma 1 (Non-Umbrella Constraint Lemma) *If constraint $j \in \tilde{\mathcal{J}}$, where $\tilde{\mathcal{J}} \subseteq \mathcal{J}$, is found to be non-umbrella when solving UCD-II for the set of constraints $\tilde{\mathcal{J}}$ then constraint j is also found to be non-umbrella when solving UCD-II for the full set of constraints $\mathcal{J}$.*

This principle is easily proved assuming that constraint j is indeed in the umbrella set of $\mathcal{J}$. It follows that if this is the case, j would also need to be umbrella when solving UCD-II over $\tilde{\mathcal{J}}$. This is because if it is to survive the UCD-II solution process, constraint j has to be umbrella for all subsets of $\mathcal{J}$. This is in contradiction of the initial premise and thus completes the proof. We note also that the converse of this lemma is not true, *i.e.* if $j \in \tilde{\mathcal{J}}$ is umbrella, j is not necessarily umbrella for $\mathcal{J}$.

The corollary of this principle is that if a constraint is found to be non-umbrella when we solve UCD-II over a subset of $\mathcal{J}$ then it is non-umbrella for the full set of constraints. This motivates the following algorithm:

Step 1: Partition the full set of constraints $\mathcal{J} = \{\mathcal{J}_1, \ldots, \mathcal{J}_M\}$ into a set of computationally-manageable constraint blocks and solve UCD-II for each of those. The UCD-II step can be executed by parallel processors.

Step 2: Recombine the umbrella constraints generated by the solution of UCD-II into computationally-manageable constraint blocks and solve UCD-II for each of those (again this can be done over parallel processors).

Step 3: Repeat Step 2 until the solution of a single UCD-II problem is obtained or when a required constraint number reduction goal is attained.

The main issues one has to consider for using the above procedure is the initial partitioning of the constraint set (in Step 1) and the way by which constraints get recombined (in Step 2). Here the goal is to set up constraint blocks large enough to ensure maximum non-umbrella constraint discovery while not overrunning memory and CPU time limitations.

One very important note is that the s variables obtained by solving an S-UCD-II problem do *not* have the same values as the s variable values if the UCD-II problem were to solved directly.

In the next section, we discuss the relative merits of two partitioning approaches for the SCOPF. There are in fact a large number of possible partitions; however, we posit that those which exploit best the SCOPF problem structure should be more successful. Recombination is a secondary issue if the initial partition was properly chosen; this is the reason why we do not address this matter in detail in this research.

2.5.3 Partitioning

Let us then partition the index set of SCOPF constraints as $\mathcal{J} = \{\mathcal{J}_\pi, \mathcal{J}_\lambda\}$. Subset $\mathcal{J}_\pi$ corresponds to the set of SCOPF constraint indices related to the power balance (2.2) and the generation limits (2.3), while $\mathcal{J}_\lambda$ is the subset of indices corresponding to the line flow limits (2.4). The constraints in $\mathcal{J}_\pi$ apply in each of the possible contingency states. On the other hand, the constraints in $\mathcal{J}_\lambda$ do depend on the contingency state and may be further partitioned along that dimension such that $\mathcal{J}_\lambda = \{\mathcal{J}_\lambda(0), \ldots, \mathcal{J}_\lambda(K)\}$, where $\mathcal{J}_\lambda(k)$ corresponds to all line flow limits associated with contingency state k. Likewise, $\mathcal{J}_\lambda$ can be partitioned on a line index basis regardless of contingency state, $\mathcal{J}_\lambda = \{\mathcal{J}_\lambda^1, \ldots, \mathcal{J}_\lambda^L\}$, where $\mathcal{J}_\lambda^\ell$ groups all constraints associated to line ℓ for all contingency states.

For most power systems, the cardinality of $\mathcal{J}_\pi$ is smaller than that of $\mathcal{J}_\lambda$ (compare $2+2I$ for $\mathcal{J}_\pi$ to $2(L + K(L-1))$ for $\mathcal{J}_\lambda$). The cardinalities of subsets $\mathcal{J}_\lambda(k)$ are $2L$ for $k = 0$ and $2(L-1)$ for $k \geq 1$, while that of $\mathcal{J}_\lambda^\ell$ is $2(K+1)$. Hence, the sizes of either $\mathcal{J}_\lambda(k)$ or $\mathcal{J}_\lambda^\ell$ are essentially the same when the SCOPF problem is enforcing $N-1$ security. Under special circumstances where outage of a line, say line j, is not considered for any reason, the cardinality of $\mathcal{J}_\lambda^\ell, \ell = j$ is larger than $\mathcal{J}_\lambda^\ell, \ell \neq j$. For such networks, the number of contingencies are smaller than the number of lines and therefore, the cardinality of $\mathcal{J}_\lambda(k)$ is smaller than $\mathcal{J}_\lambda^\ell$.

Contingency-Based Partitioning

Under a contingency-based partitioning, a UCD-II subproblem solved in Step 1 of the solution algorithm considers the SCOPF constraints associated with the power balance and generation limits, $\mathcal{J}_\pi$, on top of the constraints corresponding to line limits associated with operation under contingency k, $\mathcal{J}_\lambda(k)$. We combine each subset with $\mathcal{J}_\pi$ with the hope to

maximize the number of identified non-umbrella constraints.

Contingency-based decomposition is an intuitively attractive partition because of the natural decoupling between different contingency states. However, it is not as computationally effective as line-based partitioning (introduced below) because it tends to let through many more potential umbrella constraints in the first and in each successive iterations. It fails to generate large numbers of non-umbrella constraints, those which have the advantage of not having to be considered in the following iterations. For instance in Step 1, the UCD-II subproblems are finding all the line limits applying to each contingency considered in isolation, and they should be flagging a large proportion of line limits as umbrella because the operation of each line in the network is limited. In other words, we need to compare constraints arising from operation of a specific line in different contingency states against each other rather than comparing constraints of different lines in each contingency state k. This idea is the basis for line-based partitioning introduced below.

Line-Based Partitioning

Under a line-based partitioning, a UCD-II subproblem solved in Step 1 of the solution algorithm considers the SCOPF constraints associated with the power balance and generation limits, $\mathcal{J}_\pi$, on top of the constraints corresponding to the limits on line ℓ under each of the contingency states, $\mathcal{J}_\lambda^\ell$. This partitioning is much more effective than its contingency-based counterpart because it generates relatively large numbers of non-umbrella constraints at each step. This property stems from the fact that usually only a few contingencies lead to lines reaching their limits. Schematically, with this partitioning it is as if we are ranking up all the constraints applying to a given line over the set of contingency states and picking the most stringent ones as umbrellas while rejecting all the others as non-umbrella. The results in Section 2.7 demonstrate very well how line-based partitioning is most effective.

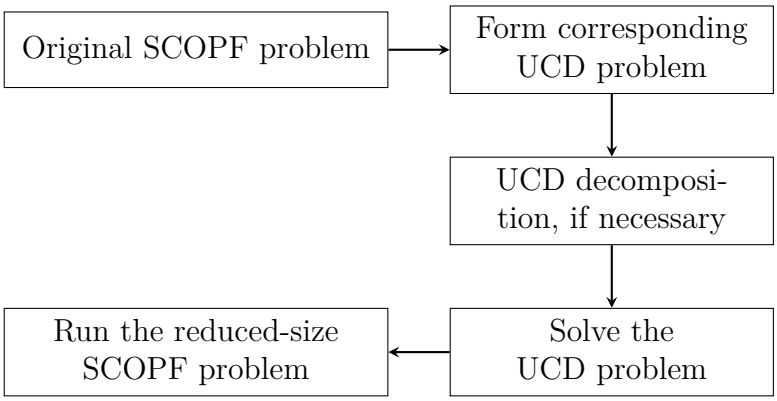

Figure 2.2 Flowchart showing the necessary steps for applying UCD on SCOPF problems

Other approaches are possible—*e.g.* random partitioning—; however, they all perform poorly when compared to line-based partitioning.

2.6 Three-Bus Example

In this Section, we demonstrate the workings of UCD problems using the three-bus power system in Fig. 2.3. We formulate the preventive dc power flow-based SCOPF as in (2.1)–(2.4) with $N-1$ security (considering the loss of each line, for a total of four contingencies). All lines have the same per unit series reactance while line capacities ($\bar{f}_\ell$) are 100, 100, 60 and 80 MW respectively for lines $\ell = 1, \ldots, 4$. The objective function is linear in the generation levels, $\sum_{i=1}^{3} c_i p_i$, where the marginal costs c_i and other generation parameters are given in Table 2.1.

Table 2.1 Generation Parameters

i	c_i (\$/MWh)	$\underline{p}_i$ (MW)	$\bar{p}_i$ (MW)
1	20	100	250
2	40	20	100
3	50	0	50

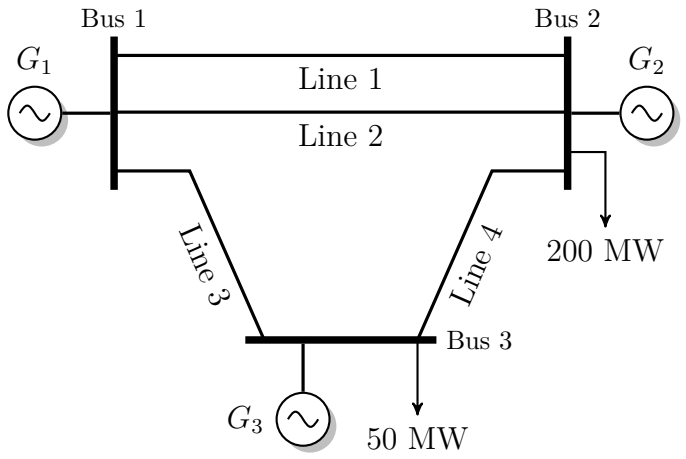

Figure 2.3 Three-bus system.

The number of constraints for this very simple SCOPF problem already reaches 40 (two inequalities for the power balance, six for the generation limits and 32 to represent the line limits in both pre- and post-contingency states). Solving UCD-II without any decomposition requires solving an LP with 1 680 constraints and 160 variables which runs in negligible time on a quad core 2.13 GHz Intel Xeon CPU with 24.0 GB of RAM using the ILOG CPLEX 12.4 LP solver called by GAMS [97]. The UCD-II solution indicates that only nine constraints are umbrella and thus necessary and sufficient to describe the feasible set of the original SCOPF problem. Hence, 77% of the constraints are non-umbrellas and can be ignored. The feasible set of solutions of this network with the given loads is shown in Fig. 2.4. Note that we are showing a projection of the feasible set of solutions here. Hence, we cannot see all of the umbrella constraints in this figure.

The set of umbrella constraints splits as follows: without much surprise two come from the power balance (not shown in the figure) three come from generation limits (lower limit on generator 1 (not shown in the figure) and upper limits on generators 2 and 3) and four from line constraints (upper limits on lines 2 and 3 as line 1 is out and upper limits on

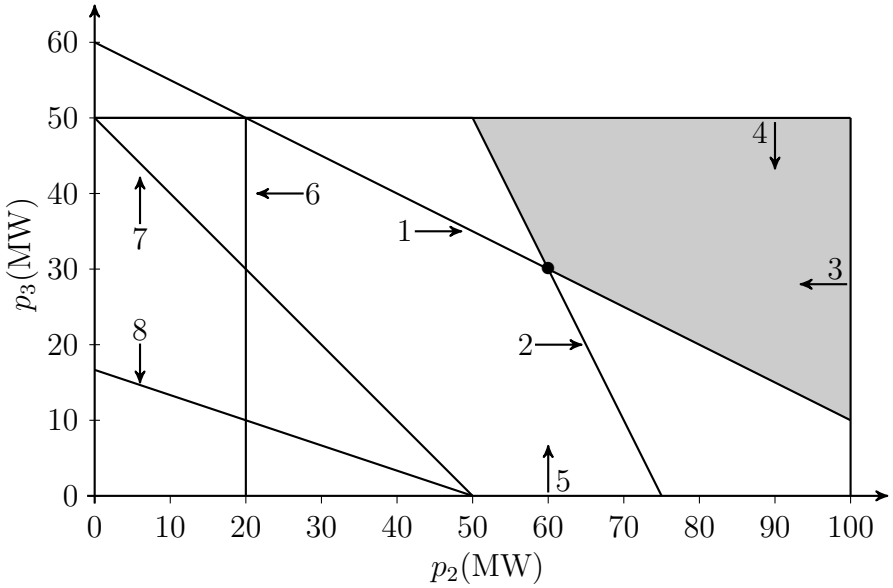

Figure 2.4 Feasibility set of solutions for three-bus system. The optimal solution is shown by the dot.

lines 1 and 3 as line 2 is out). In Fig. 2.4, line 1 represents upper limit of transmission line 3 during outage of line 1 as well as upper limit of transmission line 4 during outage of line 2. The line labeled 2 represents upper limit of line 2 during outage of line 1 as well as upper limit of line 1 during outage of line 2. Lines labeled as 3 and 4 represent upper limits of generators 3 and 2, respectively. Lines labeled 5 and 6 represent the lower limit of generators 3 and 2, respectively. The line labeled 7 represents the upper limit of transmission line 1 during outage of line 3 as well as the upper limit of line 2 during outage of line 3. The line labeled 8 is representing the upper limit of line 3 in no-contingency state.

Generator 1 is assumed to be the slack bus and therefore it is not shown in Fig. 2.4. Generator 1 is supplying the difference between the system load and the generation by generators 2 and 3 which amounts to 160 MW.

Out of five contingency states, only two, the failures of lines 1 and 2, play a role in the determination of the feasible space of the SCOPF. In the spirit of the concepts introduced

in [35], these failures are *umbrella contingencies*, since they generate the line constraints sufficient to cover all the remaining security constraints. From a power system operation point of view, this means that one has to cover for the loss of either line 1 or 2 (because they are identical) to cover the entire set of contingency states of the system. As expected, the solution of the SCOPF subjected to its nine umbrella constraints is identical to its solution when subjected to all of its 40 original constraints (\$7 100 with $p_1^* = 160$ MW, $p_2^* = 60$ MW and $p_3^* = 30$ MW). Finally, as the original SCOPF problem is much smaller than UCD-II, the solution time required to successively solve UCD-II and the SCOPF subjected to its umbrella constraints only is hardly justifiable.

In Section 2.7, we show the value of solving UCD-II in the solution of SCOPF problems in larger standard test networks.

2.6.1 Lagrange Multipliers of UCD-II Constraints

Lagrange multipliers in optimization problems are representing the sensitivity of the objective function with respect to the right hand-side value of a certain constraint. If the Lagrange multiplier for a constraint is positive (negative), it means that by moving that constraint the objective value for the problem will be increased (decreased). We analyze the Lagrange multipliers of UCD-II constraints to see if we could gain any extra information from them.

In the three-bus system in Section 2.6, we saw that UCD-II has 1 600 constraints. These constraints are originating from the two sets of constraints in (2.21) and (2.22). The Lagrange multipliers of the constraint set in (2.21) represent the change in the objective function if a change happens in the right-hand side of these constraints. In other words, if constraint j is moved 1 unit, what would be the change in the value of s_j? Inspecting the Lagrange Multipliers of these constraints shows that the Lagrange multipliers of umbrella

constraints are zero. This confirms that moving umbrella constraints infinitesimally in any direction, will not change the value of the objective function. However, if we move a non-umbrella constraint, the "distance" of that constraint to the feasible set of solutions will change and therefore, the value of s_j for that constraint will change. Therefore, we can see that the Lagrange multipliers confirm the findings of UCD-II.

Now, let us consider the special case shown in the example in Fig. 2.5. By inspection we can say that constraints 1–3 are umbrella and constraint 4 is non-umbrella. However, constraint 5 is on the border of the feasibility region, which means that it is not essential in forming the feasibility region, but, an infinitesimal change in its right-hand side can make that constraint either umbrella or non-umbrella. This type of constraint is called "weakly redundant". Nonetheless, UCD-II identifies such weak redundant constraints as umbrella. If one is interested in identifying those weakly redundant constraints, Lagrange multipliers of UCD-II problem can be very helpful.

By analyzing the corresponding Lagrange multipliers for set of equations (2.21), we observe that all Lagrange multipliers of umbrella constraints are zero, except for constraint 5 which is weakly redundant. Moving this constraint would make it non-umbrella with respect to constraints 1–3 and therefore, variable s_5 would have to have a value for a non-umbrella constraint. Hence, it has a non-zero Lagrange multiplier assigned to it. Here, we can see that by analyzing the Lagrange multipliers of UCD-II constraints we can further scrutinize the identified umbrella set and remove, if deemed necessary, the weakly redundant constraints.

If one forms the dual problem of a UCD-II problem, the Lagrange multipliers of constraints in the primal problem will be the variables in the dual problem. Therefore, solving the dual problem of UCD-II will present some more information regarding the location of constraints with respect to the feasible set of solutions.

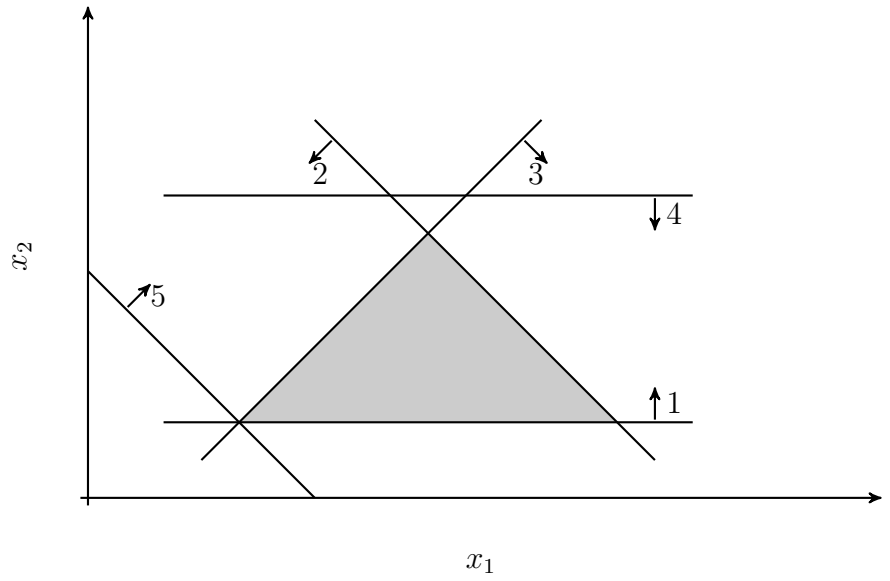

Figure 2.5 The feasible set of solutions for a problem with 5 constraints. In this problem, UCD-II identifies constraints 1–3 and constraint 5 as umbrella and constraint 4 as non-umbrella. However, inspection of Lagrange multipliers of constraint 5 shows that this constraint is weakly redundant.

2.7 Test Results

In this Section, we will apply UCD-II on corresponding SCOPF problems for two different test systems. We form the SCOPF problems following the model explained in Section 2.2.1. We identify the umbrella constraints of these SCOPF problems and we show the effectiveness of UCD-II and the time saving gained by applying UCD-II. The chosen systems are two IEEE test systems with 24 bus and 118 buses. As was pointed out in section 2.2.1, we use the PTDF coefficients to construct the line limit constraints in the SCOPF problems.

2.7.1 IEEE RTS

In this section we apply UCD-II on to the SCOPF problem corresponding to the IEEE Reliability Test System (IEEE RTS) [94]. The IEEE RTS, shown in Fig. 2.6, has 24 buses

and includes 38 transmission lines. The system has 32 generating units located at 10 buses. For this part of the studies, the system load is assumed to be the load of the first hour of the year, *i.e.* the first hour of the first day of January. We consider the $N-1$ security criterion and the line outages are the only possible system contingencies. Furthermore, the outage of line 11, which connects bus 7 to bus 8, is not a possible contingency. The outage of this line would disconnect bus 7 from the rest of the system and thus form an island. Therefore, we are considering a total of 37 line outages only. The number of constraints arising from the line limits pertaining to both pre- and post-contingency states totals 2 814 constraints ($\mathcal{J}_\lambda$). We note that we are considering both upper and lower limits of line capacities, attributing two constraints for each transmission line. The system load balance constraint is an equality constraint and is converted to two inequality constraints as shown before in (2.5) and (2.6). The generation limits at each bus are translated into two constraints accounting for 48 constraints. These 50 constraints are forming set $\mathcal{J}_\pi$. The total number of constraints in the corresponding SCOPF problem is 2 864 constraints. The objective function of the SCOPF problem is to minimize the cost of the system operation. The full details of the system data can be found in Appendix A.

For benchmarking purposes, we first solve the fully-constrained SCOPF problem, and the solution time required here is 0.015 s. The corresponding UCD problem has $2\,864 \times 2\,864 = 8\,202\,496$ constraints. The size of the UCD problem allows for a direct solution of the problem. The UCD direct solution time is 219.353 s. Obviously, the solution time is not impressing compared to the solution time of the original SCOPF problem. To reduce the solution time of UCD, we apply the proposed decomposition approaches to reduce the solution time of UCD.

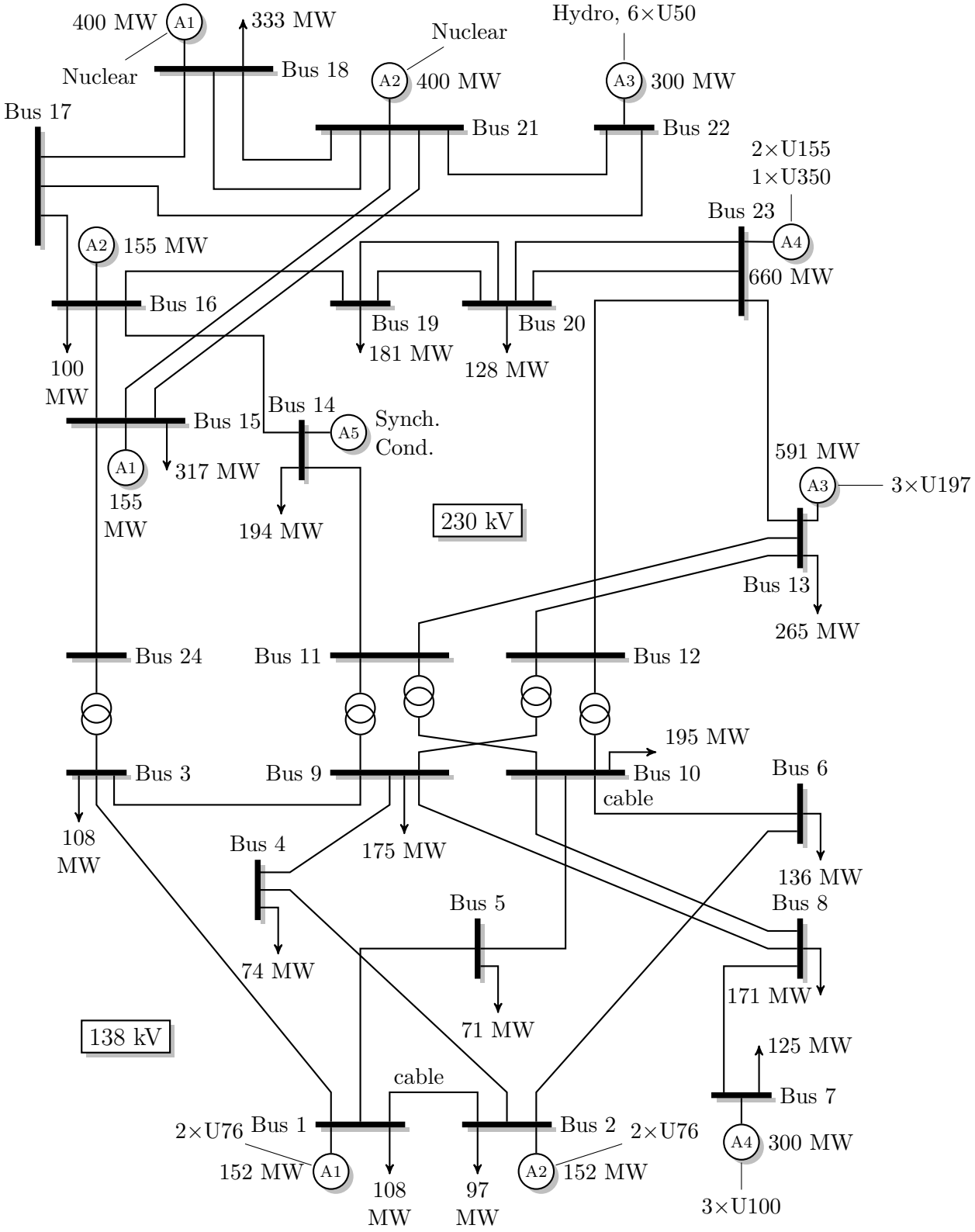

Figure 2.6 IEEE Reliability Test System 1996 [4].

2.7.2 Contingency-Based Partitioning

In contingency-based partitioning, we group all line constraints arising from the operation of the system in each contingency state. Since we are considering 37 line contingencies, we have 37 blocks, each containing 74 line flow constraints corresponding to the operation of the system under that contingency, and one block containing 76 line flow constraints representing the system operation under no-contingency state. These sub-problems are forming the set of $\mathcal{J}_\lambda^k$. We add the generation and system-wide load balance constraints —which accounts for 50 constraints and forms set $\mathcal{J}_\pi$— on top of each sub-problem, $\mathcal{J}_\lambda^k$. Thus, each sub-problem, contains 124 constraints and one sub-problem contains 126 constraints. UCD-II is run on each $\mathcal{J}_\lambda^k$ and an average solution time of 0.0871 seconds is required for each sub-problem. The total solution time, if all sub-problems were solved in series, is 3.3110 s. At the end of this step, 38 line constraints and 49 generation limits are identified as potential umbrellas. Solving UCD-II on the remaining constraints does not identify ant non-umbrella constraints. Hence, the final umbrella set contains 87 constraint.

Line-Based Partitioning

With line-based partitioning, we collect all the constraints arising from operation of each line in both pre- and post-contingency states in one sub-problem. Therefore, the number of sub-problems is equal to the number of transmission lines in the system. Therefore, we have 38 sub-problems. Each line in the network contributes two constraints for operation in each state of the system. In the pre-contingency state, there are two constraints associated with each line. However, in the case of post-contingency states, two constraints are assigned to each line while the outage of another line is considered. For example, for the outage of line 12, we assign two constraints to all other lines, but not to line 12, since this line is

assumed to be out of service for that contingency. Moreover, for the case of the lines whose outage is not listed in the possible contingency list, *e.g.* line 11 in the case of the IEEE RTS, we assign two constraints in all system states to them. So, we have 38 sub-problems, each containing 74 constraints, except for the sub-problem corresponding to line 11. This sub-problem contains 76 constraints. These sub-problems are forming the sets $\mathcal{J}_\lambda^\ell$.

Now, we add the remaining 50 constraints corresponding to $\mathcal{J}_\pi$ which includes the system load balance constraints and generation limit constraints–on top of each $\mathcal{J}_\lambda^\ell$. Each sub-problem now contains 124 constraints, except for sub-problem 11 which contains 126 constraints. Then, UCD-II is run on each of the sub-problems. At the end of this step, we have 87 constraints left as potential umbrellas. The mean solution time for each sub-problem is 0.0887 s. The total solution time, if all sub-problems were solved in series, is 3.3690 s.

Since the number of remaining umbrella constraints is small enough to run UCD-II directly, we do not take the second step of divide-and-conquer algorithm presented in Section 2.5.2. We combine all remaining potential umbrella constraints. This run of UCD-II does not identify any constraint as non-umbrella. This means that in the first step we have identified all umbrella constraints. The breakdown of the umbrella set is as follows: (i) two constraints from the system-wide load balance (ii) 45 constraints from generation limits (iii) 40 constraints from line limits.

The line-based umbrella constraints are the upper limits of line 11 for the no-contingency state and for outages of lines 1 to 10 and 12 to 38. In other words, the only line constraints in the umbrella set are the upper limits on line 11 in all of the system states. Also, the only generation limit which is not umbrella is the upper limit of the generator at bus 7. Further inspection of the system reveals that the upper limit of generator at bus 7 is 300 MW while the capacity of line 11 is 175 MW. If the load at bus 7, which is 64.2466 MW in

the first hour of the year, is increased beyond 125 MW, we will see that the upper limit of line 11 leaves the umbrella set. In Section 2.8.2 we provide a detailed sensitivity analysis of the umbrella set membership and the load changes at bus 7.

In the case of IEEE RTS and with the current loading of the system, out of the initial 2 864 constraints, only 87 are umbrella and 2 777 constraints are identified as non-umbrella. This number of non-umbrella constraints account for more than 96.96% of the original constraint set. This shows us the potential computational savings that could be gained by applying UCD-II on SCOPF problems whose solution is found repeatedly. Since each sub-problem can be solved independently, one could make UCD-II run even faster by using parallel computing.

Comparing the solution times of UCD-II with and without using partitioning, one can see the obvious benefits of partitioning, specially line-based partitioning. However, the effectiveness of each specific partitioning technique is significantly dependent upon the nature of the problem.

Finally, note that the SCOPF problem of the IEEE RTS subjected only to its umbrella constraints takes virtually zero seconds to solve as compared to 0.015 seconds solution time of the original problem.

The IEEE RTS is a small size system and the effectiveness of UCD is more obvious in large systems. In the next section, we apply UCD-II on a larger-scale system, the IEEE 118 bus system, and show the effectiveness of UCD-II formulation in reducing solution time of SCOPF problems.

2.7.3 118 Bus System

In this Section, we apply the divide-and-conquer approaches for solving UCD-II introduced in Section 2.5 on a larger power system model. To do so, first we use a modified

version of the 118 bus IEEE test system [93] with its 186 lines and 54 generating units [3]. In our tests, we are considering 176 single line contingencies [4] along with the intact network. The number of constraints generated by the SCOPF problem for this system is 65 730. The generation limit constraints contribute $118 \times 2 = 236$ constraints for both upper and lower limits. The load balance contributes two constraints. To represent the line limits, we follow the same approach as for the IEEE RTS. In the no-contingency state, we have $186 \times 2 = 372$ constraints. In each contingency, we have $185 \times 2 = 370$ constraints. Since we are considering 176 contingencies only, the total number of constraints arising from lines, for operation under no-contingency and contingency states is $372 + 370 \times 176 = 65\,492$ constraints. This full SCOPF solves in 2.808 s using the hardware and software listed in Section 2.6.

The size of the full UCD-II here is not trivial; its number of constraints is $65\,730 \times 65\,732 \approx 4.320 \times 10^9$ and the number of variables is $119 \times 65\,730 \approx 7.822 \times 10^6$. Obviously, the current size of UCD-II is impractical. Therefore, we apply the decomposition techniques proposed in Section 2.5 to find the corresponding umbrella set.

Line-Based Partitioning of UCD-II

The first step of the decomposition process is to partition the original set of constraints into appropriate subsets. As argued previously, partitioning SCOPF line constraints, group-

3. Line and generation limits and generation cost data for the IEEE 118 bus system are notoriously ill-defined in the literature. Here, we are using the set of generation costs and limits found within the MATPOWER library [98] and we modified the set of line limits used previously by researchers based at the Illinois Institute of Technology. The complete data set can be found at `http://cl.ly/3x0L3L393r24` and in Appendix B.

4. The number of line contingencies is less than the number of actual test system branches because we had to disregard the potential failure of 10 branches which serve to connect leaf nodes of the network. The loss of any of those lines leads to node islanding and ultimately infeasible UCD-II and SCOPF solutions. To consider the failure of those lines, we should add corresponding load shedding variables in the power balance and at leaf nodes.

ing all constraints pertaining to particular lines, is more effective than partitioning them according to their contingency index. Thus, in Step 1 of the divide-and-conquer algorithm, we break the constraint set into 186 line-based blocks as outlined in Section 2.5.3. Each block corresponding to the lines whose outages we consider contains 352 line constraints and 238 constraints accounting for power generation limits and the two power balance inequalities. For the 10 lines whose outages are not considered, the corresponding constraint blocks contain two more line constraints.

Running UCD-II in parallel on each of these constraint blocks takes on average 17.542 s per block using the hardware and software mentioned in Section 2.6. The result of this first UCD-II run is impressive in terms of umbrella constraint discovery: out of the 65 730 original SCOPF constraints only 1 511 are flagged as potential umbrella constraints. In other words, after a single algorithm step we eliminated 97.7% of the original SCOPF constraints. At that stage, the solution of the SCOPF, while subjected to this much reduced set of constraints, can be obtained much more rapidly (0.0470 s; 1.7% of the original solution time).

Next, we combine all the constraints flagged as umbrella in the prior round into a single constraint block, entirely skipping Step 2 of the algorithm in Section 2.5.2. After solving UCD-II for this block of constraints, we are left with the final umbrella set containing 451 constraints only, representing 0.67% of the original number of constraints in the SCOPF. Out of 65 492 constraints on line flows, only 217 (0.33% of all line constraints) are in the umbrella set. Out of 236 constraints associated with generation limits 232 are within the umbrella set and only 4 of them are identified as non-umbrella. The remaining two constraints are the system-wide load balance constraints, which are always part of the umbrella set since they are representing equality constraints. Constraints associated with 87 contingency states (out of the original 176) are contributing constraints into the umbrella

set, thus indicating that there are 87 umbrella contingencies. The size of the UCD-II problem here is quite significant and so is its solution time (480.2 s). Nonetheless, if we solve the SCOPF now subjected to those 451 umbrella constraints, we achieve a solution time of 0.0160 s (0.57% of the original solution time).

The UCD-II solution time can be reduced by partitioning the 1 511 potential umbrella set once more as in Step 2 of the algorithm. We partitioned the 1 511 constraint set into two blocks of 873 constraints each containing the generation limits and the power balance constraints flagged as potential umbrellas and half of the potential umbrella line limits. The solution time for this step is 85.582 s and reduces potential umbrella constraints to 509. Finally, running UCD-II on that set finds the same 451 constraints in 17.784 s. This result demonstrates the power of the decomposition approach as the cumulative solution time (103.366 s) with the extra step is much less than the solution time obtained with a single 1 511-constraint block.

Contingency-Based Partitioning of UCD-II

We now provide evidence validating the poor performance of contingency-based partitioning in the divide-and-conquer solution of UCD-II. Here, in Step 1 of the algorithm, we bundle line flow constraints associated to the 177 possible power system states (176 contingency states and one no-contingency state) with generation limits and the power balance. Solving UCD-II on those constraint blocks results in the flagging of 7 828 potential umbrella constraints (11.9% of the original lot), taking an average of 16.843 s per UCD-II subproblem. As expected, the initial non-umbrella constraint discovery rate is not as appealing as with line-based partitioning (88.1% versus 97.7%). The size of this set of potential umbrella constraints is too large to go ahead with a single UCD-II solution as was attempted with line-based partitioning. Hence, we complete Step 2 of the algorithm combining pairs of

potential umbrella constraint blocks and then repeatedly solving UCD-II until we find the same 451 umbrella constraints. In the end, it takes a further eight iterations and 840 s to terminate the algorithm. Clearly, this approach is inferior to the line partitioning approach and should not be used.

2.8 Sensitivity Analysis

The UCD-II solution times reported above are high, even when using the decomposition approach with line-based partitioning. In fact, it is not difficult to see that UCD-II is itself larger than the original SCOPF. Still, we have seen above the potential for SCOPF solution time improvement for the minimum cost problem on the IEEE 118 bus system, when subjected to its umbrella set only. A UCD-II pre-processing step is effectively worthless if it ends up increasing the overall solution time of the original problem. In this Section, we provide empirical evidence that the outcome of a UCD-II problem is generally insensitive to changes in the parameters defining the SCOPF constraint set. Moreover, we show that the union of all umbrella constraints arising over a full year of operation is generally small in comparison to the original set of SCOPF constraints. From this, one can conclude that an operator could reuse the results of a prior UCD-II run when facing similar operating conditions, and thus save itself the UCD-II computation time, *e.g.* on a similar hour and day in two consecutive weeks where the loading pattern and level are essentially the same. Otherwise, the operator could simply use the union of all constraints flagged as umbrella over the course of a year in lieu of the original constraint set. This union of all umbrella constraints would usually be slightly larger than what would be provided by an exact UCD-II run in each hour, but it would not lead to significant SCOPF solution time degradation.

Firstly, we do a sensitivity analysis on the three-bus system shown in Fig. 2.3 in Section

2.6. For this small network, we are able to visualize the feasibility set of solutions to see its changes as the total system load changes. Secondly, we do a sensitivity analysis on a larger network, the IEEE RTS and we show the insensitivity of its umbrella set to the changes in the system load.

2.8.1 Three-Bus System

In this section, we use the system shown in Fig. 2.3 to analyze the sensitivity of membership of constraints in the umbrella set with respect to changes in the system load at different buses.

The feasibility set of the three-bus system with the loading and conditions shown in Fig. 2.3 and Table 2.1 is shown in Fig. 2.4. To study the sensitivity of the umbrella set to the load changes in the system, we change the load at bus 3 and bus 2 (one at a time while keeping other parameters of the system constant) and identify the corresponding umbrella set/constraints. We draw one sample of the feasibility region for each load range that has the same umbrella constraints.

Load Change at Bus 3

The load at bus 3 of the system in Fig. 2.3 is 50 MW. The load at this bus is changed from 0 MW to 90 MW and every time the umbrella set changes, the corresponding umbrella set is identified. Note that, if any change happens in the system parameters, all of the constraints move. However, this move might not be enough to push a constraint in or out of the umbrella set. In this sensitivity analysis, when we talk about changes in the umbrella set, we are referring to changes in the members of the set in terms of constraints leaving and joining. Nonetheless, the reader is aware that any change in the load will change the constraints.

Table 2.2 Umbrella sets of the three-bus system for load changes at bus 3. Please note that system load balance constraints are always part of the umbrella set and they are not included in this table.

Load (MW)	Line Number	Contingency	Generation
0-19	2(U) 1(U)	1 2	1(L) 2(U) 3(U) 3(L)
20-40	2(U) 3(U) 1(U) 3(U)	1 1 2 2	1(L) 2(U) 3(U) 3(L)
41-50	2(U) 3(U) 1(U) 3(U)	1 1 2 2	1(L) 2(U) 3(U)
51-70	2(U) 3(U) 1(U) 3(U)	1 1 2 2	 2(U) 3(U)
71-90	3(U) 3(U)	1 2	2(U) 3(U)

The first column in Table 2.2 shows all the load ranges for which the umbrella set is constant. The second column indicates the line that the umbrella constraint is coming from and whether the umbrella constraint is the lower or upper limit of that line. The third column shows the contingency whose occurrence is making the line constraint on the second column an umbrella constraint. The last column contains the bus number whose generation limit constraints are in the umbrella set. The indicators (U) and (L) denote the upper and lower limits of the constraints, respectively.

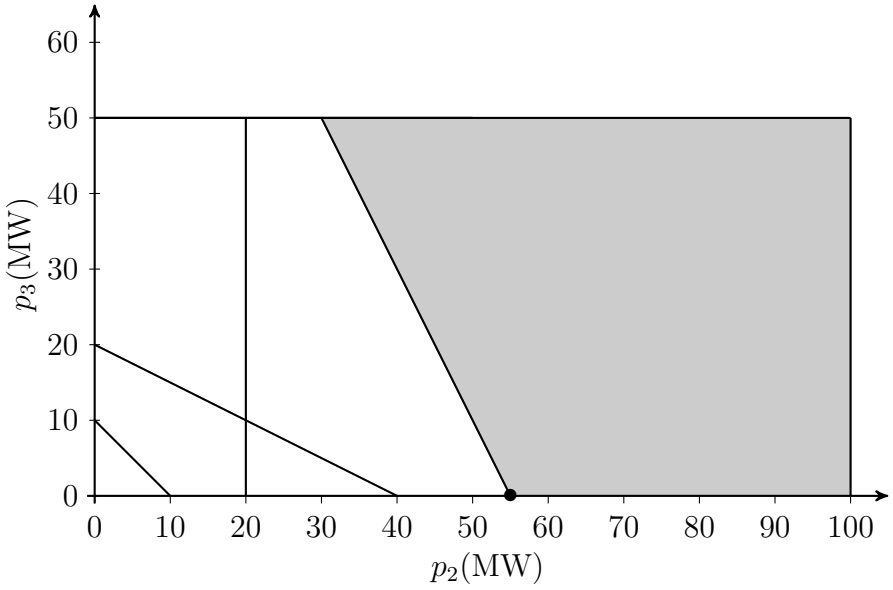

Figure 2.7 Feasible set of the three-bus system with 10 MW load at bus 3

For the interval from 0 to 19 MW, the umbrella set contains two line limits: upper limit of line 2 when line 1 is out and upper limit of line 1 when line 2 is out. Note that line 1 and 2 are identical; therefore, their corresponding constraints are identical (for similar conditions). As was explained in Section 2.4.3, identical or duplicate constraints are umbrella or non-umbrella together. Fig. 2.7 shows the feasible set of solutions for $d_3 = 10$ MW. It can be seen that the optimal solution is located at the point $p_1^* = 155$ MW, $p_2^* = 55$ MW and $p_3^* = 0$ MW and the corresponding system cost of operation is \$ 5 300. As expected, comparing with the feasible set of solutions of the original case (with $d_3 = 50$ MW), shown in Fig. 2.4, as the load decreases the line constraints become less stringent and more generation limits join the umbrella set.

For the interval of 20 to 40 MW, the membership of the umbrella constraints does not change. However, as constraints are moving closer to the feasible set, and consequently, shrinking the feasible set, two line constraint join the umbrella set. These two constraints

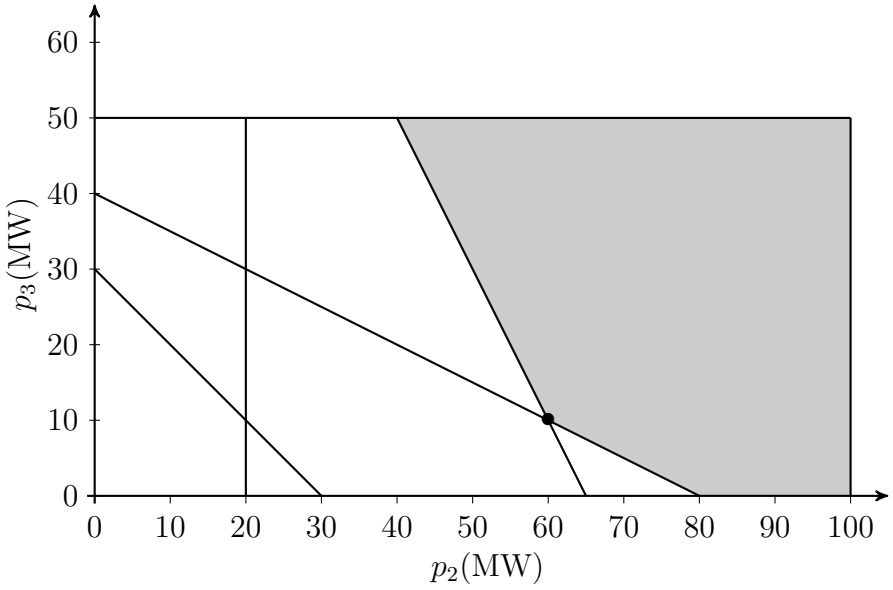

Figure 2.8 Feasible set of the three-bus system with 30 MW load at bus 3

are the upper limit of line 3 during outages of line 1 or 2. A projection of the feasible set when load at bus 3 is 30 MW is shown in Fig. 2.8. The new optimal value for objective function is \$ 6 100 which is obtained with the following generation combination: $p_1^* = 160$ MW, $p_2^* = 60$ MW and $p_3^* = 10$ MW. Movement of line constraints to the right (as opposed to Fig. 2.7) is the reason that two line constraints have joined the umbrella set. The direction of the movement of the constraints can be predicted by studying the Lagrange multipliers of UCD-II constraints, as was discussed in Section 2.4.2.

For the interval of 41 to 50 MW, the feasible set of solutions is shown in Fig. 2.9. The figure is repeated here in Fig. 2.9 for the convenience of the reader. The optimal solution for a 50 MW load at bus 3 is \$7 100 with $p_1^* = 160$ MW, $p_2^* = 60$ MW and $p_3^* = 30$ MW. The umbrella set of this network is explained in details in Section 2.6.

For the interval of 51 to 70 MW, the umbrella set consists of eight constraints. The umbrella line constraints are the same as for the interval of 41 to 50 MW but the lower

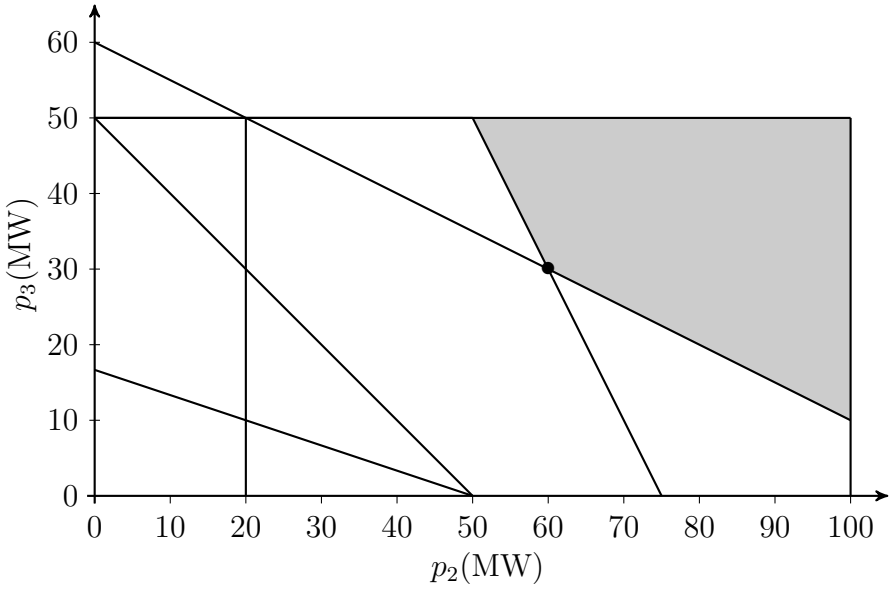

Figure 2.9 Feasible set of the three-bus system with 50 MW load at bus 3

limit of generation at bus 1 leaves the umbrella set. The feasible set of solutions for 70 MW load at bus 3 is shown in Fig. 2.10. The optimal solution for this loading is \$ 8 100 with $p_1^* = 160$ MW, $p_2^* = 60$ MW and $p_3^* = 50$ MW. Comparing the optimal answer of this case with the optimal solution for 50 MW load at bus 3, we could see that although the generator at bus 3 is the most expensive generator, and generators 1 and 3 did not hit their limits yet, any increase in the load at bus 3 is provided by generator 3. This is because transfer of power from other generators to bus 3 is not possible because of hitting the transmission line limits specially during contingencies. The price of electricity at bus 3 is 50 \$/MWh (which can be obtained by looking at Lagrange multipliers of the SCOPF constraints); therefore, for the extra 20 MW, the objective function will increase \$ 1 000 compared to the previous case.

For the interval of 71 to 90 MW, the feasible set of solutions will shrink even more. The umbrella set consists of total of six constraints, of which two line constraints are upper limit

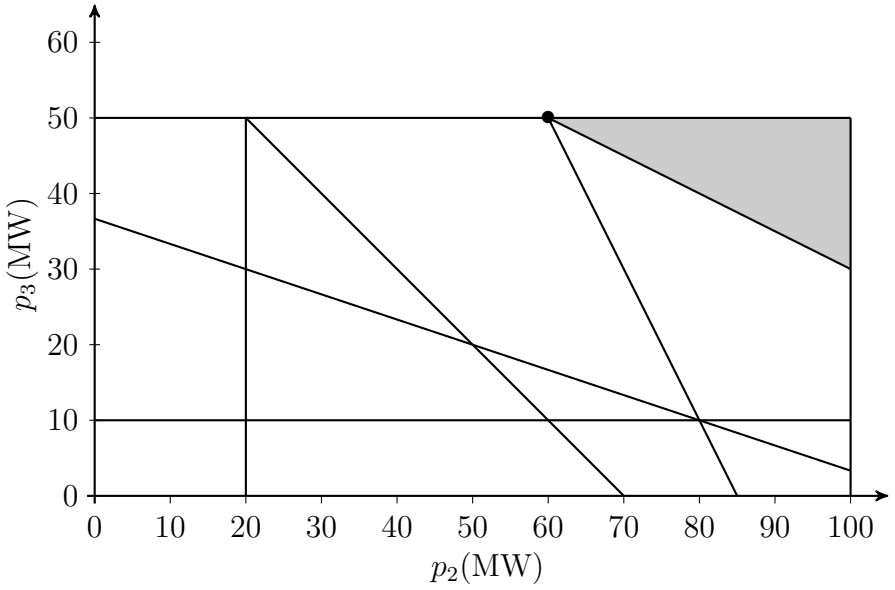

Figure 2.10 Feasible set of the three-bus system with 70 MW load at bus 3

constraints for line 3 during outage of line 1 or line 2. Another two constraints are from upper generation limits for buses 2 and 3. Of course, load balance constraints are members of the umbrella set. The feasible set for a load of 90 MW at bus 3 is shown in Fig. 2.11. For this loading, the feasible set of solutions is reduced to one single point. This point is $p_1^* = 140$ MW, $p_2^* = 100$ MW and $p_3^* = 50$, which will increase the system operation cost to \$ 9 300. Any increase in the load at bus 3 will push the system into the infeasibility and will result in the system collapse.

From analyses of the above cases, it can be seen that the more load located at bus 3, the more costly it is feeding the load. Also, it can be seen that this cost is not increasing linearly with the increase of load even when a cheaper generator is available. This happens because the line limits in the no-contingency state as well as line limits in contingency states do not allow for the transfer of power from the most economic generator to the load. Therefore, in some cases, it is necessary to use the more expensive generator while the

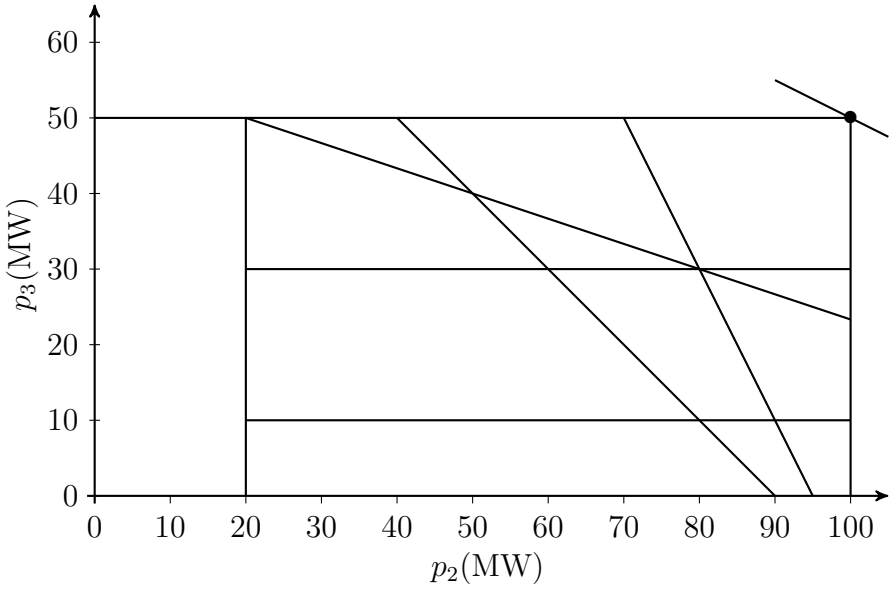

Figure 2.11 Feasible set of the three-bus system with 90 MW load at bus 3

cheaper generators are available. If the area of the projection of the feasible set of solutions for different loadings of this example are compared, it can be seen that the feasible set of solutions shrinks as the load of the system increases. These circumstances will push the problem to its infeasibility border. For this problem, if the load at bus 3 is increased to 91 MW, the SCOPF and corresponding UCD-II problem become infeasible.

Another observation is regarding the run time of UCD-II problems. The run time of UCD-II *increases* when the feasible set of solution becomes smaller. For example, the corresponding UCD-II for the case that bus 3 has 10 MW load runs at a very negligible time (the feasible set of solutions is shown in Fig. 2.7), while the corresponding UCD-II problem for the case that bus 3 has 90 MW load takes 0.015 s of the CPU time (the feasible set of solutions is shown in Fig. 2.11). UCD-II needs to find the values for its variables, $\mathbf{w}_j$ which satisfy all of the constraints. Now, the smaller the feasible set of solutions, the more time UCD-II has to spend to find feasible values for its variables. This is believed to

be the reason for the longer solution times for more stressed conditions of the network.

Load Change at Bus 2

In this section, we change the load in bus 2 and draw the feasible set of solutions for one of the loads in each interval that umbrella set is constant. We form the SCOPF for each system loading and run UCD-II on the SCOPF problem and identify the umbrella constraints. We set the load at bus 2 at 50 MW.

Since the minimum generation of the three-bus system is 120 MW, the minimum value for the load at bus 2 is 70 MW. We change the load at bus 2 from 70 MW to the point that the SCOPF problem becomes infeasible. Table 2.3 shows the load intervals for which that umbrella set remains constant. Please note that the load balance constraints are always members of the umbrella set and they are not represented in this table.

From Table 2.3, we can see that at lighter loads, none of the line constraints are umbrella. In this case, mostly lower limits of the generators are umbrella. As the load in bus 2 increases, some of the line constraints enter the umbrella set as well as the upper limits of some generators. By increasing the load even more, it can be seen that more line constraints are joining the umbrella set. For cases where the system is heavily loaded, the line constraints become the most stringent constraints in the system. As the feasibility set of solutions shrinks more and more, all lower limit constraints of generators retire from the umbrella set.

These sensitivity analyses, presented in Tables 2.2 and 2.3 show that the umbrella set for a given SCOPF problem remains unchanged for usually wide load intervals, and the system operator does not need to run UCD-II to identify the umbrella set for given ranges of load change. This observation contributes to reducing the number of times that UCD-II may need to be carried out by system operators to cover load changes in the system.

Table 2.3 Umbrella sets of the three-bus system for load changes at bus 2.

Load (MW)	Line Number	Contingency	Generation
70–99			1(L) 2(L) 3(L)
100–119	3(U) 3(U)	1 2	1(L) 2(L) 3(L)
120–149	3(U) 3(U)	1 2	1(L) 2(L) 3(L) 3(U)
150–159	3(U) 3(U)	1 2	1(L) 2(L) 3(L) 3(U) 2(U)
160–170	3(U) 3(U) 2(U) 1(U)	1 2 1 2	1(L) 2(L) 3(L) 3(U) 2(U)
171–180	3(U) 3(U) 2(U) 1(U)	1 2 1 2	1(L) 3(L) 3(U) 2(U)
181–200	3(U) 3(U) 2(U) 1(U)	1 2 1 2	1(L) 3(U) 2(U)
201–240	3(U) 3(U) 2(U) 1(U)	1 2 1 2	3(U) 2(U)
241–250	2(U) 1(U)	1 2	3(U) 2(U)

The other observation is that there are only 10 constraints (excluding the load balance constraints) that form the different umbrella sets for different system loadings. In other words, by taking the union of these umbrella sets, there is no need to run UCD-II for changes in the load of bus 3 and bus 2. One should note that the union of the umbrella set is still a small portion of the original set of umbrella constraints and can still make the solution of SCOPF problem significantly faster. We do the same analysis on the IEEE RTS in the next Section.

2.8.2 IEEE RTS

In this section, we illustrate the insensitivity of the membership of umbrella sets to changes in load using the single-area version of the IEEE Reliability Test System—1996 [94], shown in Fig. 2.6, in the first hour of the RTS year. Running UCD-II for the corresponding SCOPF in that hour results in 87 constraints forming the umbrella set (out of the original 2 864). To assess the effects of load changes on the umbrella set membership, while keeping all other parameters constant, the load at Bus 7 is increased from zero to the point where the SCOPF problem (and therefore, the corresponding UCD-II problem) becomes infeasible. In this case, the umbrella set changes only at three critical loadings (125, 126 and 159 MW) before UCD-II becomes infeasible when the demand at Bus 7 reaches 383 MW. Performing the same analysis for Bus 8 shows that the umbrella set changes also at three critical loadings (1, 9 and 183 MW), and the SCOPF becomes infeasible when the nodal load hits 350 MW. Similar results can be observed as the load is varied from zero to the level where the SCOPF becomes infeasible at other nodes. If one generalizes this analysis to multiple nodes where loads are varied, a matrix of critical loading ranges would be obtained. From this, we can expect that in between critical loading levels, the umbrella set remains constant, which entails that any pre-calculated UCD-II result can be reused under similar

system conditions.

The details of this analysis are explained in the following two sections.

Change of Load at Bus 7

In the IEEE RTS, bus 7 is one of the critical buses in defining the number of umbrella constraints since it is radially connected to the rest of the network. This bus is connected using only line 11 to bus 8. An outage of line 11 will form an island containing only bus 7. Therefore, we form the corresponding SCOPF problem, considering outage of all lines, except line 11, as possible contingencies. The corresponding UCD-II problem is saved for different load intervals at bus 7 to find the intervals that the umbrella set remains constant.

The results show that for the interval from 0 to 124 MW, the umbrella set remains constant and has 87 members. The umbrella set for this load interval breaks down as the following: two load balance constraints, 47 generation limits and 38 line limits. These line constraints are essentially coming from two lines, line 11 and line 29 (connecting buses 16 and 19–see Table A.3). The constraints corresponding to line 11 are upper limit constraints coming from no-contingency state and failures of lines 1 to 29, except for line 11 which is not considered. As was explained in Section 2.7.2, the reason why the upper limit constraint of line 11 is in the umbrella set is because the generator at bus 7 can generate up to 300 MW, while the capacity of line 11 is 175 MW. If the load at bus 7 is less than 125 MW, line 11 may be congested. The lower limit constraints of line 29 in the no-contingency case and in contingencies of lines 1 through 8 are members of the umbrella set as well. The only generation limit which is not in the umbrella set is the upper limit of the generator at bus 7. The reason for this is since the line 11 may be reaching its limit, the generation level at bus 7 cannot be increased to its limit; therefore, it is not a member of the umbrella set.

If the load at bus 7 is increased to 125 MW, the generation limit at bus 7, moves toward

the feasible set and reach the border of the feasible set, making both the upper limit of line 11 and the generation limit at bus 7 members of the umbrella set. Therefore, the number of umbrella constraints in the umbrella set increases to 88 constraints.

If the load is increased beyond 125 MW, the available power to be transferred by line 11 decreases below its capacity. Therefore, the upper limit of line 11 leaves the umbrella set along with the line limit for line 29. However, the generation limit at bus 7 remains in the umbrella set. The umbrella set now contains 50 constraints, of which 48 are generation limits and 2 load balance constraints. For the interval of 126 MW to 158 MW, the umbrella set remains constant again.

For the interval of 159 MW to 300 MW, the umbrella set has 51 members. The lower limit of generation at bus 7 leaves the umbrella set since it is replaced by the lower limit of line 12 (connecting buses 8 and 9) during failure of line 13, and the lower limit of line 13 (connecting buses 8 and 10) during failure of line 12. The reason is that with the increase of the load at bus 7, the load at bus 8 cannot be fed anymore from the generator at bus 7. Therefore, power should be imported from other generators to supply the load at bus 8, which could in turn congest the lines connected to bus 8. If the load at bus 7 is increased beyond 300 MW, generator 7 may not be able to provide all the power required by this bus. Therefore, power should be transferred to bus 7 by line 11 to feed the load.

The umbrella set remains constant until the load at bus 7 reaches 384 MW for which UCD-II, and therefore the corresponding SCOPF problem, becomes infeasible.

As can be seen from this sensitivity analysis, the umbrella set remains constant for different intervals of the load at bus 7. Therefore, if the load at bus 7 changes from 0 to 384 MW, there will be only three different umbrella sets until the problem becomes infeasible. The total number of the constraints contributing in the umbrella set in any interval is 90. In other words, the union of all different umbrella sets for the span of the

load at bus 7 only includes 90 constraints out of the original 2 864 constraints.

Change of Load at Bus 8

The load at bus 8 is supplied by lines 11, 12 and 13. To do the sensitivity analysis, the load of the first hour of the year is chosen, and the load at bus 8 is changed from 0 to the value that makes the corresponding SCOPF problem infeasible. Note that since the load at bus 7 is set at 67.354 MW, the corresponding upper limit constraints for line 11 in the no-contingency case and in contingencies 1-29 (except for contingency of line 11), and the corresponding lower limits of line 29 in the no-contingency case and in contingencies 1-8 are part of the umbrella set. Other line limits will join or leave the umbrella set in each load interval. The process is elaborated next.

If the load at bus 8 is set at zero MW, the umbrella set contains 88 constraints. The line constraints in the umbrella set are constraints arising from line 11 and 29, as well as the upper limit of line 13 during the outage of line 12 and the upper limit of line 12 during the outage of line 13. The power generated by the generating unit at bus 7 that is not consumed by the load at bus 7, is transferred using line 12 and 13. Since the load at bus 7 is 67.353 MW, the extra power produced by the generator at bus 7, which has the capacity of 300 MW, is transferred through line 11. However, line 11 has a capacity of 175 MW. If the load at bus 8 is set to zero, all 175 MW should be transferred through lines 12 and 13 to the rest of the system. In the no-contingency case, none of these two lines, which each have capacity of 175 MW, could reach their limit. Nonetheless, if any of them is out of service, the other one would be congested. Therefore, the upper limit of both lines for the contingency of the other line is part of the umbrella set. The generation limits in the umbrella set are the upper and lower generation limits of all generating units except for the upper generation limit at bus 23.

By increasing the load at bus 8, the power needed to be transferred through lines 12 and 13 is less than 175 MW. Therefore, these two lines, even in the outage of the other one, would not be congested. This means that the upper limit on line 12 during outage of line 13 and the upper limit of line 13 during outage of line 12 leave the umbrella set. In this loading, the umbrella set contains 86 constraints. This umbrella set remains constant for the load interval of 1 to 8 MW at bus 8.

If the load at this bus is increased to 9 MW, the upper generation limit of bus 23 joins the umbrella set. This increase of load in bus 8 would relieve lines 12 and 13 some more.

The umbrella set remains the same until the point where the load at bus 8 reaches 183 MW. At this point, the lower limits on lines 12 and 13, when the other line is out, join the umbrella set. Also, the lower generation limit at bus 7 leaves the umbrella set. Consequently, the umbrella set contains 88 constraints. This condition remains constant until the load at bus 8 reaches 350 MW, where, if the load is further increased, the SCOPF and consequently UCD-II becomes infeasible.

Discussion

In this section, we discuss the findings and observations made during the sensitivity analysis of the IEEE RTS. Further evidence showing how pre-calculated RTS umbrella set membership could be used is found in Fig. 2.12. Here, the RTS umbrella set has been calculated for each hour of week 1 of the RTS year. The result in Fig. 2.12 illustrates clearly the correlation between the umbrella set size and the system-wide load. As the load increases and decreases over its daily cycles, so is the number of constraints in the umbrella set. More interestingly, however, in the case of weekly load cycles, the umbrella set for hours t and $t + 168$ are generally the same. For instance, they can be identical up to 16 weeks in a row (*e.g.* in the first hour of each week in the months of November through

February).

Finally, the weekly hour which generates the umbrella set with the largest number of constraints is generally the union of all constraints flagged as umbrella in that week. Therefore, if one takes a conservative approach whereby this "peak" umbrella set is used for all hours of a week, substantial SCOPF computational savings could still be achieved, and it would guarantee that no potential umbrella constraint could be left out [5]. The difference in umbrella set size at the peak and at other hours is generally small, and it remains that the size of the peak umbrella set is still substantially smaller than that of the original SCOPF, thus resulting only in marginal SCOPF solution time increase. In the case of Fig. 2.12 the weekly peak umbrella set has 44 line constraints, in lieu of the original 2 814 line constraints, but in some hours the size of the line-only umbrella set could go as low as zero. Going even further, one could just find the peak umbrella set for a full year and use it in all hours. For the RTS, this happens in hour 42 of the year and the umbrella set contains only 44 constraints which together form the union of all line-based umbrella constraints ever entering the umbrella set over the year. Specific evidence for these is found in Fig. 2.13, 2.14 and 2.15.

Fig. 2.13 shows the number of hours in the RTS year (which contains $52 \times 7 \times 24 = 8\,736$ h) that specific lines' flow limits are umbrella constraints. Here, there are only seven such lines, and the constraints on line 11 are found in the umbrella set most of the time (8 158 h $\approx 93.4\%$ of the year), while those applying to line 23 spend the least number of hours in the umbrella set (306 h $\approx 3.5\%$ of the year). Fig. 2.14 shows which contingencies contribute at least one umbrella constraint in the RTS year. The vertical bars account for the number of umbrella constraints generated by contingencies over a full year. The dashed

5. We note, however, that the peak umbrella set does not necessarily happen at the same time as the peak in the system load.

line shows the cumulative number of umbrella constraints generated by contingencies. This number is normalized to the number of constraints generated by the original SCOPF over a full year ($2\,864 \times 8\,736 \approx 25$ million constraints). One finds that the total number of umbrella constraints generated in the RTS year represents only 1.3% of the total number of constraints generated by the original SCOPF in that year.

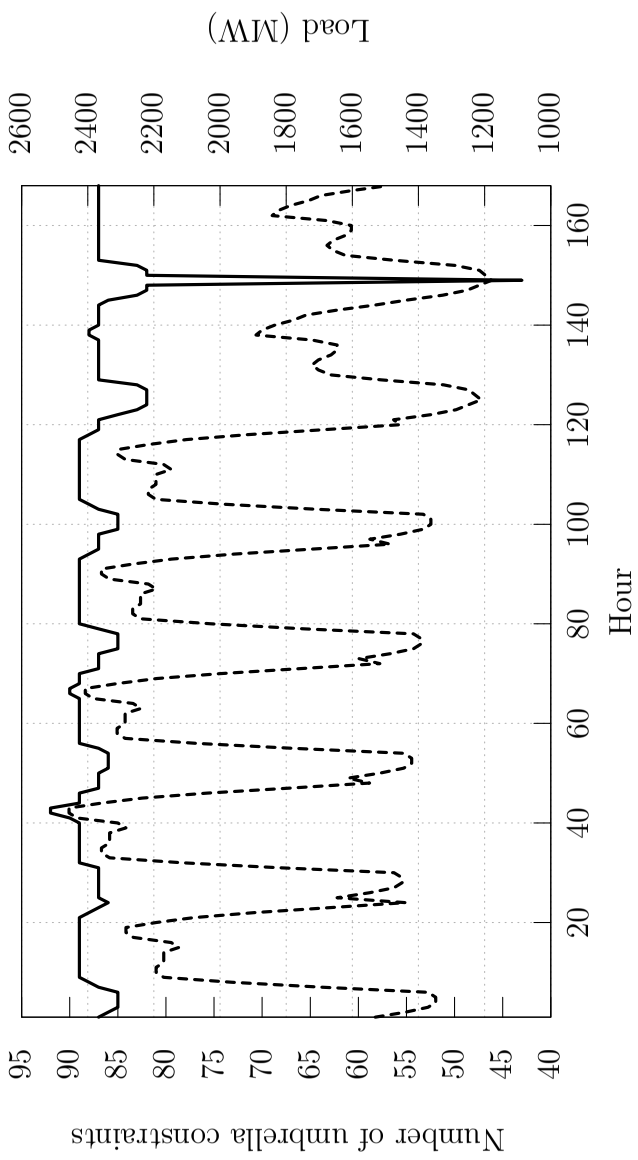

Figure 2.12 Week 1 IEEE RTS load (dashed line) [94] and size of the corresponding umbrella sets (solid line).

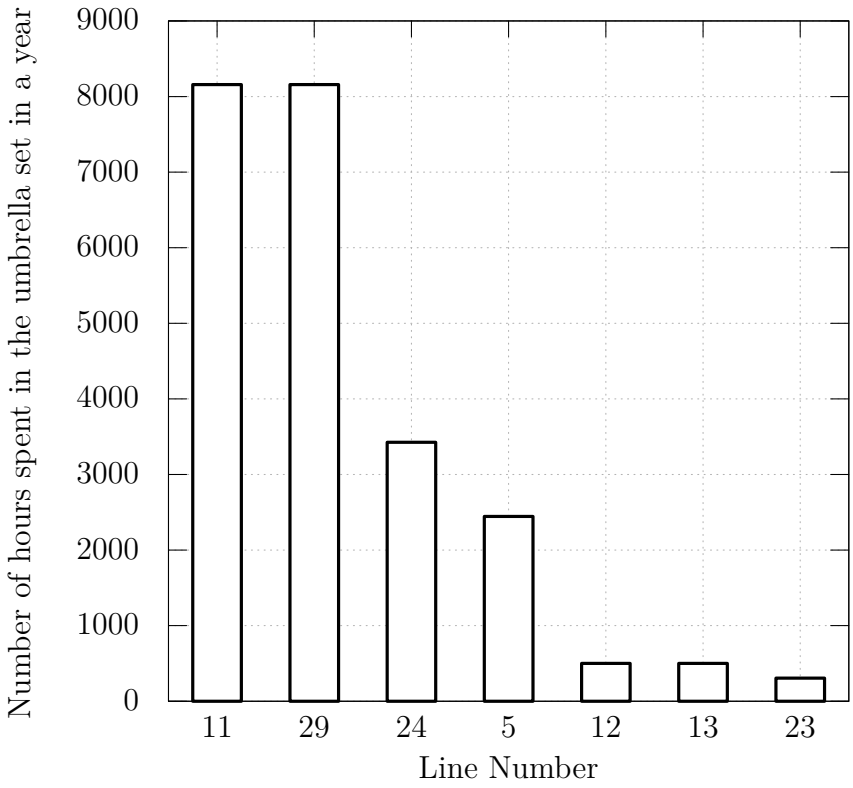

Figure 2.13 Number of hours each line in the RTS [94] contributes one or more constraints in umbrella sets. Only the seven lines listed here, out of the 38 RTS lines, contribute umbrella constraints over the year.

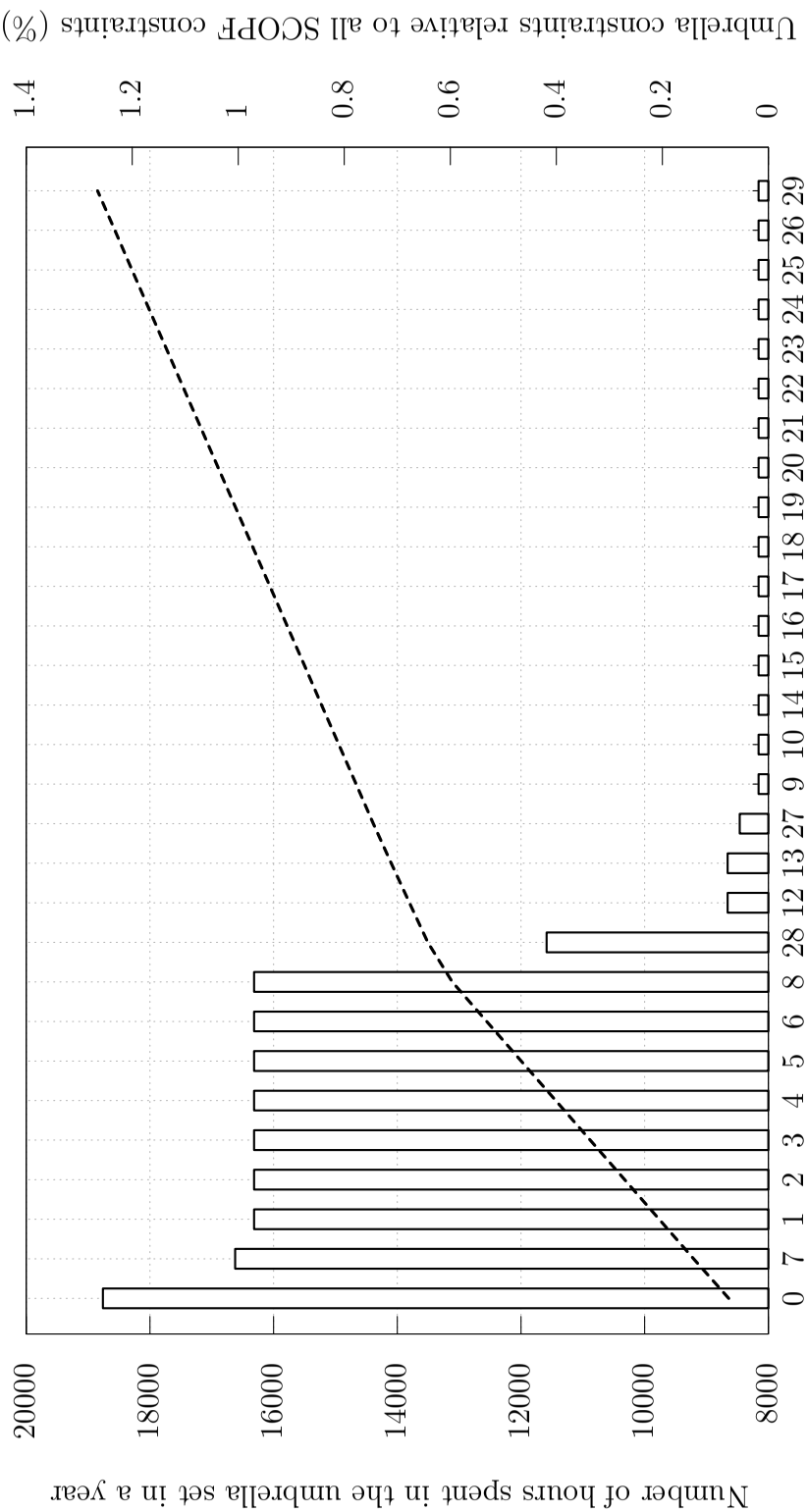

Figure 2.14 Umbrella constraints generated by all contingencies over the RTS year [94] (vertical bars) and the cumulative number of umbrella constraints relative to the total number of SCOPF constraints (dashed line). Only the 29 contingencies shown here, out of the 38 RTS contingencies, contribute umbrella constraints over the year.

Fig. 2.15 shows the number of hours each line-based umbrella constraint (the 44 constraints mentioned before) spends in the umbrella set normalized to the number of hours in the RTS year. Most notably, 38 of those line constraints spend at least 93% of the time in the umbrella set, with six more joining in at least 3.5% of the time. The first conclusion that can be drawn here is that the umbrella set membership remains grossly the same over a full year cycle. This provides further evidence of the relative insensitivity of the umbrella set membership to changes in load. Most importantly, however, given that very few constraints are potential members of the umbrella set and most of them remain in it for a significant portion of the year, we argue that using the union of all of these constraints would represent a good compromise between SCOPF compactness and potential SCOPF solution time degradation. Subjecting the SCOPF to those 44 constraints in each hour would be sufficient to cover the secure operation of the network. Yet, this set would be necessary only in a few "peak" hours. This union of these 44 constraints still only represent 1.5% of the original SCOPF constraint set.

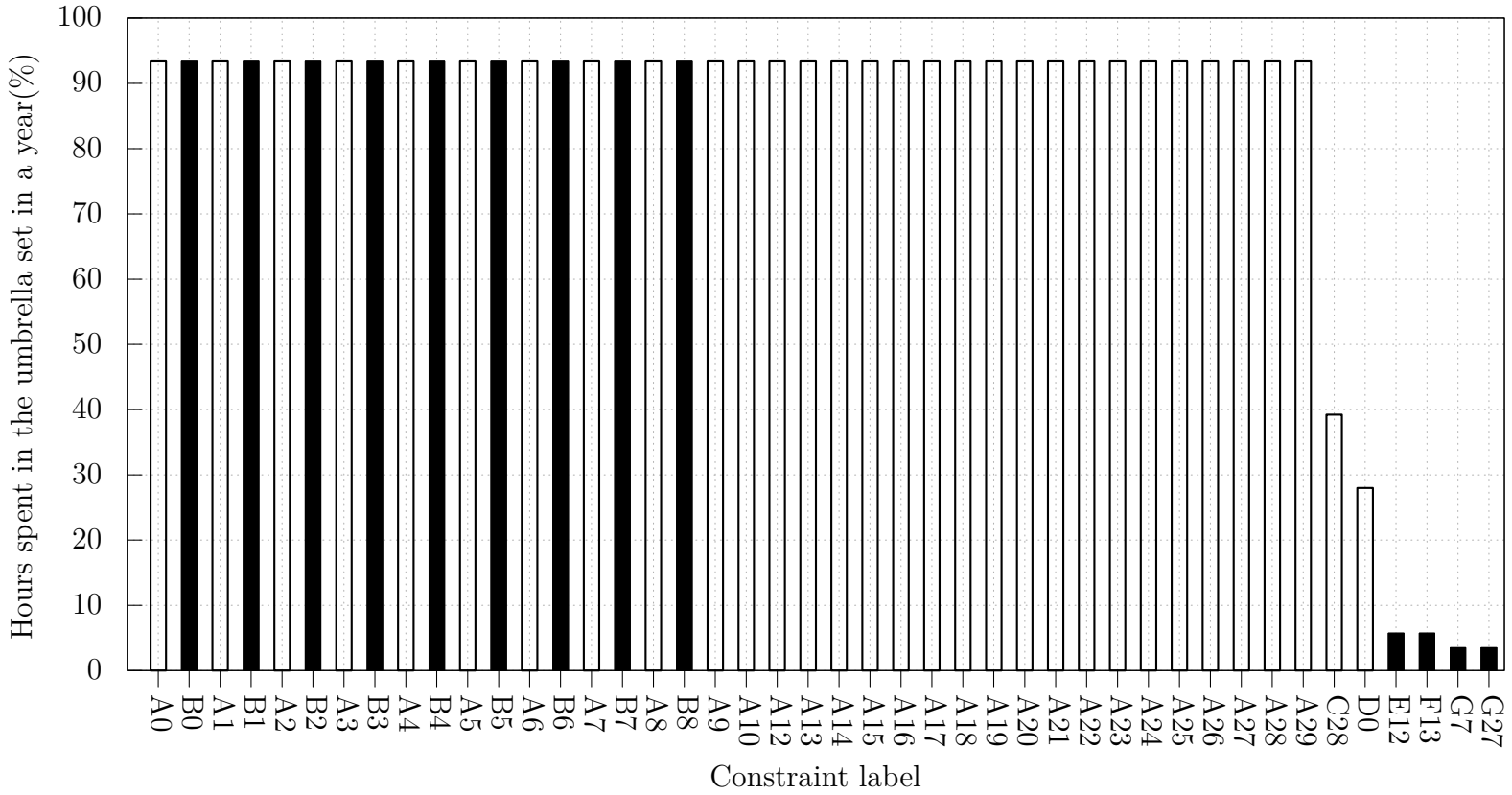

Figure 2.15 Percentage of time all constraints spend in the umbrella set in a year. Only the 44 constraints shown here, out of the 2 864 SCOPF constraints, spend some time in the umbrella set. The letters in the horizontal axis labels indicate the lines whose limits are in the umbrella set (A: line 11, B: line 29, C: line 24, D: line 5, E: line 13, F: line 12 and G: line 23). The number next to each letter indicates the contingency state associated with that limit. Black bars indicate lower flow limits, while white bars indicate upper flow limits.

2.9 Discussion

One may argue that the UCD-II solution times are prohibitive for practical power system use; however, we argue that it should not be the case if UCD-II is used in the appropriate context. UCD-II is *not* meant for directly assisting real-time operations, yet its outcomes could greatly improve the scope of application of SCOPF approaches in real time. It should be used at the operational planning stage to list out systematically the constraints operators should be concerned about and indicate which of the failures could have the most impact on operations and future dispatch decisions. In real time still, UCD-II in its separated version, (2.20)–(2.22), could be used to assess whether or not a new constraint needs to enter the current umbrella set or not. Ultimately, real-time SCOPF applications are to gain more importance as power systems are subject to ever more rapidly-changing conditions, and as limited network resources need to be allocated rapidly. A tool like UCD should contribute to streamline real-time SCOPF computations because it has the potential to make them as compact as they can realistically be.

In fact, an SCOPF formulation, of which all non-necessary constraints have been removed through the prior use of UCD-II, could be solved by an iterative dispatch-SFT process as outlined in [32]. In that case, the dispatch-SFT process would run much faster first because the number of constraints to be assessed would be significantly lower than in the original problem. Second, once the initial dispatch is assessed through the SFT, the next dispatch would be optimal because *all* binding constraints would have been found by the SFT. This is the case because once violated umbrella constraints are satisfied *all* of them have to be satisfied simultaneously. Moreover, UCD-II could be useful in assessing whether or not new line investments or line retirements may have significant impacts on the feasible operating space of a network. For example, if after adding a line, one finds that

the number of line-based umbrella constraints has decreased with respect to a base case, then this investment proposal may be beneficial because it would contribute to expand the network's operating space.

The current approaches available in the literature focus only on identifying the binding (or active) constraints, or heuristically flagging contingencies for further analysis (contingency screening)—see Section 2.1. We proposed a formulation which allows for the identification of *all* constraints in SCOPF problems which are necessary and sufficient to form the feasible set of solutions of the problems. We also argued in Section 2.4.3 that UCD-II can identify the minimum set of constraints necessary and sufficient to describe the feasible set of *any* optimization problem with convex constraints.

SCOPF solution methodologies, which only seek the optimal solution of an SCOPF problem, can be faster than successively solving UCD-II and its resulting compact SCOPF formulation. However, the empirical evidence provided in Section 2.8 demonstrates that the results of UCD are stable within often wide ranges of load, and that they are following the same weekly and daily periodic patterns as the load. Therefore, once an umbrella set is established for a given load range, it can be reused when the load falls within that range and geographical distribution. Otherwise, one may use the union of all potential umbrella constraints at all times found offline. This union set, albeit not always minimal, is still much smaller than the original set of SCOPF constraints and its use should lead to significant SCOPF solution time savings.

2.10 Summary and Conclusion

The solution of SCOPF problems is challenging because of their inherent large constraint numbers. We saw that in the case of IEEE 118 bus system, we have 65 730 constraints if

the $N-1$ security criterion is considered. As empirical evidence and longstanding operator experience show, relatively few of the constraints of SCOPF problems actually serve to enclose the feasible region of these problems. Removing these superfluous constraints can reduce the sizes of SCOPF, thus improving the solution time and numerical stability of their solution processes. In this chapter, an optimization-based formulation was proposed for identifying umbrella constraints in SCOPF problems or, in fact, *any* optimization problem with convex constraints. Note that the proposed formulation is independent of the objective function of the SCOPF problem. So, even if the objective function is not convex, the proposed formulation can be applied successfully. The most attractive umbrella constraint discovery problem formulation is a linear program, which, nonetheless, is not a trivial optimization problem when dealing with practical SCOPF problems. We addressed this matter by proposing a flexible decomposition approach amenable to parallel computation.

In the first step, we implemented the formulation on a small three-bus system as well as a medium size system, the IEEE Reliability Test System—1996. We have generated empirical evidence using both systems showing the relative insensitivity of the umbrella set to changes in demand and the correlation between system load and umbrella set membership. Also, we tested the linear programming version of UCD on an SCOPF implementation for the IEEE 118 bus test system and showed that more than 99.31% of its constraints are indeed superfluous. By removing them, the SCOPF solution time was improved by two orders of magnitude.

In the next chapter, we propose a new formulation —called *partial* UCD— based on the UCD-II formulation that can be carried out significantly faster than other proposed formulations. We implement this new method on different SCOPF problems and compare the results with UCD-II.

Chapter 3

Partial Umbrella Constraint Discovery

3.1 Introduction

In the previous chapter, we explained how the umbrella constraint discovery (UCD) problem [1] can successfully and systematically identify all umbrella constraints of a given optimization problem. We also noted that the solution time of the corresponding UCD problem is significantly longer than that of its corresponding SCOPF problem. We proposed a decomposition technique to overcome this shortcoming, and we showed the effectiveness of this technique by implementing it on different test systems. In this chapter, we propose another UCD problem formulation that can identify non-umbrella constraints very fast. This new formulation, called *partial UCD*, can be used as a pre-screening tool for constraints before solving the full UCD problem. By using this technique, the number of constraints entering UCD can be reduced significantly, resulting in a much faster solution of UCD.

1. In the remainder of this dissertation, the acronym UCD refers to the UCD-II formulation, unless otherwise stated.

We first discuss the motivation behind the proposal of this new formulation by pointing out some of the computational inefficiencies in UCD and then we present the formulation of partial UCD. Finally, we present the results of applying partial UCD on different test systems and we compare its solution time with original UCD solution times.

3.2 Computational Inefficiencies in UCD

In Chapter 2, we proposed a formulation that could identify the umbrella constraints of an optimization problem in the general form found in (2.7) and (2.8). We also proposed UCD-II, (2.14)–(2.16), as a way to identify all umbrella constraints of an SCOPF problem.

Ironically, the main drawback of UCD is also its size due to its large number of constraints. The vast majority of UCD constraints is coming from the set of constraints in (2.15). Throughout the solution process, the LP solver has to look for w_j values for each constraint in (2.16) while ensuring its feasibility against all other constraints in (2.15). In the event where such a w_j cannot be found, s_j must be increased until feasibility is re-established. The observation one makes here is that the moment $s_j > 0$, there is no longer a need to keep on searching for a feasible w_j as constraint j is proved to be non-umbrella (as per the Non-Umbrella Constraint Lemma presented in Section 2.5.2). Therefore, it is pointless to keep on comparing other constraints to a proven non-umbrella constraint. It is also equally true that it is wasteful to compare non-umbrella constraints against each other. For instance, in Section 2.7.3 and in ([99]) when considering the IEEE 118 bus test system, we found that only 451 constraints were indeed umbrella. Therefore, throughout the UCD solution process, 65 279 SCOPF non-umbrella constraints were being compared against each other without providing any more information about the actual set of umbrella constraints. Thus, as a rule of thumb, we should seek to maximize the comparison

of potentially non-umbrella constraints only with those constraints which would be likely umbrellas. Such likely umbrella constraints are the generation limits and the power balance which, in the case of the IEEE RTS, are members of the umbrella set throughout the year 2.8.2.

3.3 Partial UCD

As mentioned above, in UCD a constraint j is flagged as umbrella if the LP solver is able to find a point w_j on that constraint that satisfies all other constraints. To complete this *proof* of umbrella membership, one requires that the constraint be compared against *all* other constraints. On the other hand, to flag a constraint j as non-umbrella, a single cross-constraint comparison with j' could be enough if that comparison is able to show that there is no point on constraint j that can satisfy that other constraint j'. We recall also that if a constraint is flagged as non-umbrella at any point during the solution process, that constraint *is non-umbrella for the entire set of constraints*, according to the Non-Umbrella Constraint Lemma.

Obviously, it is not practical to interrupt the LP solution process every time an instance of $s_j > 0$ is being found. Instead, we propose here to solve an approximation of UCD as a preprocessing step to its full solution. This preprocessing step, which we call *partial UCD* (P-UCD), serves to rapidly identify non-umbrella constraints with the objective of reducing the number of necessary constraint comparisons in the solution of the full UCD. The goal of P-UCD is to identify non-umbrella constraints with as few cross-constraint comparisons as possible. In the ideal case, we aim to identify non-umbrella constraints with only one comparison. In order to achieve this goal, we should compare a non-umbrella constraint to only an umbrella constraint. Therefore, we need to know which constraints are most likely

to end up in the final umbrella set and compare the remaining constraints to them.

In P-UCD, the SCOPF constraint set is partitioned into two subsets: potential umbrella ($\mathcal{J}_\nu$) and potential non-umbrella ($\mathcal{J}_\eta$) constraints such that $\mathcal{J} = \mathcal{J}_\nu \cup \mathcal{J}_\eta$ and $\mathcal{J}_\nu \cap \mathcal{J}_\eta = \emptyset$. The membership in the potential umbrella and non-umbrella constraint sets are determined heuristically. The heuristic here should be based essentially on operator experience and/or on past UCD results. For instance, if the results of a prior UCD run are available, it is reasonable to assume that the current UCD results will be similar given similar operating conditions, as seen in [99]. Thus, in that case, $\mathcal{J}_\nu$ would contain the umbrellas from the past UCD run and $\mathcal{J}_\eta$ would contain its non-umbrellas. Another valuable partition would be to have $\mathcal{J}_\nu$ include the economic dispatch constraints (*i.e.* the generation limits and the network-wide power balance), while $\mathcal{J}_\eta$ regroups all line flow limits. This is also in line with the evidence found in [99], which shows that the vast majority of SCOPF umbrella constraints come from the generation side.

By partitioning the constraint set into a potential umbrella ($\mathcal{J}_\nu$) and a potential non-umbrella ($\mathcal{J}_\eta$) sets and comparing only these two sets against each other, we should avoid the redundant comparisons between umbrella constraints as well as between non-umbrella constraints.

3.3.1 Formulation of Partial UCD

Let us pick a constraint $j \in \mathcal{J}_\nu$. Also, let a_j denote the vector corresponding to the j^{th} row of matrix A and b_j the j^{th} element of the b vector of the system of inequalities in (2.8). Similarly, for $j' \in \mathcal{J}_\eta$, let $a_{j'}$ denote the vector corresponding to the j'^{th} row of matrix A and $b_{j'}$ the j'^{th} element of the b vector of (2.8). Let us also define an arbitrary vector $w_j \in \mathbb{R}^I$, where I is the number of variables in the SCOPF. We claim that by solving the following optimization problem, the non-umbrella constraints in the set $\mathcal{J}_\eta$ with respect to

the constraints in $\mathcal{J}_\nu$ are identified [100].

Proposition 4 (Partial UCD (P-UCD))

$$\min_{w,s\geq 0} \sum_{j\in\mathcal{J}_\eta} s_j \tag{3.1}$$

subject to,

$$a_{j'}^T w_j \leq b_{j'} \qquad j \in \mathcal{J}_\eta,\ j' \in \mathcal{J}_\nu \tag{3.2}$$

$$a_j^T w_j + s_j \geq b_j \qquad j \in \mathcal{J}_\eta \tag{3.3}$$

The interpretation of partial UCD is very similar to that of the original UCD. If constraint $j \in \mathcal{J}_\eta$ is indeed umbrella, there exists a w_j that can lie on the hyperplane $a_j^T w_j = b_j$ (as dictated by (3.3)) while still remaining feasible with respect to all constraints in subset $\mathcal{J}_\nu$, (3.2). In the case where constraint $j \in \mathcal{J}_\eta$ is not umbrella, to maintain the feasibility of P-UCD, s_j should be increased until one finds a w_j which can lie on the hyperplane $a_j^T w_j = b_j - s_j$ while simultaneously satisfying all constraints in subset $\mathcal{J}_\nu$. This is just like UCD where the slack variables s_j serve to bring all non-umbrella constraints to the border of the feasibility region to ensure the feasibility of the whole problem. In the case of the partial UCD problem, nonetheless, the feasibility region is defined by the constraints in subset $\mathcal{J}_\nu \subseteq \mathcal{J}$ only, which are predetermined based on user input. This is unlike UCD in (2.15) and (2.16) where its feasibility region is defined by all the constraints of the SCOPF.

Fig. 3.1 shows an example of P-UCD. Here, $\mathcal{J}_\nu$ comprises of all constraints except 1–4, 9 and 10. Clearly, constraints 1–4 are umbrella. The only non-umbrella constraints identified through P-UCD are constraints 9 and 10. Partial UCD would find all non-umbrellas if $\mathcal{J}_\nu$ contained only constraints 1–4. In all cases, it is necessary to follow up with a UCD run

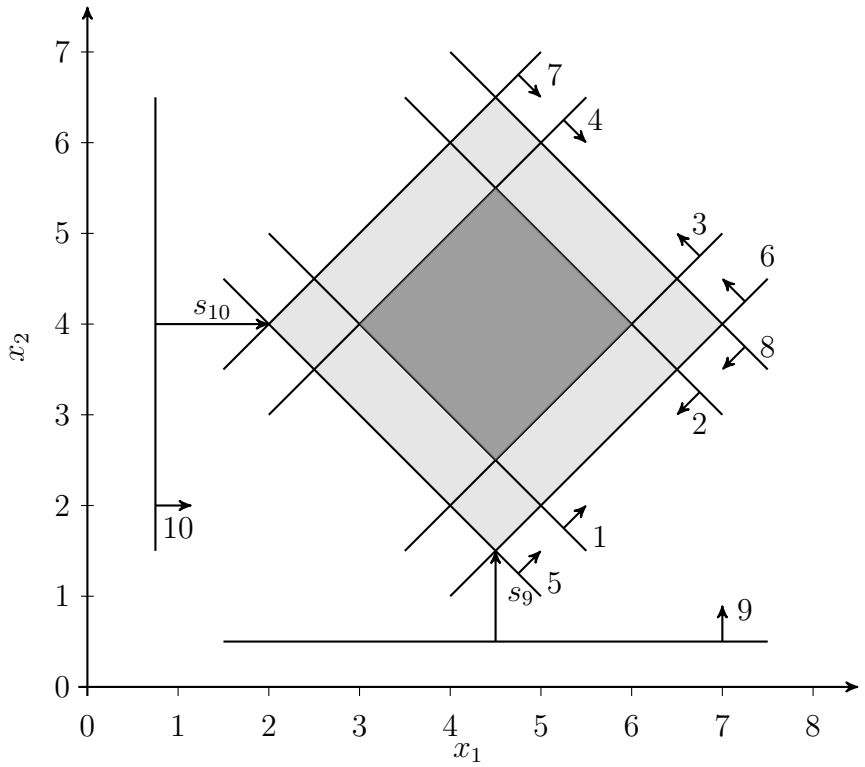

Figure 3.1 Illustration of partial UCD: we assume here that constraints 5–8 are potential umbrellas (members of $\mathcal{J}_\nu$). The remaining constraints (1–4 and 9 and 10) are potential non-umbrella constraints (members of $\mathcal{J}_\eta$). Solving partial UCD will identify constraints 9 and 10 as non-umbrella. The subsequent UCD run on constraints 1–8 would identify constraints 1–4 as umbrella.

to formally identify all umbrella constraints.

Here, we can see by inspection that constraints 1–4 are true umbrella. However, since constraints 5–8 are deemed as potential umbrella constraints, the formulation can easily find w_j for $j = 1, \ldots, 4$ that satisfies all constraints in $\mathcal{J}_\nu$. Therefore, the corresponding s_j for constraints 1–4 remains zero. As we can see, if there are actual umbrella constraints in the potential non-umbrella constraint set, $\mathcal{J}_\eta$, P-UCD will identify those constraints as umbrella constraints. This built-in feature of P-UCD assures the operator that no umbrella constraint will be left out if the set of potential umbrella constraints is not accurately built.

The only non-umbrella constraints identified through P-UCD are constraints 9 and 10. Partial UCD would find all non-umbrellas if $\mathcal{J}_\nu$ contained only constraints 1–4. Otherwise, some true non-umbrellas would not be identified as such. In all cases, it is necessary to follow up P-UCD with a UCD run to formally identify all umbrella constraints. Here, this step would eliminate constraints 1–4.

3.3.2 Size of P-UCD

P-UCD allows for s_j and w_j variables to be allocated to potentially non-umbrella constraints only and therefore, it can have a significantly lower dimensionality in comparison to UCD. It also has a much lower constraint count. As can be seen in the P-UCD formulation, to rule out the non-umbrellas in the subset $\mathcal{J}_\eta$, its elements are compared against constraints in the subset $\mathcal{J}_\nu$ only. The number of constraints in a partial UCD problem is $|\mathcal{J}_\eta| \cdot |\mathcal{J}_\nu|$ which can be significantly less than the number of the corresponding full UCD problem, that is $J(J+2)$. The number of variables in P-UCD is $|\mathcal{J}_\eta|(I+1)$ as opposed to the number of variables in the corresponding UCD problem which is $J(I+1)$. For instance, in the case of the IEEE RTS [94], if we let $\mathcal{J}_\nu$ contain all 50 economic dispatch constraints and $\mathcal{J}_\eta$ hold the remaining 2 814 line flow limits, P-UCD has 140 700 constraints and 67 536

variables. This is in stark contrast with the full UCD which would have over eight million constraints and 71 600 variables.

Obviously, the price to pay with the solution of P-UCD is that it *only identifies the constraints in $\mathcal{J}_\eta$ which are non-umbrella.* It cannot identify any umbrella constraints unless $\mathcal{J}_\nu$ is the umbrella set. As $\mathcal{J}_\nu$ is only a good guess of what the umbrella set is, $\mathcal{J}_\nu$ may contain some non-umbrellas and $\mathcal{J}_\eta$ may have umbrellas within itself. What P-UCD provides is a way to fast-track the identification of non-umbrellas so that a full UCD can be performed only on those constraints in $\mathcal{J}_\nu$ and those in $\mathcal{J}_\eta$ not ruled out as non-umbrellas by P-UCD. This way UCD can be run on a much reduced set of constraints which will be identified as umbrella or not—providing the proof of umbrella set membership.

It is important to note that P-UCD cannot leave out a *true* umbrella constraint by identifying it as a non-umbrella constraint. If a constraint $j \in \mathcal{J}_\eta$ (*i.e.* in the set of potential non-umbrellas) is indeed umbrella, one can find a w_j satisfying all constraints in (3.2). Otherwise, it is non-umbrella by the Non-Umbrella Constraint Lemma. This property ensures that the feasible set of solutions of the original SCOPF problem will never be altered by P-UCD.

As mentioned before, the closer the set $\mathcal{J}_\nu$ is to the umbrella set $\mathcal{U}$, the more non-umbrella constraints in $\mathcal{J}_\eta$ get identified by P-UCD. Therefore, a good estimation of the potential umbrella constraint set is essential for efficient function of P-UCD. In the next Section, we provide empirical evidence of the efficacy of P-UCD as a pre-processing step to a full UCD run.

3.4 Partial UCD Test Results

In this Section, we apply P-UCD on two SCOPF problems which were previously investigated in Chapter 2. We highlight the importance of potential umbrella ($\mathcal{J}_\nu$) and non-umbrella ($\mathcal{J}_\eta$) constraints set selection and how it affects the performance of P-UCD.

3.4.1 Application on IEEE RTS

We use the single-area version of the IEEE Reliability Test System–1996 [94] and form the SCOPF problem considering only line contingencies in the first hour of the RTS year. The machine which we use to run the tests is a PC with a Xeon E5606 2.13 GHz CPU and 24 GB of RAM. The corresponding SCOPF problem has a constraint set of size 2 864 (set $\mathcal{J}$), where 2 814 constraints are arising from line constraints, 48 are from generation limits at each bus —two constraints at each bus to enforce generation limits— and two constraints are from the system-wide load balance—which are stemming from the conversion of the system-wide load balance equality to two equivalent inequality constraints. Similar to the modeling done in Chapter 2, we do not include the outage of line 11 in the contingency list. The solution time of the corresponding SCOPF problem subject to all constraints is 0.015 s. By running UCD on the SCOPF constraint set, 87 umbrella constraints are identified (3% of constraints are umbrella). The run time for UCD (ran without decomposition) is 219.35 s, while using the line-based decomposition technique proposed in [99], the UCD run time can be decreased to 3.369 s.

To test partial UCD, an estimate of the actual umbrella constraints is necessary. The experience of running UCD on this network (see [99]) suggests that most of the generation limits are part of the final umbrella set along with the load balance. Therefore, a good estimation of the umbrella set $\mathcal{J}_\nu$, as suggested in the previous section, would be the set of

generation limits and the load balance constraints. The remaining constraints, which are all arising from line operations under no-contingency and contingency states, form the set $\mathcal{J}_\eta$.

These potentially umbrella and non-umbrella constraint sets are applied to (3.2) and (3.3), and the corresponding solution time for partial UCD is 0.484 s. Hence 2 776 out of 2 814 constraints in $\mathcal{J}_\eta$ (98.6%) are flagged as non-umbrella. Only 38 constraints in set $\mathcal{J}_\eta$ are flagged as potential umbrellas.

In the next stage, the 38 potential umbrellas from $\mathcal{J}_\eta$ are merged with the 50 constraints from $\mathcal{J}_\nu$. UCD is run with those 88 remaining constraints, and it takes 0.016 s to run. The result of UCD is that only one generation limit from the set $\mathcal{J}_\nu$ is finally identified as non-umbrella. Therefore, the final umbrella set has 87 constraints of which 38 are coming from line constraints and 49 are coming from generation limits and load balance constraints (as before). The total time for running P-UCD followed by UCD is 0.500 s. Following this, if the minimum cost SCOPF is solved subjected to its umbrella set only the solution time is virtually 0 s. Clearly here, P-UCD is very effective. Given the result (the elimination of one extra constraint only) of the final UCD step and the extra time it takes to run it (0.016 s), one may forgo it completely.

As it can be seen from these results, the solution time of UCD can decrease significantly if the constraints are preprocessed using P-UCD; here we see a reduction from 219.35 s (using line-based partitioning) down to 0.5 s (0.23% of the UCD original time with line-based decomposition). As was discussed before, the efficacy of P-UCD is strongly dependent upon the accuracy of the potential umbrella set $\mathcal{J}_\nu$. The estimation of the potential umbrella set is not always a simple task. As will be shown in the next subsection, it is not always enough to include generation limits and load balance constraints in $\mathcal{J}_\nu$. A poor estimation of the potential umbrella set may result in the identification of only a few

non-umbrella constraints in $\mathcal{J}_\eta$ thus making the P-UCD step counterproductive.

3.4.2 Application on IEEE 118 Bus System

In this section we use the same IEEE 118 bus system and its corresponding SCOPF that we used in Chapter 2. However, we reduce the load of the system at all nodes by 20% to represent the system load hourly variations. The corresponding SCOPF problem of the IEEE 118-bus system [2] has 65 730 constraints. Generation limits account for 236 constraints, and the load balance constraints contribute two more inequality constraints. Only 176 line contingencies are considered, and the constraints arising from the operation of the lines under these contingencies account for the remaining 65 492 constraints. The SCOPF problem takes 2.808 seconds to be solved. The corresponding UCD problem of this SCOPF is too large to be solved directly as the one formulated with for the IEEE RTS.

Line-based decomposition is used to partition UCD problems into smaller sub-problems. These sub-problems are independent from each other and can be run using parallel computing. We have 186 sub-problems and the cumulative run time of the UCD using line-based decomposition takes 3 541.6 s to complete.

Partial UCD is used here to pre-process the set of constraints and rule out some non-umbrella constraints in order to reduce the size and solution time of the full UCD. To set up P-UCD, an estimation of potential umbrella constraints is necessary. We shall assume the same $\mathcal{J}_\nu - \mathcal{J}_\eta$ partition used with the IEEE RTS above, *i.e.* all generation-based limits of the network along with the system-wide load balance constraints are forming the set $\mathcal{J}_\nu$, and all of the line-based constraints are in the set of potential non-umbrella constraints, $\mathcal{J}_\eta$. Therefore, $\mathcal{J}_\nu$ has 238 members and the rest of the constraints (line constraints) belong

2. The complete data set of 118-bus system which was used in this study can be found at http://cl.ly/3x0L3L393r24.

to $\mathcal{J}_\eta$ which has 65 492 constraints. P-UCD has about 15.5 million constraints, which is too large to be solved directly. The solution is to break down the set $\mathcal{J}_\eta$ into smaller subsets (100 here) and run partial UCD on each of them. These subsets can be formed using different approaches such as line-based or contingency-based decomposition. These sub-problems can be solved independently using parallel computing.

We note here that although we are using line-based partitioning here, in partial UCD the partitioning approach does not matter. In partial UCD we are comparing the constraints against a fixed set of constraints ($\mathcal{J}_\nu$). In other words, we assume that we know the umbrella set, and we check if the constraints in $\mathcal{J}_\eta$ are umbrella with respect to constraints in $\mathcal{J}_\nu$. There is no comparison amongst the constraints in $\mathcal{J}_\eta$. However, in UCD we try to find the umbrella set of each sub-problem by comparing all constraints present in that sub-problem. Therefore, in partial UCD we use partitioning merely as a tool to reduce the size of the problem, so we can solve the UCD using available resources.

After partitioning the set $\mathcal{J}_\eta$, each of the sub-problems are solved using partial UCD with $\mathcal{J}_\nu$ as the potential umbrella constraint set. P-UCD takes 42.819 s to run cumulatively, with 0.0654 s on average for each subset, and it identifies 39 806 constraints from the set $\mathcal{J}_\eta$ as non-umbrellas. This leaves us with 25 686 constraints as potential umbrellas in $\mathcal{J}_\eta$. The large number of remaining constraints in $\mathcal{J}_\eta$ could be because some of the generation limits in $\mathcal{J}_\nu$ are not as stringent as in the RTS case, while many of the line constraints in $\mathcal{J}_\eta$ are more demanding and cannot be flagged as non-umbrella by the generation and load balance constraints alone.

The remaining number of constraints in $\mathcal{J}_\eta$ is still too large to be considered for a single run of a UCD to identify all umbrella constraints. This is mostly because the estimation of the umbrella set was not accurate enough. To address this issue, there are two options. Firstly, the problem can be solved using decomposed UCD which will identify all umbrella

constraints at the expense of more computation time. Otherwise, we can use a better estimation of the potential umbrella constraints in the first place. An example of such a more exact estimation of the umbrella constraints could be the umbrella set of the previous operating hour.

We consider now the case where the set $\mathcal{J}_\nu$ is set to $\mathcal{U}$ from the previous hour of operation which typically has similar loading patterns to that of the current hour. redWe assume that the results presented in Section 2.7.3 are representing the results for the previous hour run of UCD. The umbrella set of the previous hour has 451 constraints, of which 234 are stemming from generation-based constraints while 217 are from line-based constraints. Since change of system load, may move some constraints in or out of the umbrella set, there might be some line-based constraints in $\mathcal{U}$ that are already identified as non-umbrella in the present hour. Therefore, we are interested in $\mathcal{J}_\eta \cap \mathcal{U}$. This set contains the line-based constraints which were umbrella in the previous hour and have not been identified as non-umbrella in the first round of P-UCD. In this case, there are six constraints in $\mathcal{U}$ which are identified as non-umbrella by P-UCD in the first round. Likewise, there might be generation-based constraints in $\mathcal{J}_\nu$ which are not in $\mathcal{U}$. We would like to move those constraints to the set $\mathcal{J}_\eta$ as they are likely to be non-umbrella. This accounts for four generation-based constraints. We remove these constraints and append them to the new $\mathcal{J}_\eta$.

At the end of the first step, we have $|\mathcal{J}_\eta| = 25\,686$ constraints. This set has 211 constraints in common with the previous hour umbrella set —$|\mathcal{J}_\eta \cap \mathcal{U}| = 211$. In other words, there are six constraints in $\mathcal{U}$ which have moved out of the umbrella set due to the load change and they are identified as non-umbrella in the first step. Since in the first step, we only compared the constraints of $\mathcal{J}_\eta$ with the generation limits and load balance constraints, it can be said that these six constraints have moved out of the hypercube built by generation

limits. So, the number of line constraints present in the new $\mathcal{J}_\eta$ is $25\,686 - 211 = 25\,475$ constraints. Now, in $\mathcal{J}_\nu$, there are four constraints from the generation-based constraints that are not in $\mathcal{U}$. Those constraints are also appended to $\mathcal{J}_\eta$. In total there are $25\,475+4 = 25\,479$ constraints in the new potential non-umbrella set, $\mathcal{J}_\eta$. As for the potential umbrella set, we should have 451 constraints from $\mathcal{U}$. But, we remove the constraints in $\mathcal{U}$ that are already identified as non-umbrella for the current hour which accounts for six constraints. Therefore, the new potential umbrella set, $\mathcal{J}_\nu$, contains $451 - 6 = 445$ constraints.

As before, the set of potential non-umbrella constraints, $\mathcal{J}_\eta$, is divided into smaller subsets, each with 100 constraints here, and partial UCD is run for each of the subsets. Each subset takes 2.44 s to run on average and the cumulative run time for all subsets is 621.83 s. At this stage, only 393 constraints remain in $\mathcal{J}_\eta$ which shows the efficiency of the alternative potential umbrella set $\mathcal{J}_\nu$. Including $\mathcal{J}_\nu$, there are now 838 constraints which have the potential to be in the final umbrella set. The number of remaining umbrella constraints is small enough to run a full UCD on them. UCD takes 85.19 s to run and identifies 390 constraints as non-umbrella. The final umbrella set contains 448 constraints, of which 213 constraints come from line constraints (about 0.3% of all line constraints in the original set of constraints) and 235 constraints come from generation limits and load balance constraints. The total run time for this method, including partial UCD followed by UCD, is 749.84 s which is around 21% of the best UCD run time using decomposition.

The 213 line constraints in the umbrella set are coming from the operation of 53 lines in 83 contingencies. The lines and the number of times its corresponding constraints are present in the umbrella set are shown in Fig. 3.2. Line 54—connecting bus 30 to 38—has the largest contribution in the umbrella set. Fig. 3.3 shows the umbrella contingencies of the SCOPF problem. The contingencies that do not contribute two or more constraints in the umbrella set are not shown in the figure.

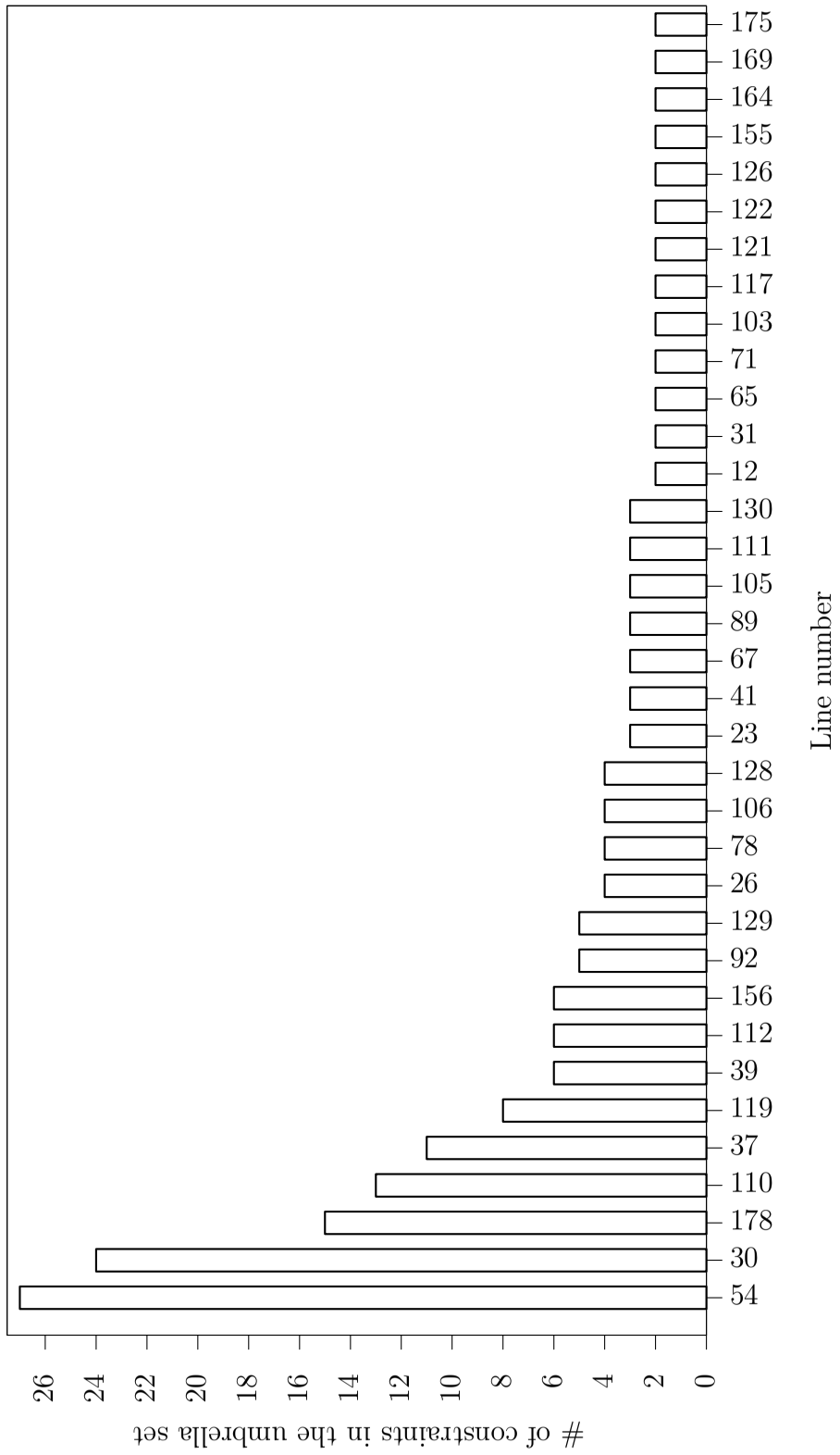

Figure 3.2 The lines that contribute more than one constraint to the umbrella set. The lines that contribute only one constraint to the umbrella set are the following: 22, 24, 44, 46, 47, 53, 57, 58, 66, 107, 109, 115, 116, 125, 136, 137, 141, 143, 145, 148, 151, 152, 153, 159.

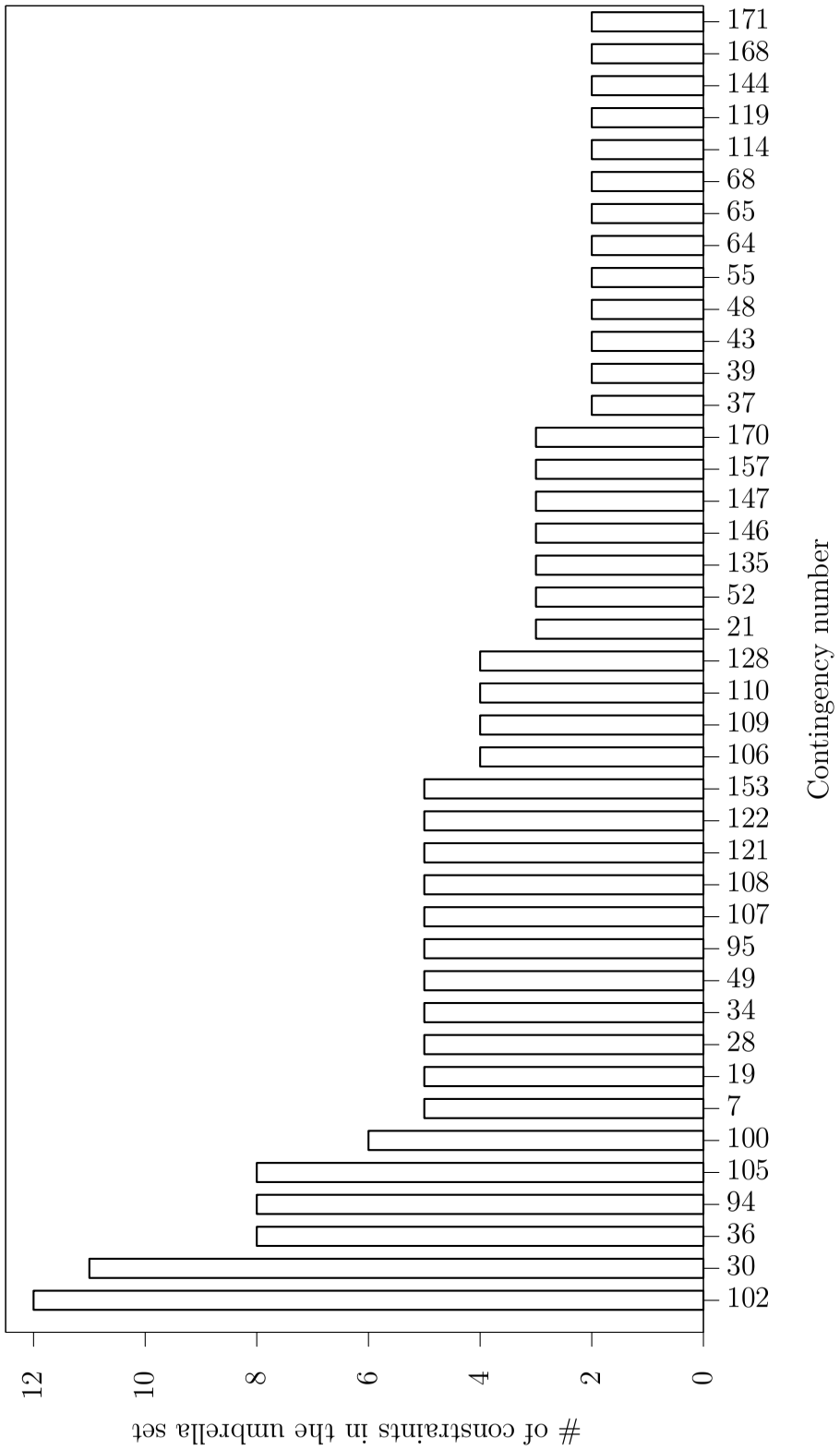

Figure 3.3 The set of contingencies contributing to the final umbrella set. Only the contingencies which contribute more than one constraint in the umbrella set are shown. The following constraints contribute only one constraint to the umbrella set: 5, 13, 14, 16, 18, 20, 23, 24, 27, 29, 31, 35, 40, 42, 46, 51, 58, 59, 75, 82, 88, 91, 92, 93, 103, 104, 111, 112, 113, 129, 130, 131, 138, 139, 141, 143, 145, 152, 154, 155, 169, 175.

Table 3.1 UCD Solution Times with and without the Application of P-UCD

Test Network	UCD	Partial UCD	Diff.
IEEE RTS	240 s	0.5 s	0.23%
IEEE 118 bus	3 541.6 s	751.2 s	20%

Table 3.1 summarizes the progress made through the use of P-UCD to streamline the solution of UCD. In the case of the IEEE RTS especially, the results are impressive. However, the observations here may be artifacts of the structure of this particular test network which is known to be *transmission strong* and *generation weak*. The fact that most of the generation limits are umbrella indicates that the generation system restricts the feasible space of the SCOPF the most, while transmission constraints do not contribute much to the restriction of operations. In the case of the IEEE 118-bus system the situation is not as clearcut, but the results show a significant improvement over the best case without P-UCD. Given those improvements in UCD performance when combined with P-UCD, one can consider its application to the security-constrained unit commitment, as we do in the next Chapter.

3.5 Summary and Conclusion

In this chapter we presented a new formulation —called *partial* UCD— that is able to identify non-umbrella constraints very quickly. Partial UCD exploits the Non-Umbrella Constraint Lemma from Chapter 2 to pre-screen some non-umbrella constraints in order to reduce the size of the umbrella set entering the UCD problem. Partial UCD decreases the number of comparisons that are necessary in UCD formulation to flag a constraint as umbrella or non-umbrella. In fact, partial UCD only identifies non-umbrella constraints since, ideally, one comparison is enough to flag a constraint as non-umbrella. On the other

hand, identifying a constraint as umbrella requires comparing that constraint against all other constraints in the constraint set. Partial UCD is applied on SCOPF problems of the IEEE RTS and the IEEE 118 bus system. For the case of the IEEE RTS, we showed that the solution time of the corresponding UCD can significantly be reduced if partial UCD is used to pre-process the constraints entering UCD. We used generation limits and load balance constraints as the potential umbrella set for this system. For the case of the IEEE 118 bus system, the size of the SCOPF problem does not allow for a direct partial UCD run. Therefore, similar to UCD, a we use partitioning and decomposition to break down the problem into smaller sub-problems. We showed that in the case of the IEEE 118 bus system, choosing generation and load balance limits as potential umbrella constraints does not identify many non-umbrella constraints. We later show that using the results of the previous run of UCD on this network is a better estimation for the potential umbrella set as it identifies most of the non-umbrella constraints. The total solution time is significantly reduced by accompanying UCD by a pre-processing step using partial UCD.

Given the improvements in UCD performance when combined with P-UCD, one can consider its application to the security-constrained unit commitment, as we do next.

Chapter 4

Application to Unit Commitment Problems

4.1 Introduction

UCD has proven to be a very effective tool in identifying non-umbrella constraints in SCOPF problems. One of the most important tools for ISOs and RTOs in day-ahead market clearing is security-constrained unit commitment (SCUC), which is solved repeatedly. By solving SCUC problems, operators aim to minimize the operation cost of the system or the total bid cost while satisfying a subset of technical constraints of the power system. Technical constraints arise from operation of the system in pre- and post-contingency states and include system load demand, line limits and generation units constraints, such as ramping limits, minimum up/down times, *etc.* A generic SCUC problem formulation is presented in this Chapter. SCUC problems are more challenging than SCOPF problems mainly due to the presence of binary variables and because of time couplings. Thus, it could be beneficial to apply UCD as a preprocessing step to SCUC because of the relative

stability of the power system feasibility region over time spans of 12 to 24 hours. In this Chapter, we first explain that how UCD treats the mixed-integer problems (MIP) and then we implement UCD on different UC and SCUC problems.

4.2 UCD and Mixed-Integer Problems

In power systems, unit commitment problems and their variations, such as SCUC, belong to the class of problems called mixed-integer problems (MIP) since they include binary variables representing the status of the generating units in the system. A general MIP can be represented by the set of equations in (4.1)–(4.3).

$$\min f(p,u) \tag{4.1}$$

subject to

$$[A|B]\begin{bmatrix} p \\ - \\ u \end{bmatrix} \leq \begin{bmatrix} b \\ - \\ c \end{bmatrix} \tag{4.2}$$

$$u \in \{0,1\}^M \tag{4.3}$$

where p is a vector in $\mathbb{R}^N$ lumping all of the network's continuous decision variables, u is a vector representing all (M) binary decision variables of the network, $f(p,u)$ is some objective function, A and B are constant matrices and b and c are constant vectors all with appropriate dimensions.

We argue here that the nature of variables are immaterial in applying UCD. Therefore, if the original optimization problem includes binary variables, to form the corresponding

UCD, we use 0-1 relaxations on these variables by adding two constraints corresponding to each variable to the set of constraints. These two constraints bound the value of each variable between 0 and 1. Therefore, if a constraint is umbrella for the MIP, it will be umbrella for the LP relaxation problem. Also, a non-umbrella constraint of the LP relaxation problem, will be non-umbrella to the MIP. Nonetheless, it is possible to have a constraint which is identified as umbrella for the LP relaxation and which may turn out to be non-umbrella for the MIP. As a result, the application of UCD onto the LP relaxation of (4.1)–(4.3) would generate *the most compact MIP formulation*, but *not necessarily the tightest one* (corresponding to its convex hull). We demonstrate this concept next using an example.

Assume we have the following optimization problem and whose feasible set of solutions is defined by (4.5)–(4.9).

$$\min f(x) \tag{4.4}$$

subject to,

$$x_2 \geq 1 \tag{4.5}$$

$$x_1 + x_2 \leq 8 \tag{4.6}$$

$$-x_1 + x_2 \leq -1 \tag{4.7}$$

$$x_2 \leq 4 \tag{4.8}$$

$$x_1 + x_2 \geq 3 \tag{4.9}$$

The coloured area in Fig. 4.1 shows the feasible set of solutions for the above problem. The optimum solution of this problem can be located at any of the vertices of the triangle

depending on the objective function for this optimization problem [1]. Note that the feasible set of solutions is indeed independent of the objective function.

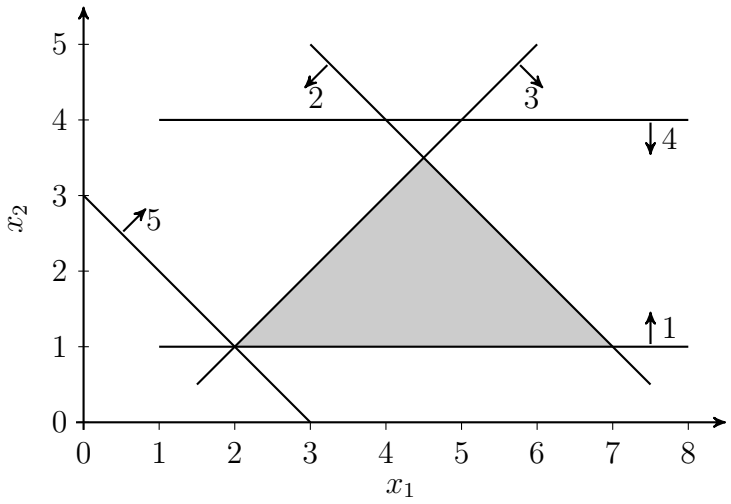

Figure 4.1 Feasible set of region of a given example with continuous variables

Now, assume that both variables x_1 and x_2 are restricted to be integer. The feasible set of solutions for this case, is shown in Fig. 4.2. Note that only the black dots represent feasible solutions of this problem.

By inspection of Fig. 4.2 and Fig. 4.1, we can see that by applying a 0-1 relaxation of the binary variables we still able to identify the non-umbrella constraints of this problem, *i.e.* constraints 4 and 5. Constraint 5 is actually weakly redundant as was explained in Chapter 2, Section 2.6.1.

Therefore, it can be seen that UCD can still be applied on problems with binary (or integer) variables. By relaxing of these variables, we keep UCD as an LP, which makes UCD a very amenable problem for off-the-shelf LP solvers.

1. We know that for linear problems, the optimal solution should be placed on a vertex of the feasible set of solutions. If the problem has multiple solutions, one of them *must* be located on a vertex [92].

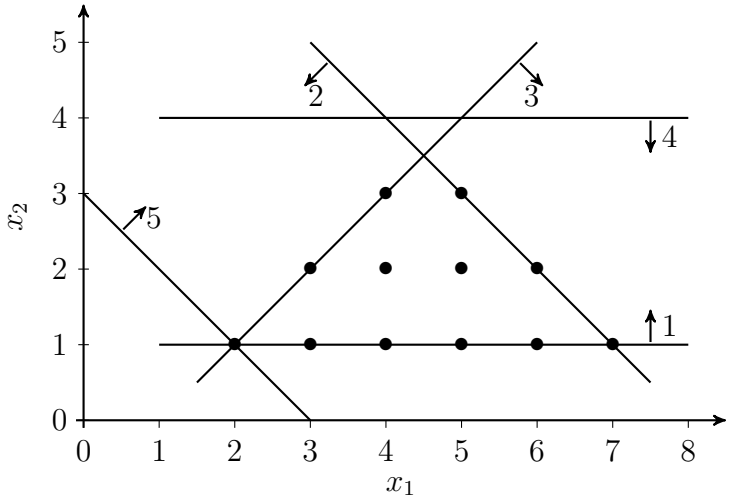

Figure 4.2 Feasible set of an example with binary variables

4.3 Formulation of the Unit Commitment Problem

The goal of an SCUC problem is to find the dispatch level and status of each generating unit such that the operational cost of a network, is minimized while all technical constraints are satisfied. These technical constraints include system-wide demand, generation limits of each unit, line limits, system-wide reserve requirements, ramping limits of generating units and minimum up and down times of each generating unit in both pre- and post-contingency states. We present the formulation and constraints that we have considered in the following.

The SCUC objective function, shown in (4.10), generally minimizes the cost of operation

$$\min \sum_{i=1}^{I} \sum_{t=1}^{T} C_i(p_{i,t}) + \sum_{i=1}^{I} S_i(u_{i,t}) \tag{4.10}$$

where $C_i(\cdot)$ is the generation cost function at generating unit i, $p_{i,t}$ is the generation level of generating unit i at time t and I is the number of network buses. Variable $u_{i,t}$ is a binary variable indicating the status of generating unit i in period t. if $u_{i,t} = 1$, the generating

unit i is turned on and if $u_{i,t} = 0$, the generating unit i is turned off. $S_i(\cdot)$ is the cost function representing the total cost for starting up or shutting down unit i at time t. The above objective function is subjected to the system-wide load balance, for which we ignore losses here,

$$\sum_{i=1}^{I} p_{i,t} = \sum_{i=1}^{I} d_{i,t} \tag{4.11}$$

where i is the index for the network buses and $d_{i,t}$ is the load at bus i at time t.

There are two constraints associated with each transmission line; the lower and the upper limit. Similar to the SCOPF problem, the SCUC problem is subjected to the line constraint and should satisfy

$$-\bar{f}_\ell(k) \leq \sum_{i=1}^{I} h_{\ell i}(k)(p_{i,t} - d_{i,t}) \leq \bar{f}_\ell(k) \tag{4.12}$$

where $h_{\ell l}(k)$ and $h_{\ell i}$ are the linear generation shift factors (*a.k.a.* power transmission distribution factors (PTDF)) relating power injections at bus l and i to the flow in line ℓ while contingency state k is occurring [15, 32].

Generation levels have to be bounded for each generating unit

$$u_{i,t}\underline{p}_i \leq p_{i,t} \leq u_{i,t}\bar{p}_i \tag{4.13}$$

The total system spinning reserve should also be met in each period, t.

$$\sum_{i=1}^{I} r_{i,t} \geq SR_t \tag{4.14}$$

where SR_t is the total spinning reserve requirement for the system at time t and $r_{i,t}$ is the contribution of each generating unit to the total reserve. Reserve contribution, $r_{i,t}$, is also

bounded for each generating unit depending on the current generation of the unit and the maximum reserve the unit can contribute

$$r_{i,t} = u_{i,t} \min\{\bar{r}_i, \bar{p}_i - p_{i,t}\}. \tag{4.15}$$

The ramp up and down rate for each unit is limited

$$|p_{i,t} - p_{i,t-1}| \leq \Delta_i \tag{4.16}$$

where $p_{i,t}$ and $p_{i,t-1}$ are generations of unit i at time t and $t-1$, respectively, and Δ_i is the ramp up/down limit of unit i. The above constraints for ramp up and down of each unit should be active only if the unit remains on at time $t-1$ and t. Parameter $p_{i,0}$ corresponds to the initial condition of the unit, which is usually determined by previous runs of the unit commitment problem.

Minimum up and down times for each unit specify that if a unit is turned on it should stay on for at least its minimum up time or, if it is turned off, it should stay off for at least its minimum down time. These constraints are modeled using the constraints proposed in [101]. For the minimum up time of the units, the following constraints should be satisfied depending on the time that the unit is turned on.

$$\sum_{t=1}^{G_i}[1 - u_i(t)] = 0 \tag{4.17}$$

$$\sum_{n=t}^{t+UT_i-1} u_i(n) \geq UT_i[u_i(t) - u_i(t-1)] \tag{4.18}$$

$$\forall t = G_j + 1, \ldots, T - UT_i + 1$$

$$\sum_{n=t}^{T} u_i(n) - [u_i(t) - u_i(t-1)] \geq 0 \tag{4.19}$$

$$\forall t = T - UT_i + 2, \ldots, T$$

where UT_i is the minimum up time for unit i and G_i is the number of time intervals that unit i must remain on after $t = 0$. If the status of unit i at $t = 0$ is on, G_i will essentially be the minimum of time horizon and the difference between minimum up time of the unit and the number of time intervals that unit i has been on before $t = 0$. If the status of unit i at $t = 0$ is off, G_i is zero. (4.18) ensures that minimum up time requirement is respected for units that are on at $t = 0$. (4.19) enforces the minimum up time for unit i at time intervals between G_i and $T - UT_i + 1$, while (4.20) ensures that if any unit is turned on after $T - UT_i + 1$, it will remain online until the end of the time horizon. The minimum down time of the units is formulated similarly.

$$\sum_{t=1}^{L_i} u_i(t) = 0 \tag{4.20}$$

$$\sum_{n=t}^{t+DT_i-1} [1 - u_i(n)] \geq DT_i[u_i(t-1) - u_i(t)] \tag{4.21}$$

$$\forall t = L_j + 1, \ldots, T - DT_i + 1$$

$$\sum_{n=t}^{T} 1 - u_i(n) - [u_i(t-1) - u_i(t)] \geq 0 \tag{4.22}$$

$$\forall t = T - DT_i + 2, \ldots, T$$

where DT_i is the minimum down time for unit i and L_i is the number of time intervals that unit i must remain off after $t = 0$. If the status of unit i at $t = 0$ is off, L_i will essentially be the minimum of time horizon and the difference between minimum down time of the unit and the number of time intervals that unit i has been off before $t = 0$. If the status of unit i at $t = 0$ is on, L_i is zero. (4.20) ensures that minimum down time requirement is respected for units that are off at $t = 0$. (4.22) enforces the minimum down time for unit i at time intervals between L_i and $T - DT_i + 1$, while (4.22) ensures that if any unit is turned on after $T - DT_i + 1$, it will remain online until the end of the time horizon.

4.4 Application of UCD to SCUC

What we investigate next is the application of UCD and P-UCD to the 0-1 LP relaxation of an SCUC formulation. We also discuss some non-umbrella constraint identifications which could have significant computational benefits for SCUC. Here we make use of the IEEE RTS to illustrate the potential benefits and drawbacks of UCD and P-UCD on the SCUC solution. Fig. 4.3 shows the steps that are taken in order to apply UCD and P-UCD

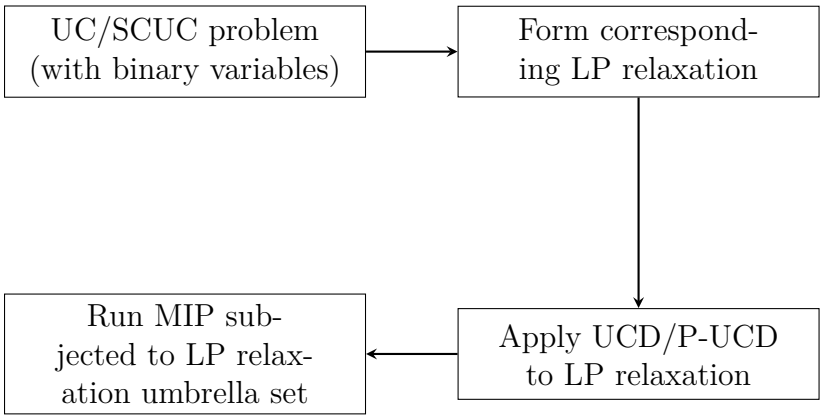

Figure 4.3 Flowchart showing the necessary steps for UCD-based size reduction for SCUC

on SCUC.

4.4.1 Application of UCD on Static Unit Commitment

In this section, we apply UCD on the corresponding single-period (static) unit commitment problem of the IEEE RTS without considering the network for illustrative purposes. We will add the network constraints in the next Section.

In order to form a UCD problem for the static unit commitment problem (UC), we need to consider its 0-1 linear programming relaxation, wherein all binary variables are converted to continuous variables and a lower (0) and upper (1) bounds are added to the set of constraints for each variable.

The IEEE RTS has 32 generating units; therefore, in the corresponding UC, the generation limits contribute 64 constraints—one for the lower and one the for upper generation limits. The load balance equality constraint contributes two equivalent inequality constraints. When forming the corresponding UCD problem, 64 constraints are added for upper and lower limits on the relaxed binary variables. Therefore, in total, the set of constraints for the corresponding UCD problem has 130 elements.

The system load has been varied and the corresponding UC and UCD problems are solved. For different ranges of loads, constraints join or retire from the umbrella set of the problem as expected. All of these constraints are umbrella for loads below 3 005 MW. The interesting observation is that if a lower limit constraint for a binary variable is non-umbrella, *i.e.* $u_i \geq 0$ is non-umbrella, this indicates that the generating unit corresponding to that binary variable would have to be "on" in that range of load when the UC is solved. This observation determines which generators are *must run* for certain transmission conditions. This is very interesting in the context of reliability and market power analysis. If a generator is *must run*, then this generator is needed to participate for reliability purposes. Consequently, it is likely that from the perspective of market power, the offer from that generator should be mitigated. For the IEEE-RTS this situation happens for loads over 3 005 MW where, for example at 3 006 MW, lower limit constraints of units 22 and 23 become non-umbrella, signalling that these two generating units must remain online for any load above that threshold. Also, if the load is increased even more, we observe that the minimum generation limits of those units will also leave the umbrella set. The same phenomenon repeats itself with other units if we keep increasing the load. This observation continues until the load reaches a point where the problem becomes infeasible. Thus, if the lower bound of a relaxed binary variable is flagged as non-umbrella, the corresponding generating unit has to be online in the UC. A similar argument can be made in the case of upper bounds on relaxed binary variables which are non-umbrella, *i.e.* $u_i \leq 1$ is non-umbrella. In that case, the corresponding generator has to be offline. This happens with very light loads of the system.

Knowing ahead of time that some of the binary variables should be fixed prior to the UC solution process is quite advantageous as it would contribute to decrease the computational cost of the corresponding UC branch-and-cut algorithm. This type of information

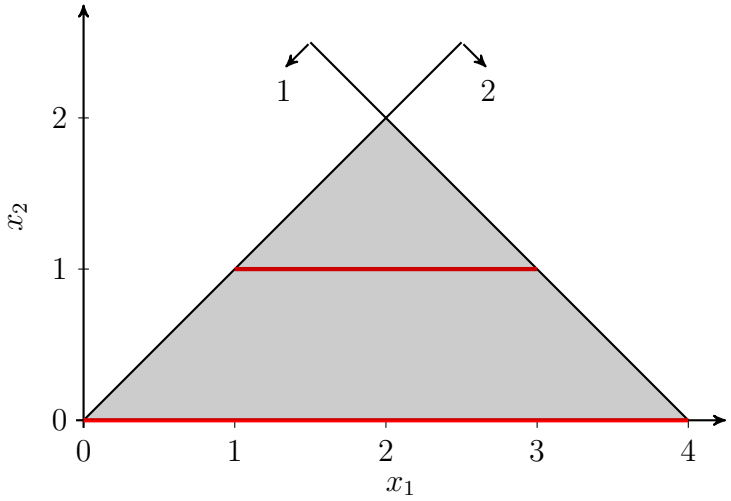

Figure 4.4 The feasible set of a problem with one binary variable and one continuous variable

is only available when the system is either highly or lightly loaded, however. This type of information is not usually available at mid-range loads of the system when binary variable limits are umbrella constraints.

We illustrate this concept using a simple two-variable example. Geometrically, assume the feasible set of the two variable optimization problem shown in Fig. 4.4 where x_1 is a continuous variable and x_2 is a binary variable. The constraints of this problem are defined by (4.23)–(4.26).

$$x_1 - x_2 \geq 0 \tag{4.23}$$

$$x_1 + x_2 \leq 4 \tag{4.24}$$

$$x_2 \in \{0, 1\} \tag{4.25}$$

The feasible set of solutions of this problem are the red lines shown in Fig. 4.4. Equations (4.26)–(4.29) show the binary relaxation formulation of this problem.

$$x_1 - x_2 = 0 \tag{4.26}$$

$$x_1 + x_2 \leq 4 \tag{4.27}$$

$$x_2 \leq 1 \tag{4.28}$$

$$x_2 \geq 0 \tag{4.29}$$

The feasible set of solutions for the 0-1 relaxation problem is shown by the gray area in Fig. 4.4. Running UCD on the 0-1 relaxation will identify all constraints as umbrella. Now, assume that the following constraint is added to the problem $x_2 \geq 0.5$. This constraint can be a non-umbrella constraint that has moved towards the feasibility region because of the increase in the system load. The new feasible set of solutions for the binary problem is shown by the red line and for the 0-1 relaxation is shown by the gray area in Fig. 4.5.

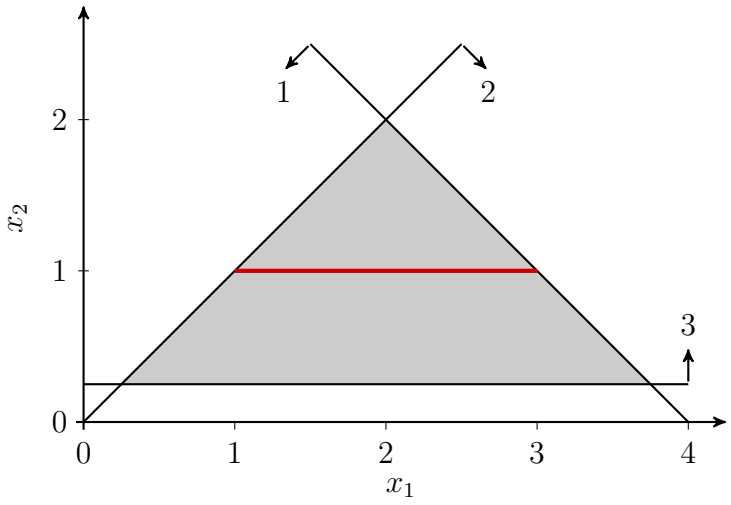

Figure 4.5 The feasible set of the above problem with the new constraint

Now, if we run UCD on this problem, it will identify constraint (4.29) as no-umbrella. As argued before, if the lower limit of a relaxed binary variable is flagged as umbrella,

that variable can only be equal to 1. Inspection of Fig. 4.5 reveals that the feasible set of solutions for this problem consists of points for which $x_2 = 1$. The same argument can be made when the upper limit of a binary variable is flagged as non-umbrella.

4.4.2 Application of UCD on Dynamic Unit Commitment

In this section, we apply UCD and P-UCD on multi-period (dynamic) UC problems with pre-contingency network constraints. The test network is still the IEEE RTS (See Appendix A) and the UC problem is modeled as was explained in Section 4.3.

For the purpose of this study, a planning horizon comprising the first four hours of the IEEE RTS year is considered. This system has 32 generating units and 38 transmission lines. The corresponding SCUC has 1 404 constraints of which 304 come from line limits, while the rest are associated to generation-related inequalities. For each time period we have 76 line constraints, therefore, the total line constraints for a four hour horizon would be $76 \times 4 = 304$ constraints—$2 \times L \times T$ where L is the number of lines in the system and T is the time horizon. As for generation limits, the constraints breakdown is as follows: (i) Load balance constraints count for two constraints in each time period—$2 \times T$, where T is the time horizon, eight constraints in this case, (ii) The reserve requirement counts for one constraint in each time period, T—four constraints in this case, (iii) The total number of constraints assigned to units' reserve limits counts for $3 \times I \times T$ constraints, where I is the number of generating units in the network—384 constraints, (iv) The generation limits count for $2 \times I \times T$ constraints for upper and lower limits—256 constraints (v) The minimum up/down time limits counts for $2 \times I \times T$ constraints—256 constraints, and finally (vi) The ramp up limits count for $2 \times I \times (T - 1)$—192 constraints.

The solution time for the SCUC problem here is 0.063 s with the hardware used previously.

Now, if we consider the corresponding UCD problem, it has an extra 256 constraints associated with the 0-1 relaxation of the binary variables. Therefore, UCD has 1 660 constraints in total here. By running UCD, which takes 69.701 s to solve, only 491 constraints are identified as non-umbrella (29.6%). From the constraints corresponding to the line limits, all of them are non-umbrella for the whole time horizon, except for the upper flow limit on line 11 (between buses 7 and 8) in each time period. This result was expected as the net generation at bus 7 is over the upper flow limit of line 11. From generation-related constraints, all system spinning reserve requirements are non-umbrella as well as most of ramp limits. The most interesting result is that the ramp limits are not restricting unit commitment decisions when it comes to the inter-period couplings. The minimum up/down time restrictions are those playing this role as they are never flagged as non-umbrella. The compact size original problem takes 0.047 s to solve (25% faster than with all constraints). Table 4.1 summarizes the results of application of UCD on static and dynamic unit commitment problems associated with the RTS.

In a scenario where both ramp limits and minimum up/down time constraints are flagged as non-umbrella would be very interesting from an SCUC computational point of view. This would indicate that two successive time periods have no coupling. If this were the case for all generating units simultaneously, it would be possible to split the SCUC between the periods where those non-umbrella constraints arise and then solve them independently. This is obviously desirable property; however, it is very unlikely to happen in practice.

For time horizons over four hours in the case of the IEEE RTS, UCD becomes intractable and cannot be solved directly. In this case, we can use P-UCD to pre-identify some of the non-umbrella constraints. The results of P-UCD when $\mathcal{J}_\eta$ contains all line constraints and $\mathcal{J}_\nu$ holds all generation limits match the results presented in [53].

Table 4.1 Application of UCD on Static and Dynamic Unit Commitment

	Static UC	Dynamic UC
Horizon	1 hr	4 hr
# of constraints	66	1 404
UC run time	0 s	0.063 s
# of UCD constraints	130	1 660
UCD run time	0.109 s	69.701 s
# of non-umbrella	0	491
Compact UC run time	0	0.047 s

4.4.3 Discussion

As it can be seen from the results of the application of UCD on dynamic SCUC problems, not many constraints are proven non-umbrellas. Most of the non-umbrella constraints, as expected, are line flow constraints, and most of constraints arising from generation limits are umbrella. One observation here is that what makes line flow limits good non-umbrella constraint candidates is that they couple a large number of the problem's decision variables [see (2.4) which couples all p_i variables]. Geometrically speaking, these constraints affect multiple dimensions of the problem simultaneously. On the other hand, generation-based constraints contribute to restrict at most four variables simultaneously ($u_{i,t}$, $u_{i,t-1}$, $p_{i,t}$ and $p_{i,t-1}$). Therefore, whether a constraint pertaining to a specific generating unit is flagged as umbrella or not is essentially independent from the constraints on other generating units (unless the system load is very high or very low). In addition, with the introduction of a new time period or a new generating unit, new dimensions are added to the original feasible space. For a constraint which was non-umbrella before the addition of a new variable, this constraint will become umbrella of the new feasible space unless it is explicitly coupled

with the added dimension.

The effective conclusion here is that one should use UCD and P-UCD to reduce the number of transmission constraints (as with SCOPF). However, it is clear that the benefit of applying UCD and P-UCD on unit commitment constraints is very slim given their computational cost.

4.5 Summary and Conclusion

In this chapter, we implemented UCD and P-UCD on unit commitment and security-constrained unit commitment problems. We showed that UCD can successfully identify non-umbrella constraints in these problems. However, the structure of these problems does not generate many non-umbrella constraints, especially in the generation-based constraints. Results of application of P-UCD on UC problems are compared with [53] and the same results are obtained. In the next chapter, we demonstrate that it is possible to exploit the cyclical nature of umbrella constraint/sets over a year to predict the umbrella set using heuristic methods.

Chapter 5

Prediction of Umbrella Sets

5.1 Introduction

In this short chapter, we explore the possibility of predicting the membership in umbrella sets using heuristic methods. The observation that led to this work is the cyclic nature of umbrella sets as well as the system load as can be seen in Fig. 2.12. This figure along with Fig. 2.15 show that the membership of constraints in the umbrella set is relatively insensitive to the changes in system parameters, in this case the system load. Moreover, the constraints that are constructing the umbrella sets are usually constant in the sense that the same constraints are joining or leaving the umbrella set as the system load changes. As seen in Chapter 2, the union of all umbrella constraints consists of few constraints which can move in and out of the umbrella set for the changes of the system load. This fact can inspire the idea that by taking the union of all constraints in the umbrella set of each hour of an operation year, we could circumvent running UCD entirely. By using machine learning techniques, we aim to develop a tool that can "learn" the characteristics of umbrella sets over a span of a time horizon and to be able to predict the umbrella set of a given system

conditions. Moreover, this tool can help system operators to avoid solving UCD for every minor changes in the system. Although the decomposition techniques, proposed in Chapter 2, can make UCD problems run faster, but once a predictive tool is developed, it can predict the umbrella sets very fast and can circumvent solution of UCD altogether.

To predict the umbrella set of a given SCOPF problem, historical load/UCD results are used *i.e.* a training set. In every data sample we need the nodal load (the value and the geographical position of the loads) of the system and the corresponding umbrella set for that loading. Also, one could develop a dataset for changes in the system topology.

5.2 Neural Networks

We use artificial neural networks (ANNs) [102] to explore the possibility of umbrella set prediction. Since proposal of ANNs, they have been used to solve variety of problems. In the context of power systems, they have been successfully applied to different problems such as electricity price forecasting and wind forecasting [103–107].

ANNs include an input, an output, and some hidden layers. ANNs consist of some "neurons" where the weights of their connecting links are adjusted to minimize the mapping error of the input to the output. The output of each neuron is a combination of its inputs,

$$y = f(\sum_{i=1}^{N} w_i d_i). \tag{5.1}$$

A general representation of an artificial neural network is shown in Fig. 5.1. Neural networks can contain more than one hidden layer depending on the complexity of the problem. However, theoretically, a neural network with one hidden layer can approximate any function [108].

The problem of adjusting the weights of connecting links between neurons can be re-

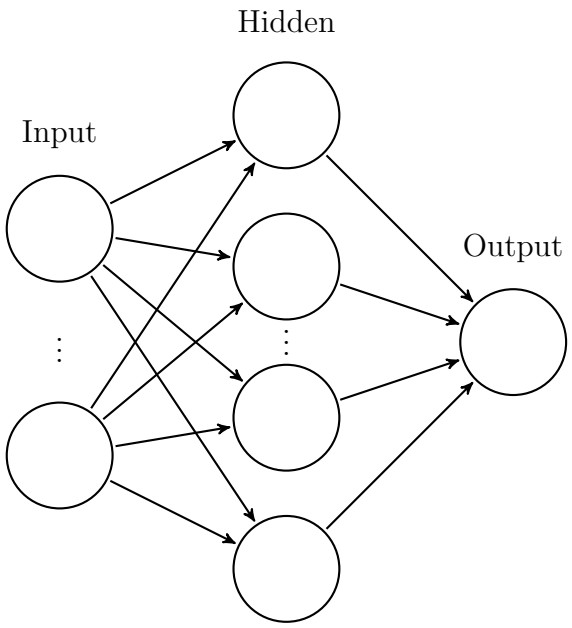

Figure 5.1 A general neural network with one hidden layer.

duced to an optimization problem and can be solved using any optimization algorithm. We are using the standard back propagation (BP) algorithm [109] to train the neural networks. Back-propagation algorithm uses gradient descent algorithm to find the minimum error. This method usually uses the mean squared error (MSE) to calculate the prediction error.

5.3 Test System

We have used the IEEE Reliability Test System 1996 [94] for this study. The system is well-defined in the literature and the hourly load of the system as well as its line flow limits are available in details —See Appendix A. Additionally, the size of its SCOPF problem allows for direct solution of its corresponding UCD problem. Since the preventive control is used in this work, the long-term capacity of lines is used as their limits in the formulations.

The annual peak load of the IEEE RTS is 2 850 MW and it happens in week 51 of the

RTS year. The RTS year is assumed to start in January. Therefore, the load peak happens in December. The system includes 24 buses, of which loads are located at 17 buses and generations are located at 11 buses. The IEEE RTS generation data can be found in Appendix A. As can be seen from this data, if all of the system units were committed, *i.e.* turned on, the minimum load that this system can supply is 1 036 MW. There are certain hours during the RTS year that the system load is below the minimum generation of the system. For those hours, which counts for 72 hours, the SCOPF problem does not have a solution and becomes infeasible. Those hours and the results of their SCOPF are not included in this study. The corresponding SCOPF problem of the IEEE RTS has 2 864 constraints, of which 50 constraints are coming from the generation limits and load balance constraints and the remaining 2 814 constraints are coming from the operation of lines under non contingent and contingent states.

We solve the UCD problem corresponding to the RTS over the span of a year (8 664 hours) and store the corresponding umbrella set of each hour along with the system loading. Each run of UCD for a load instance takes 219.353 s without any decomposition technique, see Section 2.7.1, and takes 0.5 s using P-UCD, see Section 3.4.1. We use this dataset for the training of neural networks.

5.4 Implementation

We assign one neural network to each constraint to "learn" the membership of that constraint in the umbrella set. Therefore, we need to form one neural network for each constraint in the SCOPF problem. Thus, for the SCOPF problem corresponding to the RTS, we form 2 864 neural networks. Now, we form different types of neural networks, with different number of neurons and activation functions on the last layer to compare their

performance for this specific problem. Then, each neural networks is trained, validated and tested several times to ensure that the random weight assigning for the training process initialization has been considered. Also, since the training samples of each network is randomly selected from the dataset, by simulating a network several times, we ensure that the network performance is not affected by data samples.

In order to train the neural networks, from the available samples, 80% (6 931 samples) are randomly selected to train and validate the neural networks. From the set of training data, 85% (5 891 samples) are assigned to the training of the neural networks and the remaining 15% (1 040 samples) are assigned to the validation of the training process. The remaining 20% of the total data (1 733 samples) are used for testing the neural networks. To capture the whole characteristics of the problem, these training samples are chosen randomly from the database. Then, all of the networks are trained using back-propagation algorithm, validated and tested.

The criterion to compare different neural networks is the validation errors. By training and validating neural networks using the training set, the minimum validation error obtained is 0.128% on a neural network with one hidden layer, 5 neurons on the hidden layer and a linear activation function on the output layer. The error is the total miscategorizations occurred in the prediction of the validation set. For an SCOPF problem with 2 864 constraints, this error means about 3.5 extra constraints in each run. Given that the average number of umbrella constraints over an RTS year is about 84 constraints, the solution time degradation for having three more constraints in the umbrella set is extremely marginal.

The three neural networks with minimum errors are listed in Table 5.1. As it can be seen, the networks with the least errors in the train and validation steps have the minimum test error as well. Table 5.2 shows the networks with the minimum average errors over 10

Table 5.1 Comparisons of the different neural networks results with back-propagation as the training algorithm. HL stands for hidden layer. All errors are in %.

Network #	# of HL	Neurons	Act. Func.	Train Er.	Val. Er.	Test Er.
1	1	5	Linear	0.143	0.128	0.135
2	1	50	Linear	0.143	0.128	0.135
3	2	20–10	Linear	0.144	0.129	0.135

Table 5.2 Comparisons of the average performance of different neural networks results with back-propagation as the training algorithm. HL stands for hidden layer. All errors are in %.

Network #	# of HL	Neurons	Act. Func.	Train Er.	Val. Er.	Test Er.
1	1	5	Linear	0.140	0.141	0.138
2	1	50	Linear	0.140	0.141	0.138
3	2	20–10	Linear	0.140	0.141	0.138

runs. It can be seen that on average the three networks have the same error. The standard deviation for all of the networks for the training error is 0.002, for validation error is 0.009 and for the test error is 0.003.

5.5 Error Types

There are two types of errors than can occur in the process of prediction in neural networks. These errors are called error type I and error type II. Error type I occurs when a constraint is not umbrella but is categorized as umbrella. This type of error is also called “false positive error”. On the other hand, error type II occurs when neural network categorizes a constraint as non-umbrella while that constraint is indeed a member of the umbrella set. This type of error is also called “false negative error”. In back-propagation

Table 5.3 Comparisons of false negative and false positive errors in neural networks trained with the back-propagation algorithm. All errors are in %.

Network #	Train Er. (FN/FP)	Val. Er. (FN/FP)	Test Er. (FN/FP)
1	0.023/0.120	0.022/0.105	0.024/0.110
2	0.023/0.120	0.022/0.105	0.024/0.111
3	0.022/0.121	0.021/0.107	0.023/0.112

algorithm, when calculating the prediction error, both types of error have the same weight and the algorithm tries to minimize the MSE, regardless of the type of errors. However, in the application of neural networks for prediction of umbrella sets, leaving out umbrella constraints is unacceptable since it will alter the feasibility region of the problem. Therefore, it is extremely vital to avoid the false negative errors to avoid changing the feasible set of solutions. Occurrence of false negative errors may result in infeasible solutions of the corresponding SCOPF problems. On the other hand, occurrence of false positive errors (error type I) adds non-umbrella constraints to the predicted umbrella set. This type of error does *not* cause an alteration of the umbrella set beyond its umbrella size. It will, however, augment the umbrella set which causes a very marginal solution time degradation.

The errors reported in Section 5.2 include both false negative and false positive errors. Table 5.3 shows the false negative and false positive errors in the neural networks with the minimum errors.

In order to avoid the false negative errors during the test, we should implement a training algorithm that differentiates between the types of errors and allows only for false positive errors. The back-propagation algorithm does not differentiate between types of errors and uses mean squared or sum of squared error functions to calculate the prediction errors. Given the size of the problem and the fact that we are dealing with an optimization problem, a meta-heuristic evolutionary optimization method called particle swarm optimization

(PSO), has been selected for this purpose.

5.6 Modified Training Algorithm

As was discussed before, for the application of prediction of umbrella sets, a more conservative neural network is preferable since false negative errors cannot be tolerated. Therefore, the value of the validation error, without paying attention to the type of errors, is not the best criterion to choose a neural network for this specific application. The selected neural network should have zero false negative errors and overall minimum validation error.

With regards to the above mentioned observation, it is necessary to have a customized training algorithm for neural networks to replace the back-propagation algorithm. The motivation for this replacement is that the back propagation algorithm does not differentiate between false negative and false positive errors in the training process, while, for this application, it is imperative to have no false negative errors while minimizing the number of false positive errors. Therefore, it is *more possible* for a network trained by back-propagation to incur false negative errors compared to a network that was trained to avoid false negative errors.

As was mentioned before, the problem of neural network training boils down to an optimization problem with the objective function of minimizing the prediction error. The weights of the links between neurons are the variables of this optimization problem. Here, we use PSO [110] with the objective function to minimize the false negative errors as the training algorithm. We repeat the process of training, validation and test of the same neural networks as in Section 5.2, only with a different training algorithm and with the goal of minimizing false negative errors.

All of the neural networks that obtained the minimum validation error and did not

Table 5.4 Comparisons of the average performance of different neural networks results with back-propagation as the training algorithm. HL stands for hidden layer. All errors are in %.

HL	Neurons	Act. Func.	Train Er.	Val. Er.	Test Er.
1	5/10/15/20/25/30/40/50	sigmoid/hard limit	0.3367	0.3252	0.3338
2	10-5/20-10/20-15	sigmoid/hard limit	0.3367	0.3252	0.3338

make any false negative errors have hard limit [1] and log-sigmoid [2] activation functions in their output layer. Moreover, these networks make the same number of false positive errors in the training, validation and test. These networks have between 5 to 50 neurons and contain one or two hidden layers. All of the networks have 0.325 % validation error with no false negative test error. Table 5.4 lists all of these networks with their errors in each train, validation and test step.

The test error for these networks is 0.3338 % and this means that for each run of SCOPF, there will be about nine extra constraints compared to the same problem subjected to its umbrella set obtained by solving its UCD.

We can see that the errors of the modified training algorithm is comparable with back-propagation results. The advantage of this method is that it is *less probable* for the networks trained with the goal of minimizing the false negative errors, to make a false negative error when the network is being tested. However, we note that the network is incurring false positive errors at the same rate as false negative and positive errors combined in back-propagation algorithm. The reason for this is that there is no penalty assigned to incurring false positive errors in the objective function. Therefore, to improve the performance of neural networks, we modify the objective function of the training algorithm by including false positive errors in the objective function. However, we still assign a heavy penalty for

1. A hard limit transfer function is a function with outputs of 0 or 1 (a Boolean value).
2. log-sigmoid is an S-shaped function defined by $S(n) = \frac{1}{1+e^{-n}}$.

Table 5.5 Comparisons of different neural networks and their training algorithm objective function. FN and FP stand for false negative and false positive errors, respectively. HL stands for hidden layer. All errors are in %.

Obj. Func.	Network Specs.			Errors (%)		
	HL	Neurons	Act. Func.	Train Er.	Val. Er.	Test Er.
$FP + 2 \times FN$	1	5	log-sig.	0.333 (0.001)	0.338 (0.007)	0.332 (0.006)
$FP + 3 \times FN$	1	5	log-sig.	0.334 (0.001)	0.335 (0.006)	0.334 (0.007)
$FP+FN^2$	1	5	log-sig.	0.335 (0.002)	0.334 (0.015)	0.330 (0.006)
$FP+FN^3$	1	5	log-sig.	0.334 (0.001)	0.335 (0.006)	0.334 (0.007)

incurring false negative errors in order to avoid those errors. We examine four different objective functions: two linear combination of errors and two non-linear combination of errors. Table 5.5 shows these functions and the neural networks with minimum errors for each of these objective functions.

The numbers in front of the errors in parentheses are the standard variations. It can be seen that for the objective function $FP+FN^2$, the validation error is the least of all networks. Also, the output layer activation function for these networks is log-sigmoid function. This is expected since the outputs of the neural networks are in the form of 0 and 1.

5.7 Conclusion

In this chapter, we briefly introduced the possibility of prediction of umbrella set to replace solving UCD problems directly. Since our intention was to establish the possibility of this task, we used standard tools. Of course, further research could look into possible modifications and probably more suitable tools for the task of umbrella set prediction to reduce the errors. We also pointed out the importance of different error types and the issues that standard back-propagation training algorithm have with this application of

neural networks. Then, we used PSO as an optimization tool to train neural networks with the goal of minimizing false negative errors.

However, we can see that the number of constraints arising from the errors in the prediction of umbrella sets are very few compared to the original size of the SCOPF problem. This size increase does not incur significant solution time degradation. By improving the prediction tools, these errors could be significantly reduced.

Chapter 6

Conclusion

6.1 Dissertation Overview

With the rise of uncertainties in modern power systems, system operators need to explicitly represent these uncertainties in their models to ensure a secure operation of power systems. Representation of these uncertainties along with the large sizes of interconnected modern power networks make the size of system models intractable. The system operators need to solve these models as many times as possible to optimize the system operation, economically and technically. The large number of constraints that must be included in these models, increases significantly their solution time. However, the empirical evidence and previous studies suggest that only a small portion of constraints actually contribute to the enclosure of the problem's feasible set of solutions. In this dissertation, we proposed a formulation to identify those constraints, so-called *umbrella constraints*. The proposed formulation can be generalized to be applied on any convex optimization problem. The proposed formulation, called umbrella constraint discovery (UCD), is an optimization-based formulation and uses a series of combinatorial cross-constraint comparisons to identify the

umbrella constraints.

In this dissertation, we first defined the concepts of "umbrella" and "non-umbrella" constraints. In order to set apart umbrella and non-umbrella constraints, we observed that it is possible to find a point on an umbrella constraint that satisfies all other constraints simultaneously. However, there is no point available on non-umbrella constraints that can satisfy all other constraints simultaneously. Based on these observation, we proposed a formulation, called UCD-I. UCD-I is a mixed-integer problem (MIP). This formulation uses binary variables to indicate the status of a constraint as umbrella or non-umbrella. Given the size of UCD-I and the computational burden of MIPs, application of UCD-I on large problems seems impractical. Later, we proposed an LP version of UCD-I, called UCD-II. This new formulation has the same number of constraints as UCD-I but it does not include binary variables, which makes UCD-II appropriate for off-the-shelf solvers. We demonstrated the abilities of UCD-II on several test systems, ranging from a small three-bus system to a large IEEE 118 bus system.

One of the main features of UCD-II is exploited by utilizing the Non-umbrella Constraint Lemma. Based on this lemma, if a constraint is non-umbrella in a subset of a set of constraints, that constraint will be non-umbrella with respect to the original set of constraints. The Non-umbrella Constraint Lemma can be compared to the transitivity property in set algebra. This lemma allows us to break down a UCD-II problem into smaller sub-problems which can be run independently from each other. We can utilize parallel computation to expedite the solution time. We noted that it is important how constraints are divided into sub-problems. Some dividing patterns result in the elimination of more non-umbrella constraints rapidly. The decomposition method with the highest efficiency is a line-based decomposition in which we group all constraints arising from the operation of a line in its no-contingency and contingency states in one sub-problem. The other method could be

grouping all constraints arising from each contingency in one sub-problem. We showed that this method is not as efficient as the line-based decomposition approach.

Next, we showed that umbrella sets are relatively insensitive to a wide range of changes in system load. We showed that by taking the union of all umbrella constraints in a system year, the operator could run the SCOPF problem of each hour only subjected to a small portion of the set of constraints, without actually running the UCD problem corresponding to each operational hour. For example, for one year of the IEEE RTS, the union of all umbrella constraints has about 90 constraints, while the SCOPF problem of one hour has 2 864 constraints. Using this approach the operators can run SCOPF problems a lot faster while making sure that none of the umbrella constraints are left out.

Next, we proposed a formulation which can quickly identify non-umbrella constraints—called *partial* UCD. In this formulation, we avoid some of the inefficiencies of UCD-II by avoiding some unnecessary cross-constraint comparisons. In partial UCD, the set of constraints is partitioned into two subsets: potential umbrella and potential non-umbrella constraints. In the process of solving partial UCD, the only comparisons that are done are between potential non-umbrella and potential umbrella constraints, *i.e.* there is no comparisons among non-umbrella constraints themselves nor among umbrella constraints. This modification can reduce significantly the solution time of partial UCD. Since the potential umbrella and non-umbrella sets are not exact, partial UCD formulation does not identify all non-umbrella constraints. Therefore, it is imperative to follow up a partial UCD problem with a UCD-II run to identify all umbrella constraints. Another note is that partial UCD never leaves out any umbrella constraint, *i.e.* even that the potential umbrella and non-umbrella constraints are not exact, if an umbrella constraint is among potentially non-umbrella constraints, it will not be identified as non-umbrella. Instead, it will be carried on to the next level, where UCD-II can formally identify it as an umbrella

constraint. This method was applied on the IEEE RTS and IEEE 118 bus systems. The results show significant UCD-II solution time gains.

Following the remarkable results of UCD on SCOPF problems, we went on and applied UCD (both UCD-II and partial UCD) on unit commitment problems. Unit commitment problems are MIPs and UCD is applied on their 0-1 linear programming relaxations. Another characteristic of unit commitment problems is that they contain more generation-based constraints than line-based constraints. We applied UCD on security-constrained unit commitment problems (SCUC) and observed that there are not as many non-umbrella constraints in these problems as with SCOPF. Most of the non-umbrella constraints are coming from line-based constraints and only a few of generation-based constraints are non-umbrella. We notice that, in unit commitment problems, if a generation or a time horizon is added to the problem, several variables are added. In turn, those variables add new dimensions to the problem and change previously non-umbrella constraints in to umbrella constraints. Moreover, unlike the line constraints, the generation constraints do not link many variables together. This is also another reason that most of the generation-based constraints are indeed umbrella.

In the last part of this work, we explored the possibility of predicting the umbrella set of a given network, IEEE RTS in this case, if the information about the umbrella set of the past hours is available. We use artificial neural networks for this task. Further, we demonstrate that a traditional neural network is not adequate for this purpose. The reason is that in prediction of umbrella constraints it is vital not to leave out any umbrella constraints, since such errors will alter the feasibility set of region of the problem. On the other hand, leaving a non-umbrella constraint in the predicted umbrella set does not do much harm. Therefore, we modified the training algorithm of the neural networks to accommodate for this new requirement.

6.2 Recommendations for Future Work

As this research is an initial step in identifying umbrella constraints, there are several aspects of this work that can be taken further by researchers. In this section, we summarize some of these future research areas.

- UCD has many constraints and considerably fewer number of variables. By forming the dual problem of UCD, we might be able to run the dual problem faster than the original UCD problem. The solution of the dual problem is the Lagrange multipliers of the original problem. As was explained in Chapter 2, by having the Lagrange multipliers of UCD constraints, we can infer which constraints are umbrella or non-umbrella and even which ones are weakly redundant. Analyzing and forming the dual problem of UCD can be a promising frontier.
- As was mentioned in Section 2.4.1, the values of s_j^* and and their sensitivities (*e.g.* $\partial s_j^*/\partial b_j$) could serve to predict under which conditions a specific constraint joins or leaves the umbrella set. Moreover, values of $\partial s_j^*/\partial b_j$ can signal the directions that constraints are moving to. These information can be vital for system operators to be alerted if a line has some potential to join the umbrella set if some change happens in the system.
- One could look into application of large change sensitivity analysis [111] on UCD-II to analyze the movements of constraints in order to determine if a constraints has joined or left the umbrella set. This method has already been successfully applied in power systems [112].
- In the decomposition technique, we are able to separate the sub-problems as small as we wish. One future work can be looking into finding an optimal size for decomposition problems in order to trade off between complexity of each sub-problem and the

overall solution time of UCD-II.

- In this work, we showed that it is possible to predict the umbrella set of a given SCOPF problem. The prediction of umbrella constraints can be improved by fine adjustments on artificial neural networks. Other methods such as data mining can be applied for this purpose. Also, more inputs can be considered for the neural networks such as topology and configuration of the network.
- UCD can be generalized to solve other problems in power systems. One of these problems is identification of the infeasible constraints in an infeasible SCOPF or unit commitment problem. By doing changes in the UCD formulation, it is possible to identify the constraints that are making a problem infeasible.
- UCD can be applied on stochastic analyses of power system where different scenarios augment the size of the problems significantly.
- In this dissertation, we have used a linearized representation of power systems in our models. An extension of this work could include ac models of power systems to represent exact behaviour of power systems. These exact models contain non-linear non-convex constraints which will introduce new challenges in solving SCOPF and SCUC problems.

Appendix A

IEEE Reliability Test System Data

This appendix presents the data of IEEE RTS 1979, which is taken from the "case24_ieee_rts.m" case file, provided with MATPOWER [98]. Table A.1 presents the bus data, Table A.2 contains the generation data. Finally, the branch data is included in Table A.3.

Table A.1 IEEE RTS bus data.

Bus	p_d	q_d	g_s	b_s	v_{base}	v_{max}	v_{min}
1	108	22	0	0	138	1.05	0.95
2	97	20	0	0	138	1.05	0.95
3	180	37	0	0	138	1.05	0.95
4	74	15	0	0	138	1.05	0.95
5	71	14	0	0	138	1.05	0.95
6	136	28	0	-100	138	1.05	0.95
7	125	25	0	0	138	1.05	0.95
8	171	35	0	0	138	1.05	0.95
9	175	36	0	0	138	1.05	0.95
10	195	40	0	0	138	1.05	0.95
11	0	0	0	0	230	1.05	0.95
12	0	0	0	0	230	1.05	0.95
13	265	54	0	0	230	1.05	0.95
14	194	39	0	0	230	1.05	0.95
15	317	64	0	0	230	1.05	0.95
16	100	20	0	0	230	1.05	0.95
17	0	0	0	0	230	1.05	0.95
18	333	68	0	0	230	1.05	0.95
19	181	37	0	0	230	1.05	0.95
20	128	26	0	0	230	1.05	0.95
21	0	0	0	0	230	1.05	0.95
22	0	0	0	0	230	1.05	0.95
23	0	0	0	0	230	1.05	0.95
24	0	0	0	0	230	1.05	0.95

Table A.2 IEEE RTS generator data.

Bus	p_{max}	p_{min}	v_g	q_{max}	q_{min}	Type
1	152	30.4	1.035	60	-50	U76
2	152	30.4	1.035	60	-50	U76
7	300	75	1.025	180	0	U100
13	591	207	1.02	240	0	U197
14	0	0	0.98	200	-50	SynCond
15	155	54.3	1.014	80	-50	U155
16	155	54.3	1.017	80	-50	U155
18	400	100	1.05	200	-50	U400
21	400	100	1.05	200	-50	U400
22	300	60	1.05	96	-60	U50
23	310	108.6	1.05	160	-100	U155
23	350	140	1.05	150	-25	U350

Table A.3 IEEE RTS branch data.

Line#	From	To	r	x	b_c	s_{max}	τ	θ_{shift}
1	1	2	0.0026	0.0139	0.4611	175	0	0
2	1	3	0.0546	0.2112	0.0572	175	0	0
3	1	5	0.0218	0.0845	0.0229	175	0	0
4	2	4	0.0328	0.1267	0.0343	175	0	0
5	2	6	0.0497	0.192	0.052	175	0	0
6	3	9	0.0308	0.119	0.0322	175	0	0
7	3	24	0.0023	0.0839	0	400	1.03	0
8	4	9	0.0268	0.1037	0.0281	175	0	0
9	5	10	0.0228	0.0883	0.0239	175	0	0
10	6	10	0.0139	0.0605	2.459	175	0	0
11	7	8	0.0159	0.0614	0.0166	175	0	0
12	8	9	0.0427	0.1651	0.0447	175	0	0
13	8	10	0.0427	0.1651	0.0447	175	0	0
14	9	11	0.0023	0.0839	0	400	1.03	0
15	9	12	0.0023	0.0839	0	400	1.03	0
16	10	11	0.0023	0.0839	0	400	1.02	0
17	10	12	0.0023	0.0839	0	400	1.02	0
18	11	13	0.0061	0.0476	0.0999	500	0	0
19	11	14	0.0054	0.0418	0.0879	500	0	0
20	12	13	0.0061	0.0476	0.0999	500	0	0
21	12	23	0.0124	0.0966	0.203	500	0	0
22	13	23	0.0111	0.0865	0.1818	500	0	0
23	14	16	0.005	0.0389	0.0818	500	0	0
24	15	16	0.0022	0.0173	0.0364	500	0	0
25	15	21	0.0063	0.049	0.103	500	0	0
26	15	21	0.0063	0.049	0.103	500	0	0
27	15	24	0.0067	0.0519	0.1091	500	0	0
28	16	17	0.0033	0.0259	0.0545	500	0	0
29	16	19	0.003	0.0231	0.0485	500	0	0
30	17	18	0.0018	0.0144	0.0303	500	0	0
31	17	22	0.0135	0.1053	0.2212	500	0	0
32	18	21	0.0033	0.0259	0.0545	500	0	0
33	18	21	0.0033	0.0259	0.0545	500	0	0
34	19	20	0.0051	0.0396	0.0833	500	0	0
35	19	20	0.0051	0.0396	0.0833	500	0	0
36	20	23	0.0028	0.0216	0.0455	500	0	0
37	20	23	0.0028	0.0216	0.0455	500	0	0
38	21	22	0.0087	0.0678	0.1424	500	0	0

Appendix B

IEEE 118 Bus System Data

In this appendix, we include the information that we used for our simulations on IEEE 118 bus system. We used the set of generation costs and limits found within the MATPOWER library [98] and we modified the set of line limits used previously by researchers based at the Illinois Institute of Technology. The complete data set can be found at http://cl.ly/3x0L3L393r24. We provide bus, generation and line data here. For the sake of brevity, we have not presented some of the information that could be easily accessed in MATPOWER. The type column in Table B.1 refers to the bus type according to the following labeling (i) Type 1 is for PQ buses; (ii) Type 2 represents PV buses; and (iii) Type 3 is the reference bus [98].

In Table B.2, all real power values, P, are in MW and all reactive power, Q, values are in MVAr.

Table B.1 IEEE 118 bus system data.

Bus	Type	P_d (MW)	Q_d (MVAr)	Bus	Type	P_d (MW)	Q_d (MVAr)
1	2	51	27	38	1	0	0
2	1	20	9	39	1	27	11
3	1	39	10	40	2	66	23
4	2	39	12	41	1	37	10
5	1	0	0	42	2	96	23
6	2	52	22	43	1	18	7
7	1	19	2	44	1	16	8
8	2	28	0	45	1	53	22
9	1	0	0	46	2	28	10
10	2	0	0	47	1	34	0
11	1	70	23	48	1	20	11
12	2	47	10	49	2	87	30
13	1	34	16	50	1	17	4
14	1	14	1	51	1	17	8
15	2	90	30	52	1	18	5
16	1	25	10	53	1	23	11
17	1	11	3	54	2	113	32
18	2	60	34	55	2	63	22
19	2	45	25	56	2	84	18
20	1	18	3	57	1	12	3
21	1	14	8	58	1	12	3
22	1	10	5	59	2	277	113
23	1	7	3	60	1	78	3
24	2	13	0	61	2	0	0
25	2	0	0	62	2	77	14
26	2	0	0	63	1	0	0
27	2	71	13	64	1	0	0
28	1	17	7	65	2	0	0
29	1	24	4	66	2	39	18
30	1	0	0	67	1	28	7
31	2	43	27	68	1	0	0
32	2	59	23	69	3	0	0
33	1	23	9	70	2	66	20
34	2	59	26	71	1	0	0
35	1	33	9	72	2	12	0
36	2	31	17	73	2	6	0
37	1	0	0	74	2	68	27

Table B.1 IEEE RTS bus data–Cont'd

Bus	Type	P_d (MW)	Q_d (MVAr)	Bus	Type	P_d (MW)	Q_d (MVAr)
75	1	47	11	97	1	15	9
76	2	68	36	98	1	34	8
77	2	61	28	99	2	42	0
78	1	71	26	100	2	37	18
79	1	39	32	101	1	22	15
80	2	130	26	102	1	5	3
81	1	0	0	103	2	23	16
82	1	54	27	104	2	38	25
83	1	20	10	105	2	31	26
84	1	11	7	106	1	43	16
85	2	24	15	107	2	50	12
86	1	21	10	108	1	2	1
87	2	0	0	109	1	8	3
88	1	48	10	110	2	39	30
89	2	0	0	111	2	0	0
90	2	163	42	112	2	68	13
91	2	10	0	113	2	6	0
92	2	65	10	114	1	8	3
93	1	12	7	115	1	22	7
94	1	30	16	116	2	184	0
95	1	42	31	117	1	20	8
96	1	38	15	118	1	33	15

Table B.2 IEEE 118 bus system generation data

Bus	P_g	Q_g	Q_{max}	Q_{min}	V_g (pu)	P_{max}	P_{min}
1	0	0	15	-5	0.955	100	0
4	0	0	300	-300	0.998	100	0
6	0	0	50	-13	0.99	100	0
8	0	0	300	-300	1.015	100	0
10	450	0	200	-147	1.05	550	0
12	85	0	120	-35	0.99	185	0
15	0	0	30	-10	0.97	100	0
18	0	0	50	-16	0.973	100	0
19	0	0	24	-8	0.962	100	0
24	0	0	300	-300	0.992	100	0
25	220	0	140	-47	1.05	320	0
26	314	0	1000	-1000	1.015	414	0
27	0	0	300	-300	0.968	100	0
31	7	0	300	-300	0.967	107	0
32	0	0	42	-14	0.963	100	0
34	0	0	24	-8	0.984	100	0
36	0	0	24	-8	0.98	100	0
40	0	0	300	-300	0.97	100	0
42	0	0	300	-300	0.985	100	0
46	19	0	100	-100	1.005	119	0
49	204	0	210	-85	1.025	304	0
54	48	0	300	-300	0.955	148	0
55	0	0	23	-8	0.952	100	0
56	0	0	15	-8	0.954	100	0
59	155	0	180	-60	0.985	255	0
61	160	0	300	-100	0.995	260	0
62	0	0	20	-20	0.998	100	0
65	391	0	200	-67	1.005	491	0
66	392	0	200	-67	1.05	492	0
69	516.4	0	300	-300	1.035	805.2	0
70	0	0	32	-10	0.984	100	0
72	0	0	100	-100	0.98	100	0
73	0	0	100	-100	0.991	100	0
74	0	0	9	-6	0.958	100	0
76	0	0	23	-8	0.943	100	0
77	0	0	70	-20	1.006	100	0

Table B.2 IEEE 118 bus system generation data–Cont'd

Bus	P_g	Q_g	Q_{max}	Q_{min}	V_g (pu)	P_{max}	P_{min}
80	477	0	280	-165	1.04	577	0
85	0	0	23	-8	0.985	100	0
87	4	0	1000	-100	1.015	104	0
89	607	0	300	-210	1.005	707	0
90	0	0	300	-300	0.985	100	0
91	0	0	100	-100	0.98	100	0
92	0	0	9	-3	0.99	100	0
99	0	0	100	-100	1.01	100	0
100	252	0	155	-50	1.017	352	0
103	40	0	40	-15	1.01	140	0
104	0	0	23	-8	0.971	100	0
105	0	0	23	-8	0.965	100	0
107	0	0	200	-200	0.952	100	0
110	0	0	23	-8	0.973	100	0
111	36	0	1000	-100	0.98	136	0
112	0	0	1000	-100	0.975	100	0
113	0	0	200	-100	0.993	100	0
116	0	0	1000	-1000	1.005	100	0

Table B.3 IEEE 118 bus system branch data

Line#	From	To	R(p.u.)	X(p.u.)	B(p.u.)	Limit (MW)
1	1	2	0.0303	0.0999	0.0254	100
2	1	3	0.0129	0.0424	0.01082	100
3	4	5	0.00176	0.00798	0.0021	500
4	3	5	0.0241	0.108	0.0284	100
5	5	6	0.0119	0.054	0.01426	100
6	6	7	0.00459	0.0208	0.0055	100
7	8	9	0.00244	0.0305	1.162	500
8	8	5	0	0.0267	0	500
9	9	10	0.00258	0.0322	1.23	500
10	4	11	0.0209	0.0688	0.01748	100
11	5	11	0.0203	0.0682	0.01738	100
12	11	12	0.00595	0.0196	0.00502	100
13	2	12	0.0187	0.0616	0.01572	100
14	3	12	0.0484	0.16	0.0406	100
15	7	12	0.00862	0.034	0.00874	100
16	11	13	0.02225	0.0731	0.01876	100
17	12	14	0.0215	0.0707	0.01816	100
18	13	15	0.0744	0.2444	0.06268	100
19	14	15	0.0595	0.195	0.0502	100
20	12	16	0.0212	0.0834	0.0214	100
21	15	17	0.0132	0.0437	0.0444	500
22	16	17	0.0454	0.1801	0.0466	100
23	17	18	0.0123	0.0505	0.01298	100
24	18	19	0.01119	0.0493	0.01142	100
25	19	20	0.0252	0.117	0.0298	100
26	15	19	0.012	0.0394	0.0101	100
27	20	21	0.0183	0.0849	0.0216	100
28	21	22	0.0209	0.097	0.0246	100
29	22	23	0.0342	0.159	0.0404	100
30	23	24	0.0135	0.0492	0.0498	100
31	23	25	0.0156	0.08	0.0864	500
32	26	25	0	0.0382	0	500
33	25	27	0.0318	0.163	0.1764	500
34	27	28	0.01913	0.0855	0.0216	100
35	28	29	0.0237	0.0943	0.0238	100
36	30	17	0	0.0388	0	500
37	8	30	0.00431	0.0504	0.514	100

Table B.3 IEEE 118 bus system branch data–Cont'd

Line#	From	To	R(p.u.)	X(p.u.)	B(p.u.)	Limit (MW)
38	26	30	0.00799	0.086	0.908	500
39	17	31	0.0474	0.1563	0.0399	100
40	29	31	0.0108	0.0331	0.0083	100
41	23	32	0.0317	0.1153	0.1173	100
42	31	32	0.0298	0.0985	0.0251	100
43	27	32	0.0229	0.0755	0.01926	100
44	15	33	0.038	0.1244	0.03194	100
45	19	34	0.0752	0.247	0.0632	100
46	35	36	0.00224	0.0102	0.00268	100
47	35	37	0.011	0.0497	0.01318	100
48	33	37	0.0415	0.142	0.0366	100
49	34	36	0.00871	0.0268	0.00568	100
50	34	37	0.00256	0.0094	0.00984	500
51	38	37	0	0.0375	0	500
52	37	39	0.0321	0.106	0.027	100
53	37	40	0.0593	0.168	0.042	100
54	30	38	0.00464	0.054	0.422	100
55	39	40	0.0184	0.0605	0.01552	100
56	40	41	0.0145	0.0487	0.01222	100
57	40	42	0.0555	0.183	0.0466	100
58	41	42	0.041	0.135	0.0344	100
59	43	44	0.0608	0.2454	0.06068	100
60	34	43	0.0413	0.1681	0.04226	100
61	44	45	0.0224	0.0901	0.0224	100
62	45	46	0.04	0.1356	0.0332	100
63	46	47	0.038	0.127	0.0316	100
64	46	48	0.0601	0.189	0.0472	100
65	47	49	0.0191	0.0625	0.01604	100
66	42	49	0.0715	0.323	0.086	100
67	42	49	0.0715	0.323	0.086	100
68	45	49	0.0684	0.186	0.0444	100
69	48	49	0.0179	0.0505	0.01258	100
70	49	50	0.0267	0.0752	0.01874	100
71	49	51	0.0486	0.137	0.0342	100
72	51	52	0.0203	0.0588	0.01396	100
73	52	53	0.0405	0.1635	0.04058	100
74	53	54	0.0263	0.122	0.031	100

Table B.3 IEEE 118 bus system branch data–Cont'd

Line#	From	To	R(p.u.)	X(p.u.)	B(p.u.)	Limit (MW)
75	49	54	0.073	0.289	0.0738	100
76	49	54	0.0869	0.291	0.073	100
77	54	55	0.0169	0.0707	0.0202	100
78	54	56	0.00275	0.00955	0.00732	100
79	55	56	0.00488	0.0151	0.00374	100
80	56	57	0.0343	0.0966	0.0242	100
81	50	57	0.0474	0.134	0.0332	100
82	56	58	0.0343	0.0966	0.0242	100
83	51	58	0.0255	0.0719	0.01788	100
84	54	59	0.0503	0.2293	0.0598	100
85	56	59	0.0825	0.251	0.0569	100
86	56	59	0.0803	0.239	0.0536	100
87	55	59	0.04739	0.2158	0.05646	100
88	59	60	0.0317	0.145	0.0376	100
89	59	61	0.0328	0.15	0.0388	100
90	60	61	0.00264	0.0135	0.01456	500
91	60	62	0.0123	0.0561	0.01468	100
92	61	62	0.00824	0.0376	0.0098	100
93	63	59	0	0.0386	0	500
94	63	64	0.00172	0.02	0.216	500
95	64	61	0	0.0268	0	500
96	38	65	0.00901	0.0986	1.046	500
97	64	65	0.00269	0.0302	0.38	500
98	49	66	0.018	0.0919	0.0248	500
99	49	66	0.018	0.0919	0.0248	500
100	62	66	0.0482	0.218	0.0578	100
101	62	67	0.0258	0.117	0.031	100
102	65	66	0	0.037	0	500
103	66	67	0.0224	0.1015	0.02682	100
104	65	68	0.00138	0.016	0.638	500
105	47	69	0.0844	0.2778	0.07092	100
106	49	69	0.0985	0.324	0.0828	100
107	68	69	0	0.037	0	500
108	69	70	0.03	0.127	0.122	500
109	24	70	0.00221	0.4115	0.10198	100
110	70	71	0.00882	0.0355	0.00878	100

Table B.3 IEEE 118 bus system branch data–Cont'd

Line#	From	To	R(p.u.)	X(p.u.)	B(p.u.)	Limit (MW)
111	24	72	0.0488	0.196	0.0488	100
112	71	72	0.0446	0.18	0.04444	100
113	71	73	0.00866	0.0454	0.01178	100
114	70	74	0.0401	0.1323	0.03368	100
115	70	75	0.0428	0.141	0.036	100
116	69	75	0.0405	0.122	0.124	500
117	74	75	0.0123	0.0406	0.01034	100
118	76	77	0.0444	0.148	0.0368	100
119	69	77	0.0309	0.101	0.1038	100
120	75	77	0.0601	0.1999	0.04978	100
121	77	78	0.00376	0.0124	0.01264	100
122	78	79	0.00546	0.0244	0.00648	100
123	77	80	0.017	0.0485	0.0472	500
124	77	80	0.0294	0.105	0.0228	500
125	79	80	0.0156	0.0704	0.0187	100
126	68	81	0.00175	0.0202	0.808	500
127	81	80	0	0.037	0	500
128	77	82	0.0298	0.0853	0.08174	100
129	82	83	0.0112	0.03665	0.03796	100
130	83	84	0.0625	0.132	0.0258	100
131	83	85	0.043	0.148	0.0348	100
132	84	85	0.0302	0.0641	0.01234	100
133	85	86	0.035	0.123	0.0276	500
134	86	87	0.02828	0.2074	0.0445	500
135	85	88	0.02	0.102	0.0276	100
136	85	89	0.0239	0.173	0.047	100
137	88	89	0.0139	0.0712	0.01934	500
138	89	90	0.0518	0.188	0.0528	500
139	89	90	0.0238	0.0997	0.106	500
140	90	91	0.0254	0.0836	0.0214	100
141	89	92	0.0099	0.0505	0.0548	500
142	89	92	0.0393	0.1581	0.0414	500
143	91	92	0.0387	0.1272	0.03268	100
144	92	93	0.0258	0.0848	0.0218	100
145	92	94	0.0481	0.158	0.0406	100
146	93	94	0.0223	0.0732	0.01876	100
147	94	95	0.0132	0.0434	0.0111	100
148	80	96	0.0356	0.182	0.0494	100

Table B.3 IEEE 118 bus system branch data–Cont'd

Line#	From	To	R(p.u.)	X(p.u.)	B(p.u.)	Limit (MW)
149	82	96	0.0162	0.053	0.0544	100
150	94	96	0.0269	0.0869	0.023	100
151	80	97	0.0183	0.0934	0.0254	100
152	80	98	0.0238	0.108	0.0286	100
153	80	99	0.0454	0.206	0.0546	100
154	92	100	0.0648	0.295	0.0472	100
155	94	100	0.0178	0.058	0.0604	100
156	95	96	0.0171	0.0547	0.01474	100
157	96	97	0.0173	0.0885	0.024	100
158	98	100	0.0397	0.179	0.0476	100
159	99	100	0.018	0.0813	0.0216	100
160	100	101	0.0277	0.1262	0.0328	100
161	92	102	0.0123	0.0559	0.01464	100
162	101	102	0.0246	0.112	0.0294	100
163	100	103	0.016	0.0525	0.0536	500
164	100	104	0.0451	0.204	0.0541	100
165	103	104	0.0466	0.1584	0.0407	100
166	103	105	0.0535	0.1625	0.0408	100
167	100	106	0.0605	0.229	0.062	100
168	104	105	0.00994	0.0378	0.00986	100
169	105	106	0.014	0.0547	0.01434	100
170	105	107	0.053	0.183	0.0472	100
171	105	108	0.0261	0.0703	0.01844	100
172	106	107	0.053	0.183	0.0472	100
173	108	109	0.0105	0.0288	0.0076	100
174	103	110	0.03906	0.1813	0.0461	100
175	109	110	0.0278	0.0762	0.0202	100
176	110	111	0.022	0.0755	0.02	137
177	110	112	0.0247	0.064	0.062	100
178	17	113	0.00913	0.0301	0.00768	100
179	32	113	0.0615	0.203	0.0518	500
180	32	114	0.0135	0.0612	0.01628	100
181	27	115	0.0164	0.0741	0.01972	100
182	114	115	0.0023	0.0104	0.00276	100
183	68	116	0.00034	0.00405	0.164	500
184	12	117	0.0329	0.14	0.0358	100
185	75	118	0.0145	0.0481	0.01198	100
186	76	118	0.0164	0.0544	0.01356	100

References

[1] M. Huneault, F. Galiana, and G. Gross, "A review of restructuring in the electricity business," in *Proc. 13th Power Systems Computation Conference*, Jun. 1999, pp. 19–31.

[2] M. Milligan, E. Ela, J. Hein, T. Schneider, G. Brinkman, and P. Denholm, "Exploration of high-penetration renewable electricity futures. vol. 4 of renewable electricity futures study," National Renewable Energy Laboratory, Tech. Rep., 2012.

[3] U.S.-Canada Power System Outage Task Force, "Final report on the August 14, 2003 blackout in the United States and Canada: Causes and recommendations," North American Electric Reliability Corporation, Tech. Rep., Apr. 2004.

[4] R. W. Lincoln, "Learning to trade power," Ph.D. dissertation, University of Strathclyde, May 2011.

[5] L. Fink, "Security: its meaning and objectives," in *Proc. Int. Symposium on Power System Security Assessment*, 1988, pp. 35–41.

[6] L. Fink and K. Carlsen, "Power/energy: Operating under stress and strain," *IEEE Spectrum*, vol. 15, no. 3, pp. 48–53, Mar. 1978.

[7] T. Dy Liacco, "The adaptive reliability control system," *IEEE Trans. Power App. Syst.*, no. 5, pp. 517–531, 1967.

[8] A. Monticelli, M. V. F. Pereira, and S. Granville, "Security-constrained optimal power flow with post-contingency corrective rescheduling," *IEEE Trans. Power Syst.*, vol. 2, no. 1, pp. 175–180, Feb. 1987.

[9] The Joint Board on Economic Dispatch for the Northeast Region, "Study and recommendations regarding security constrained economic dispatch (SCED) in the northeast," Tech. Rep., May 2006.

[10] M. B. Cain, R. P. O'Neill, and A. Castillo, "History of optimal power flow and formulations," *Federal Energy Regulatory Commission*, Dec. 2012. [Online]. Available: http://www.isone.com/committees/comm_wkgrps/prtcpnts_comm/pac/mtrls/2013/mar202013/a2_planning_technical_guide.pdf

[11] M. Huneault and F. Galiana, "A survey of the optimal power flow literature," *IEEE Trans. Power Syst.*, vol. 6, no. 2, pp. 762–770, May 1991.

[12] R. B. Squires, "Economic dispatch of generation directly from power system voltages and admittances," *IEEE Trans. Power App. Syst.*, vol. PAS-79, no. 3, pp. 1235–1244, Apr. 1960.

[13] R. B. Shipley and M. Hochdorf, "Exact economic dispatch - digital computer solution," *IEEE Trans. Power App. Syst.*, vol. PAS-75, no. 3, pp. 1147–1153, Jan. 1956.

[14] J. F. Calvert and T. W. Sze, "A new approach to loss minimization in electric power systems," *IEEE Trans. Power App. Syst.*, vol. PAS-76, no. 3, pp. 1439–1446, Apr. 1957.

[15] A. J. Wood and B. F. Wollenberg, *Power Generation Operation and Control*, 2nd ed. New York, NY: Wiley-Interscience, 1996.

[16] J. M. Arroyo and F. D. Galiana, "Energy and reserve pricing in security and network-constrained electricity markets," *IEEE Trans. Power Syst.*, vol. 20, no. 2, pp. 634–643, May 2005.

[17] F. D. Galiana, F. Bouffard, J. M. Arroyo, and J. F. Restrepo, "Scheduling and pricing of coupled energy and primary, secondary, and tertiary reserves," *Proc. IEEE*, vol. 93, no. 11, pp. 1970–1983, Nov. 2005.

[18] J. Wang, N. E. Redondo, and F. D. Galiana, "Demand-side reserve offers in joint energy/reserve electricity markets," *IEEE Trans. Power Syst.*, vol. 18, no. 4, pp. 1300–1306, Nov. 2003.

[19] P. A. Ruiz, C. R. Philbrick, E. Zak, K. W. Cheung, and P. W. Sauer, "Uncertainty management in the unit commitment problem," *IEEE Trans. Power Syst.*, vol. 24, no. 2, pp. 642–651, May 2009.

[20] J. Wang, M. Shahidehpour, and Z. Li, "Contingency-constrained reserve requirements in joint energy and ancillary services auction," *IEEE Trans. Power Syst.*, vol. 24, no. 3, pp. 1457–1468, Aug. 2009.

[21] K. Hedman, R. O'Neill, E. Fisher, and S. Oren, "Optimal transmission switching with contingency analysis," *IEEE Trans. Power Syst.*, vol. 24, no. 3, pp. 1577–1586, Aug. 2009.

[22] K. W. Hedman, M. C. Ferris, R. P. O'Neill, E. B. Fisher, and S. S. Oren, "Co-optimization of generation unit commitment and transmission switching with $n-1$ reliability," *IEEE Trans. Power Syst.*, vol. 25, no. 2, pp. 1052–1063, May 2010.

[23] F. Bouffard, "Electricity market-clearing with stochastic security," Ph.D. dissertation, McGill University, Feb. 2006.

[24] Federal Energy Regulatory Commission. (2013, Oct.) Electric power markets: National overview. [Online]. Available: https://www.ferc.gov/market-oversight/mkt-electric/overview.asp

[25] A. Gomez-Exposito, A. J. Conejo, and C. Cañizares, *Electric energy systems: analysis and operation.* CRC Press, 2008.

[26] F. Capitanescu, J. M. Ramos, P. Panciatici, D. Kirschen, A. M. Marcolini, L. Platbrood, and L. Wehenkel, "State-of-the-art, challenges, and future trends in security constrained optimal power flow," *Elect. Power Syst. Res.*, vol. 81, no. 8, pp. 1731–1741, Aug. 2011.

[27] J. Carpentier, "Contribution to the economic dispatch problem," *Bulletin de la Société Française des Électriciens*, vol. 3, no. 8, pp. 431–447, 1962.

[28] O. Alsac and B. Stott, "Optimal load flow with steady-state security," *IEEE Trans. Power App. Syst.*, vol. PAS-93, no. 3, pp. 745–751, May 1974.

[29] A. Berizzi, M. Delfanti, P. Marannino, M. Pasquadibisceglie, and A. Silvestri, "Enhanced security-constrained OPF with FACTS devices," *IEEE Trans. Power Syst.*, vol. 20, no. 3, pp. 1597–1605, Aug. 2005.

[30] J. Momoh, R. Koessler, M. Bond, B. Stott, D. Sun, A. Papalexopoulos, and P. Ristanovic, "Challenges to optimal power flow," *IEEE Trans. Power Syst.*, vol. 12, no. 1, pp. 444–455, Feb. 1997.

[31] B. Stott, O. Alsac, and A. Monticelli, "Security analysis and optimization," *Proc. IEEE*, vol. 75, no. 12, pp. 1623–1644, Dec. 1987.

[32] J. Zhu, *Optimization of Power System Operation*. Hoboken, NJ: Wiley, 2008, ch. 3.

[33] X. Ma, H. Song, M. Hong, J. Wan, Y. Chen, and E. Zak, "The security-constrained commitment and dispatch for Midwest ISO day-ahead co-optimized energy and ancillary service market," in *Proc. IEEE Power & Energy Society General Meeting*, Calgary, AB, Jul. 2009.

[34] F. Bouffard, F. D. Galiana, and A. J. Conejo, "Market-clearing with stochastic security—Part II: Case studies," *IEEE Trans. Power Syst.*, vol. 20, no. 4, pp. 1827–1835, Nov. 2005.

[35] F. Bouffard, F. D. Galiana, and J. M. Arroyo, "Umbrella contingencies in security-constrained optimal power flow," in *Proc. 15th Power Systems Computation Conf.*, Liège, Belgium, Aug. 2005.

[36] P. Giesbertz and R. van Amerongen, "On the identification of redundant constraints in optimisation problems," *Archiv für Elektrotechnik*, vol. 72, no. 5, pp. 341–347, 1989. [Online]. Available: http://dx.doi.org/10.1007/BF01573715

[37] A. Boneh, S. Boneh, and R. J. Caron, "Constraint classification in mathematical programming," *Math. Program.*, vol. 61, no. 1-3, pp. 61–73, Jun. 1990.

[38] E. D. Andersen and K. D. Andersen, "Presolving in linear programming," *Math. Program.*, vol. 71, no. 2, pp. 221–245, Dec. 1995.

[39] A. Brearley, G. Mitra, and H. P. Williams, "Analysis of mathematical programming problems prior to applying the simplex algorithm," *Math. Program.*, vol. 8, no. 1, pp. 54–83, Aug. 1975.

[40] R. Caron, J. McDonald, and C. Ponic, "A degenerate extreme point strategy for the classification of linear constraints as redundant or necessary," *J. Optim. Theory Appl.*, vol. 62, no. 2, pp. 225–237, Aug. 1989.

[41] H. J. Greenberg, "Consistency, redundancy, and implied equalities in linear systems," *Ann. Math. Artificial Intelligence*, vol. 17, no. 1, pp. 37–83, 1996.

[42] J. Telgen, "Identifying redundant constraints and implicit equalities in systems of linear constraints," *Manag. Sci.*, vol. 29, no. 10, pp. 1209–1222, Oct. 1983.

[43] G. L. Thompson, F. M. Tonge, and S. Zionts, "Techniques for removing nonbinding constraints and extraneous variables from linear programming problems," *Manag. Sci.*, vol. 12, no. 7, pp. 588–608, Mar. 1966.

[44] S. Paulraj and P. Sumathi, "A comparative study of redundant constraints identification methods in linear programming problems," *Mathematical Problems in Engineering*, vol. 2010, Sep. 2010.

[45] P. Sumathi and S. Paulraj, "Identification of redundant constraints in large scale linear programming problems with minimal computational effort," *Applied Mathematical Sciences*, vol. 7, no. 80, pp. 3963–3974, 2013.

[46] I. Ioslovich, "Robust reduction of a class of large-scale linear programs," *SIAM J. on Optimization*, vol. 12, no. 1, pp. 262–282, Jan. 2001.

[47] A. Geoffrion, "Generalized Benders decomposition," *Journal of optimization theory and applications*, vol. 10, no. 4, pp. 237–260, 1972.

[48] Y. Li and J. McCalley, "Decomposed SCOPF for improving efficiency," *IEEE Trans. Power Syst.*, vol. 24, no. 1, pp. 494–495, Feb. 2009.

[49] M. Shahidehpour, H. Yamin, and Z. Li, *Security–Constrained Unit Commitment*. John Wiley & Sons, Inc., 2002, pp. 275–310.

[50] T. Overbye, X. Cheng, and Y. Sun, "A comparison of the ac and dc power flow models for lmp calculations," in *Proc. 37th Ann. Hawaii Int. Conf. on System Sciences*, Jan. 2004, p. 9 pp.

[51] A. Marano-Marcolini, F. Capitanescu, J. Martinez-Ramos, and L. Wehenkel, "Exploiting the use of DC SCOPF approximation to improve iterative ac scopf algorithms," *IEEE Trans. Power Syst.*, vol. 27, no. 3, pp. 1459–1466, Aug. 2012.

[52] L. Platbrood, F. Capitanescu, C. Merckx, H. Crisciu, and L. Wehenkel, "A generic approach for solving nonlinear-discrete security-constrained optimal power flow problems in large-scale systems," *IEEE Transactions on Power Systems*, vol. 29, no. 3, pp. 1194–1203, May 2014.

[53] Q. Zhai, X. Guan, J. Cheng, and H. Wu, "Fast identification of inactive security constraints in SCUC problems," *IEEE Trans. Power Syst.*, vol. 25, no. 4, pp. 1946–1954, Nov. 2010.

[54] H. Wang, C. Murillo-Sanchez, R. Zimmerman, and R. Thomas, "On computational issues of market-based optimal power flow," *IEEE Trans. Power Syst.*, vol. 22, no. 3, pp. 1185–1193, Aug. 2007.

[55] G. Ejebe and B. Wollenberg, "Automatic contingency selection," *IEEE Trans. Power App. Syst.*, vol. PAS-98, no. 1, pp. 97–109, Jan. 1979.

[56] T. A. Mikolinnas and B. Wollenberg, "An advanced contingency selection algorithm," *IEEE Trans. Power App. Syst.*, vol. PAS-100, no. 2, pp. 608–617, Feb. 1981.

[57] G. Irisarri and A. Sasson, "An automatic contingency selection method for on-line security analysis," *IEEE Trans. Power App. Syst.*, vol. PAS-100, no. 4, pp. 1838–1844, Apr. 1981.

[58] R. Fischl, T. Halpin, and A. Guvenis, "The application of decision theory to contingency selection," *IEEE Trans. Circ. Syst.*, vol. 29, no. 11, pp. 712–723, Nov. 1982.

[59] R. Schlueter, J. E. Sekerke, K. L. Burnett, and A. G. Costi, "Improved contingency measures for operation and planning applications," *IEEE Trans. Power Syst.*, vol. 4, no. 4, pp. 1430–1437, Nov. 1989.

[60] Q. Jiang, Z. Huang, and K. Xu, "Contingency filtering technique for transient stability constrained optimal power flow," *IET Gener. Transm. Distrib.*, vol. 7, no. 12, pp. 1536–1546, Dec. 2013.

[61] Q. Wang, J.-P. Watson, and Y. Guan, "Two-stage robust optimization for n-k contingency-constrained unit commitment," *IEEE Trans. Power Syst.*, vol. 28, no. 3, pp. 2366–2375, Aug. 2013.

[62] Y. Chen and A. Bose, "An adaptive pre-filter for the voltage contingency selection function," *IEEE Trans. Power Syst.*, vol. 5, no. 4, pp. 1478–1486, Nov. 1990.

[63] V. C. Ramesh and X. Li, "A fuzzy multiobjective approach to contingency constrained opf," *IEEE Trans. Power Syst.*, vol. 12, no. 3, pp. 1348–1354, Aug. 1997.

[64] T. Sidhu and L. Cui, "Contingency screening for steady-state security analysis by using FFT and artificial neural networks," *IEEE Trans. Power Syst.*, vol. 15, no. 1, pp. 421–426, Feb. 2000.

[65] V. Brandwajn, A. B. R. Kumar, A. Ipakchi, A. Bose, and S. Kuo, "Severity indices for contingency screening in dynamic security assessment," *IEEE Trans. Power Syst.*, vol. 12, no. 3, pp. 1136–1142, Aug. 1997.

[66] L. Wehenkel, "Contingency severity assessment for voltage security using non-parametric regression techniques," *IEEE Trans. Power Syst.*, vol. 11, no. 1, pp. 101–111, Feb. 1996.

[67] N. Amjady and M. Esmaili, "Application of a new sensitivity analysis framework for voltage contingency ranking," *IEEE Trans. Power Syst.*, vol. 20, no. 2, pp. 973–983, May 2005.

[68] C. Davis and T. Overbye, "Multiple element contingency screening," *IEEE Trans. Power Syst.*, vol. 26, no. 3, pp. 1294–1301, Aug. 2011.

[69] C.-L. Chang and Y.-Y. Hsu, "A new approach to dynamic contingency selection," *IEEE Trans. Power Syst.*, vol. 5, no. 4, pp. 1524–1528, Nov. 1990.

[70] F. M. Echavarren, E. Lobato, and R. Rouco, "Contingency analysis: feasibility identification and calculation algorithm," *Proc. IEE Gener. Transm. Distrib.*, vol. 152, no. 5, pp. 645–652, Sep. 2005.

[71] Y. Jia, P. Wang, X. Han, J. Tian, and C. Singh, "A fast contingency screening technique for generation system reliability evaluation," *IEEE Trans. Power Syst.*, vol. 28, no. 4, pp. 4127–4133, Nov. 2013.

[72] Y.-Y. Hsu and H.-C. Kuo, "Fuzzy-set based contingency ranking [power system security]," *IEEE Trans. Power Syst.*, vol. 7, no. 3, pp. 1189–1196, Aug. 1992.

[73] Y. Mansour, E. Vaahedi, and M. El-Sharkawi, "Dynamic security contingency screening and ranking using neural networks," *IEEE Trans. Neural Net.*, vol. 8, no. 4, pp. 942–950, Jul. 1997.

[74] P. Ruiz and P. Sauer, "Voltage and reactive power estimation for contingency analysis using sensitivities," *IEEE Trans. Power Syst.*, vol. 22, no. 2, pp. 639–647, May 2007.

[75] F. Capitanescu, M. Glavic, D. Ernst, and L. Wehenkel, "Contingency filtering techniques for preventive security-constrained optimal power flow," *IEEE Trans. Power Syst.*, vol. 22, no. 4, pp. 1690–1697, Nov. 2007.

[76] J. Zaborszky, K.-W. Whang, and K. Prasad, "Fast contingency evaluation using concentric relaxation," *IEEE Trans. Power App. Syst.*, vol. PAS-99, no. 1, pp. 28–36, Jan. 1980.

[77] V. Brandwajn, "Efficient bounding method for linear contingency analysis," *IEEE Trans. Power Syst.*, vol. 3, no. 1, pp. 38–43, Feb. 1988.

[78] E. Hnyilicza, S. T. Y. Lee, and F. C. Schweppe, "Steady state security regions: Set-theoretic approach," in *Proc. IEEE PICA*, New Orleans, LA, 1975, pp. 347–355.

[79] R. Fischl, G. C. Ejebe, and J. A. De Maio, "Identification of power system steady-state security regions under load uncertainty," in *Proc. IEEE PES Summer Meeting*, Portland, OR, 1976.

[80] C. G. Ejebe and B. F. Wollenberg, "Automatic contingency selection," *IEEE Trans. Power App. Syst.*, vol. PAS-98, no. 1, pp. 97–109, Jan. 1979.

[81] M. H. Banakar and F. D. Galiana, "Power system security corridors concept and computation," *IEEE Trans. Power App. Syst.*, vol. PAS-100, no. 11, pp. 4524–4532, Nov. 1981.

[82] R. Fischl, T. F. Halpin, and A. Guvenis, "The application of decision-theory to contingency selection," *IEEE Trans. Circuits Syst.*, vol. CAS-29, no. 11, pp. 712–723, Nov. 1982.

[83] V. Brandwajn and M. G. Lauby, "Complete bounding for AC contingency analysis," *IEEE Trans. Power Syst.*, vol. 4, no. 2, pp. 724–729, May 1989.

[84] A. B. R. Kumar, V. Brandwajn, A. Ipakchi, and R. Adapa, "Integrated framework for dynamic security analysis," *IEEE Trans. Power Syst.*, vol. 13, no. 3, pp. 816–821, Aug. 1998.

[85] C. Fu and A. Bose, "Contingency ranking based on severity indices in dynamic severity analysis," *IEEE Trans. Power Syst.*, vol. 14, no. 3, pp. 980–986, Aug. 1999.

[86] D. Ernst, D. Ruiz-Vega, M. Pavella, P. M. Hirsch, and D. Sobajic, "A unified approach to transient stability contingency filtering, ranking and assessment," *IEEE Trans. Power Syst.*, vol. 16, no. 3, pp. 435–443, Aug. 2001.

[87] F. Capitanescu and L. Wehenkel, "A new iterative approach to the corrective security-constrained optimal power flow problem," *IEEE Trans. Power Syst.*, vol. 23, no. 4, pp. 1533–1541, Nov. 2008.

[88] A. Street, F. Oliveira, and J. Arroyo, "Contingency-constrained unit commitment with $n-k$ security criterion: A robust optimization approach," *IEEE Trans. Power Syst.*, vol. 26, no. 3, pp. 1581–1590, Aug. 2011.

[89] J. Momoh, R. Adapa, and M. El-Hawary, "A review of selected optimal power flow literature to 1993. i. nonlinear and quadratic programming approaches," *IEEE Trans. Power Syst.*, vol. 14, no. 1, pp. 96–104, Feb. 1999.

[90] J. Momoh, M. El-Hawary, and R. Adapa, "A review of selected optimal power flow literature to 1993. ii. newton, linear programming and interior point methods," *IEEE Trans. Power Syst.*, vol. 14, no. 1, pp. 105–111, Feb. 1999.

[91] A. Papalexopoulos, "Challenges to on-line opf implementation," *IEEE Trans. Power Syst.*, vol. 12, no. 1, pp. 449–451, Feb. 1997.

[92] D. Bertsimas and J. N. Tsitsiklis, *Introduction to Linear Optimization.* Belmont, MA: Athena Scientific, 1997.

[93] IEEE 118 bus power flow test case. [Online]. Available: http://www.ee.washington.edu/research/pstca/pf118/ieee118psp.txt

[94] Reliability Test System Task Force, "The IEEE reliability test system—1996," *IEEE Trans. Power Syst.*, vol. 14, no. 3, pp. 1010–1020, Aug. 1999.

[95] C. A. Floudas, *Nonlinear and Mixed-Integer Optimization: Fundamentals and Applications.* New York, NY: Oxford University Press, 1995.

[96] R. Baldick, *Applied Optimization.* Cambridge, U.K.: Cambridge University Press, 2006.

[97] GAMS Development Corporation, *GAMS—A User's Guide.* Washington, DC: GAMS, Jul. 2014.

[98] R. D. Zimmerman, C. E. Murillo-Sánchez, and D. Gan. MATPOWER 4.1: A MATLAB power system simulation package. Cornell University. [Online]. Available: http://www.pserc.cornell.edu/matpower/

[99] A. Ardakani and F. Bouffard, "Identification of umbrella constraints in dc-based security-constrained optimal power flow," *IEEE Trans. Power Syst.*, vol. 28, no. 4, pp. 3924–3934, Nov. 2013.

[100] ——, "Acceleration of umbrella constraint discovery in generation scheduling problems," IEEE Trans. Power Syst., Aug. 2014, in press.

[101] M. Carrión and J. Arroyo, "A computationally efficient mixed-integer linear formulation for the thermal unit commitment problem," *IEEE Trans. Power App. Syst.*, vol. 21, no. 3, pp. 1371–1378, Aug. 2006.

[102] S. Haykin, *Neural networks: a comprehensive foundation*. Prentice Hall PTR, 1994.

[103] B. R. Szkuta, L. A. Sanabria, and T. Dillon, "Electricity price short-term forecasting using artificial neural networks," *IEEE Trans. Power Syst.*, vol. 14, no. 3, pp. 851–857, Aug. 1999.

[104] J. Contreras, R. Espinola, F. Nogales, and A. Conejo, "Arima models to predict next-day electricity prices," *IEEE Trans. Power Syst.*, vol. 18, no. 3, pp. 1014–1020, Aug. 2003.

[105] J.-B. Park, K.-S. Lee, J.-R. Shin, and K. Lee, "A particle swarm optimization for economic dispatch with nonsmooth cost functions," *IEEE Trans. Power Syst.*, vol. 20, no. 1, pp. 34–42, Feb. 2005.

[106] D. Park, M. El-Sharkawi, I. Marks, R.J., L. Atlas, and M. Damborg, "Electric load forecasting using an artificial neural network," *IEEE Trans. Power Syst.*, vol. 6, no. 2, pp. 442–449, May 1991.

[107] H. Hippert, C. Pedreira, and R. Souza, "Neural networks for short-term load forecasting: a review and evaluation," *IEEE Trans. Power Syst.*, vol. 16, no. 1, pp. 44–55, Feb. 2001.

[108] K. Hornik, "Approximation capabilities of multilayer feedforward networks," *Neural networks*, vol. 4, no. 2, pp. 251–257, 1991.

[109] D. E. Rumelhart, G. E. Hinton, and R. J. Williams, "Learning representations by back-propagating errors," *Cognitive modeling*, 1988.

[110] J. Kennedy, R. Eberhart *et al.*, "Particle swarm optimization," in *Proc. IEEE Int. Conf. on Neural Net.*, vol. 4, no. 2. Perth, Australia, 1995, pp. 1942–1948.

[111] W. Butler and S. Haykin, "Multiparameter sensitivity problems in network theory," *Proc. IEE*, vol. 117, no. 12, pp. 2228–2236, Dec. 1970.

[112] A. Kalantari and S. M. Kouhsari, "An exact piecewise method for fault studies in interconnected networks," *International Journal of Electrical Power & Energy Systems*, vol. 30, no. 3, pp. 216–225, Mar. 2008.